eCAM
Evidence-Based Complementary and Alternative Medicine

Immunomodulatory Activity of Complementary and Alternative Medicines

Guest Editors: Kuzhuvelil Bhaskaran-Nair Harikumar, Roland Hardman, Jesil Mathew Aranjani, Vineesh Vimala Raveendran, and Punathil Thejass

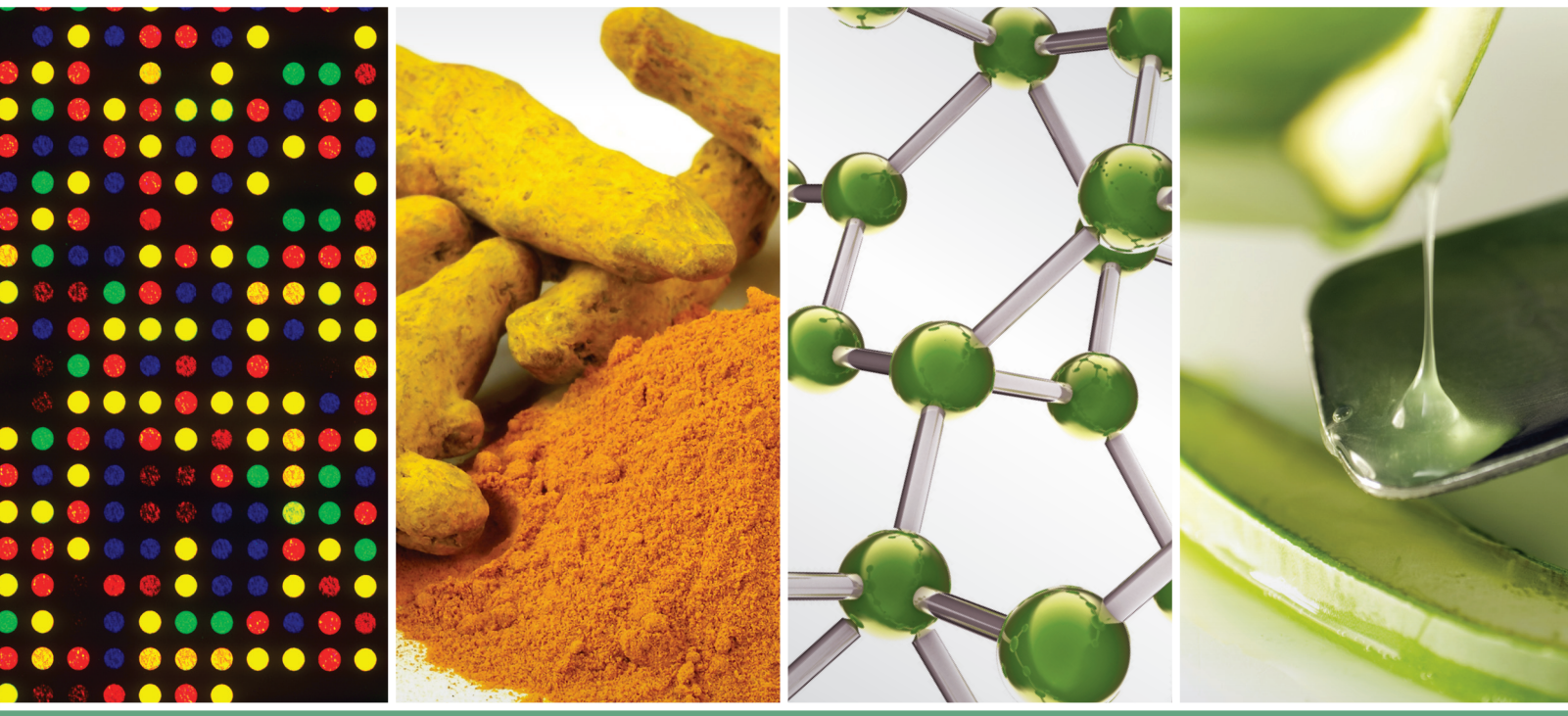

Immunomodulatory Activity of Complementary and Alternative Medicines

Evidence-Based Complementary and Alternative Medicine

Immunomodulatory Activity of Complementary and Alternative Medicines

Guest Editors: Kuzhuvelil Bhaskaran-Nair Harikumar, Roland Hardman, Jesil Mathew Aranjani, Vineesh Vimala Raveendran, and Punathil Thejass

Editorial Board

Contents

Hindawi Publishing Corporation
Evidence-Based Complementary and Alternative Medicine
Volume 2014, Article ID 765107, 2 pages
http://dx.doi.org/10.1155/2014/765107

Editorial

Immunomodulatory Activity of Complementary and Alternative Medicines

Kuzhuvelil Bhaskaran-Nair Harikumar,[1] Roland Hardman,[2] Jesil Mathew Aranjani,[3] Vineesh Vimala Raveendran,[4] and Punathil Thejass[5]

[1] *Cancer Research Program, Rajiv Gandhi Centre for Biotechnology, Thiruvananthapuram 695014, India*
[2] *School of Pharmacy and Pharmacology, University of Bath, Bath BA2 7AY, UK*
[3] *Department of Pharmaceutical Biotechnology, Manipal College of Pharmaceutical Sciences, Manipal University, Manipal 576104, India*
[4] *Division of Allergy, Clinical Immunology and Rheumatology, University of Kansas Medical Center, Kansas City, KS 66160, USA*
[5] *Department of Zoology, Government College, Madappally, Vadakara 673102, India*

Correspondence should be addressed to Kuzhuvelil Bhaskaran-Nair Harikumar; harikumar@rgcb.res.in

Received 8 January 2014; Accepted 8 January 2014; Published 2 March 2014

Around the world, the majority of people tend to adopt different health care approaches outside of the mainstream Western medicine for diseases or general well-being. These nonmainstream health care approaches are commonly referred to as complementary and alternative medicine (CAM).

Although people use the words "complementary and alternative" interchangeably, they refer to two different concepts. "Complementary" confers the intention to add to conventional medicines by the use of phytomedicines, which are nonmainstream medicines. While "alternative" refers to a purely nonmainstream approach using phytomedicines, instead of a combinational medicinal treatment.

The main drawback, raised by the Western medical community, is the lack of scientific evidence for the ascribed healing power of CAM, as well as the failure of large placebo controlled clinical trials to show the therapeutic efficacy of certain CAM. Nevertheless, in certain instances, the research relying on herbal products has led to the discovery of potent anticancer lead molecules such as taxol and camptothecin, and today many other candidate plant molecules are under investigation as anticancer agents. Similarly, plant activity for cardiovascular disease and other inflammatory diseases is relevant. Evidence continues to build up in support of the effects of these therapies on immunomodulation and maintenance of the physiological balance between anti- and proinflammatory mechanisms.

In vitro and in vivo animal studies have shown the plausible mechanisms of CAM in preventing or curing disease to be linked to antioxidant effects, alterations in proinflammatory cell signaling, production of cytokines, and other proinflammatory mediators.

To better understand and adopt these nonmainstream health approaches to complement the current standard (Western) healthcare, scientific evidence is required which is obtained via properly controlled experimentation. In this special issue we have some research papers which hold evidence of efficacy in various disease conditions.

Three papers of this special issue show the effect of either hydrogen dissolved purified water or herbal natural products on atopic dermatitis (AD) like skin inflammation. The authors of one of the articles compared the effect of drinking hydrogen water (HW) or purified water (PW) on AD and showed therapeutic effect by HW over PW by effectively modulating Th1 and Th2 response. In another article, the authors induced AD like inflammation in Balb/c mice by 2, 4-dinitrofluorobenzene and studied the effect of Qingpeng ointment (QP) on alleviation of lesion severity. The authors correlated the effect of QP on AD with the inhibition

of infiltration of CD4+T cells and mast cells, suppression of production of IgE and IL-4, and increase in the levels of IFN-γ. One of the papers also deals with a natural remedy for AD. The authors used a nona natural product mixture (NPM-9), which effectively suppressed Th2-mediated allergic inflammation on skin of the mouse model.

Another paper attempted to study the effect Korean red ginseng (KRG) on *vif* gene in HIV. Patients receiving KRG and highly active antiretroviral therapy (HAART) exhibited high frequency of premature stop codons (PSC) for *vif* compared to patients on KRG alone or the placebo group. On the other hand, KRG induced more in-frame deletions compared to the placebo group. This study therefore suggests a therapeutic strategy for a better outcome in HIV patients by combining KRG along with HAART.

Another paper demonstrates the effect of a Chinese medicine granule, Shu-Feng-Xuan-Fei (SFXF), on the gross change in the gene expression profile in T-cell-mediated immunity, during influenza virus infection. The authors studied different doses of SFXF and compared the efficacy with the control group as well as with mice which received oseltamivir. The authors concluded that SFXF restored the immune function and helped the rapid clearance of viral particles by regulating the T-cell gene expression patterns.

We believe the above selected research papers, taken from those appearing in this special issue, will improve our knowledge and understanding of the immunomodulatory functions of complementary and alternative medicines.

Acknowledgments

We, the editorial team, sincerely thank all the authors for submitting their manuscripts and for their patience. We also acknowledge the sincere assistance from the eCAM team for facilitating this special issue.

Kuzhuvelil Bhaskaran-Nair Harikumar
Roland Hardman
Jesil Mathew Aranjani
Vineesh Vimala Raveendran
Punathil Thejass

Hindawi Publishing Corporation
Evidence-Based Complementary and Alternative Medicine
Volume 2014, Article ID 976364, 15 pages
http://dx.doi.org/10.1155/2014/976364

Research Article

Gene Expression Profiles Underlying Selective T-Cell-Mediated Immunity Activity of a Chinese Medicine Granule on Mice Infected with Influenza Virus H1N1

Na-na Lu,[1] Qi Liu,[1,2] Li-gang Gu,[1] Shi-jie Ge,[1] Jun Wu,[1] Qiu Ze-ji,[1] Ze-ji Qiu,[3] Hong-chun Zhang,[3] En-xiang Chao,[1] and Zhuo-nan Yu[1]

[1] *Laboratory of Chinese Medicine on Viral Disease, Basic Medical College, Beijing University of Chinese Medicine, Beijing 100029, China*
[2] *Shanxi University of Traditional Chinese Medicine, Taiyuan, Shanxi 030024, China*
[3] *Department of Respiratory Medicine, China-Japan Friendship Hospital, Beijing 100029, China*

Correspondence should be addressed to Li-gang Gu; lggulg@163.com

Received 21 August 2013; Revised 25 October 2013; Accepted 18 November 2013; Published 8 January 2014

Academic Editor: V. R. Vineesh

A Chinese medicine granule, Shu-Feng-Xuan-Fei (SFXF), is critical for viral clearance in early phase of influenza virus infection. In this study, 72 ICR mice were randomly divided into six groups: normal control group, virus control group, Oseltamivir group, low-dose SFXF, medium-dose SFXF, and high-dose SFXF. Mice were anesthetized and inoculated with 4LD50 of influenza virus A (H1N1) except normal control group. Oseltamivir group received 11.375 $mg \cdot kg^{-1} \cdot d^{-1}$ Oseltamivir Phosphate. SFXF 3.76, 1.88 and 0.94 $g \cdot kg^{-1} \cdot d^{-1}$ were administrated to mice in all SFXF groups. Each group was in equal dose of 0.2ml daily for 4 consecutive days. Mice were sacrificed and then total RNA was extracted in lung tissue. Some genes involved in T-cell-mediated immunity were selected by DNA microarray. These candidate genes were verified by Real-Time PCR and western immunoblotting. Compared with virus control group, in Toll-like receptor signaling pathway, 12 virus-altered genes were significantly reduced following medium-dose SFXF treatment. Eighteen antigen processing presentation-associated genes were upregulated by medium-dose SFXF. In the process of T cell receptor signaling pathway, 19 genes were downregulated by medium-dose SFXF treatment. On exploration into effector T cells activation and cytokines, all of altered genes in virus control group were reversed by medium-dose SFXF. Real-time PCR and western immunoblotting showed that the regulation of medium-dose SFXF in IL-4, IFN-γ, TNF-α, IL-1β, TLR7, MyD88, p38, and JNK was superior to Oseltamivir and high-dose SFXF group. Therefore, SFXF granules could reduce influenza infected cells and activation of T cells.

1. Introduction

Influenza virus A (H1N1) has emerged every year and remained a public health threat worldwide. Influenza virus not only can damage the epithelial cells, of the lung and airways, but also may lead to complications of extrarespiratory diseases. Today the main option for prevention and treatment is the neuraminidase inhibitor (NAI), Oseltamivir Phosphate, which prolongs influenza virus shedding, decreases the signs of infection, reduces the spread of H1N1pdm influenza virus in the lungs of ferrets, and impedes the development of viral pneumonia [1]. However, the risk of Oseltamivir for virus strain resistance, possible side effects, and financial cost outweigh the small benefits for the prophylaxis and treatment of healthy individuals [2]. To address these issues, other effective alternative treatments of symptomatic influenza, especially Chinese herbal granules, will be additionally needed to have maximal reduction in incidence and mortality of influenza. For example, it was reported that Yin-Qiao-San could reduce time of fever resolution in patients with H1N1 influenza virus infection [3]. This paper studies Shu-Feng-Xuan-Fei granules (SFXF) whose major ingredients are based upon classical Yin-Qiao-San formula. Before this study, based on the guidelines issued by the Chinese Ministry of Health, the data of

pyretic patients in fever clinic of Chinese-Japanese Friendship Hospital were collected by rapid influenza diagnostic tests (RIDT) from February to April, 2012. Clinical trials of this herbal granule had demonstrated its efficacy in reducing the duration of fever in patients with influenza A (H3N2) virus infection [4]. However, the molecular mechanisms of this herbal granule are still unclear. DNA microarray analysis has emerged as an important tool in the characterization of changes in host gene expression following infection by influenza virus. In this study, we reported a systematic evaluation of its immune-modulatory activities *in vivo*.

2. Methods and Materials

2.1. Virus. The virus strain used in the study was a mouse-adapted strain of influenza A/FM/1/47 (H1N1), kindly offered by the Chinese Center for Disease and Prevention. Virus was grown in 9-day-old embryonated chicken eggs and virus-containing allantoic fluids were used in experiments. The supernatants were clarified, harvested, and stored at −70°C. The viral titer in the viral stocks, or tissue homogenates, was determined using a medium lethal dose (LD50) assay and then calculated by the Muench-Reed method (1938) [5]. The medium lethal dose (LD50) was determined in mice after serial dilution of the stock. Two times value of LD50 were used for viral challenge in all of the experiments. LD50 value $= 10^{-2.24}$.

2.2. Preparation of Herbal Extracts. Oseltamivir Phosphate was purchased from the F. Hoffmann-La Roche Ltd. (Basel, Swiss) (no. J20040058). SFXF granule was manufactured and provided by Beijing Tcmages Pharmaceutical Co., Ltd. SFXF consists of *lonicera japonica* (10 g), *forsythia* (10 g), *dyers woad leaf* (10 g), *great burdock achene* (10 g), *periostracum cicadae* (8 g), *thunberg fritillary bulb* (10 g), *scutellaria* (10 g), *radix asteris* (15 g), almond (10 g), *platycodon grandiflorum* (10 g), *glycyrrhiza uralensis* (6 g), and *radix isatidis* (10 g). One hundred grams of granules was dissolved in 500 mL water and kept at 4°C over night. The autoclaved herbal juice was then concentrated by continuous freeze-drying operation for 72 hours until the solvent was completely removed. These granules were kept in airtight containers at −70°C until further use.

2.3. Animal Experiments. Seventy-two male ICR mice (13 to 15 g body weight) were purchased from SPF Lab Animal, Ltd. (Beijing, China). All mice were housed at an animal facility under specific-pathogen-free conditions. Mice were housed in individually ventilated cages provisioned with water and standard feed and were monitored daily for health and condition. All H1N1 *in vivo* experiments were performed under biosafety level 3 enhanced (BSL3+) containment. Mice were exposed to 4LD50 of virus by the intranasal (i.n.) route. All animal experiments were handled to the protocol approved by the university animal committee. According to random number table, 72 ICR mice were randomly divided into six groups ($n = 12$): normal control group (N), virus control group (M), Oseltamivir group, low-dose SFXF (SL), medium-dose SFXF (SM), and high-dose SFXF (SH). Mice were anesthetized with 2,2,2-tribromoethanol in tert-amyl alcohol and inoculated (i.n.) with 4LD50 of virus except normal control group. Normal control group was given isotonic saline 0.05 mL in nasal drops. After 2 hours of inoculation, Oseltamivir group received 11.375 $mg \cdot kg^{-1} \cdot d^{-1}$ Oseltamivir Phosphate. SFXF 3.76, 1.88, and 0.94 $g \cdot kg^{-1} \cdot d^{-1}$ were administrated to mice in SL, SM, and SH groups by gastric irrigation, respectively. The medium dosage SFXF granule for mouse study was equivalent to the human dosage in clinical practice, while the SL was half and the SH was twice of the human clinical dosage, respectively. Each group was in equal dose of 0.2 mL daily for 4 consecutive days. Total RNA was extracted in each group.

2.4. Microarray Data Analysis. One microgram of total RNA was prepared for the cDNA reversed transcription reaction and performed using Amino Allyl MessageAmp II aRNA Amplification Kit (Ambion no. AM1753, CA, USA) according to manufacture's instructional resources information system. Double stranded cDNA was synthesized and as a template followed by an *in vitro* transcription reaction to amplify aRNA while biotin was incorporated into the synthesized aRNA probe. 40 μg of unlabeled aRNA was subsequently used in each labeling reaction to generate sufficient Cy5-labeled aRNA for the microarray hybridization in triplicate. Before the microarray hybridization, the Cy5-labeled aRNAs were fragmented by using the reagents and protocol provided in Ambion RNA Fragmentation Reagents kit (Ambion Inc., Austin, TX). Each 10 μg fragmented Cy5-labeled aRNA was suspended in OneArray hybridization buffer at a final volume of 180 μL for microarray hybridization to the mouse Whole Genome One Array Version 5.1 (HOA 5.1, Phalanx Biotech Group, Inc., Taiwan). After an overnight hybridization at 50°C, nonspecific binding targets were washed out three times (Wash, 42°C, 5 min; Wash II, 42°C, 5 min; Wash III 25°C, 5 min). The arrays were dried by centrifugation and were scanned by AXON4000B scanner (Molecular Devices, CA, USA). The fluorescent intensities of each spot were analyzed by GenePix 4 (Molecular Device, CA, USA). And then the data were averaged from the three technical replicates and were normalized using Rosetta Resolver System software (Rosetta Biosoftware, USA). The spots that flags reported as −50 were filtered out. Rosetta error models were available in the Rosetta Resolver system for gene expression analysis in two different groups. Five pairwise comparisons were performed. For example, the comparison between normal control group and virus control group was scattered, indicating that a large number of genes were altered in response to H1N1-infected mouse lung. Changes in gene expression were attributable to the SH, SM, SL, and Oseltamivir intervention which were done by comparing genes in virus control group. Gene Cluster 3.0 and Eisen's Treeview software (Stanford University) were used to compare similarities among individual samples. The log 2 transformed intensity of any two gene expression profiles was plotted and compared, while a fold change (FC) over 2 or under 0.5 ($|\log_2 FC| \geq 1$), as well as P value <0.05, was considered to indicate differential

expression. Genes whose relative expression levels showed $\log_2\text{FC} \geq 1$ and $P < 0.05$ were considered significantly upregulated, and those with $\log_2\text{FC} \leq -1$ and $P < 0.05$ were considered significantly downregulated. The correlation of expression profiles between biological replicates and treatment conditions was demonstrated by unsupervised hierarchical clustering analysis. The functions of differentially expressed genes involved in immunomodulatory biological pathways were analyzed by Kyoto Encyclopedia of Genes and Genomes (KEGG) Pathway databases in Database for Annotation, Visualization, and Integrated Discovery (DAVID, http://david.abcc.ncifcrf.gov/).

2.5. Real-Time PCR Analysis. Real-Time PCR, a technology used for the detection and quantification of RNA targets, is considered as "gold standard" for verifying the microarray data. Total RNA was extracted from 50 to 100 mg of lung tissue with TRIzol (Invitrogen) according to the protocol described for the SYBR Green PCR kit (Takara Bio Inc., Shiga, Japan). For smaller samples, homogenization in liquid nitrogen could be done using mortar and pestle. Phase separation was achieved by adding chloroform (0.2 mL/mL Trizol), vortexing, and incubation at room temperature for 3 min. The tubes were centrifuged at 12000 ×g at 4°C for 15 min. The top, aqueous phase was transferred into a fresh RNA tube. Isopropanol was added and samples were mixed thoroughly and incubated at room temperature to precipitate RNA. Isopropanol was then replaced by 75% ethanol (1 mL/mL Trizol), mixed thoroughly, and centrifuged at 7500 ×g for 5 min at 4°C. The supernatant was removed. The RNA pellet redissolved in DEPC-H_2O (50 μL). The primer sequences of the expected PCR products were as follows: GAPDH (141 bp), Forward primer: 5′-GCAAGTTCAACGGCACAG-3′, and reverse primer: 5′-CGCCAGTAGACTCCACGAC-3′; IL-4 (142 bp), forward primer: 5′-TGTACCAGGAGCCATATC-CA-3′, and reverse primer: 5′-CTGTGGTGTTCTTCGTTG-CT-3′; IFN-γ (179 bp), forward primer: 5′-AGGCCATCA-GCAACAACATA-3′, and reverse primer: 5′-TGAGCT-CATTGAATGCTTGG-3′; TNF-α (133 bp), forward primer: 5′-CCAAAGGGATGAGAAGTTCC-3′, and reverse primer: 5′-CTCCACTTGGTGGTTTGCTA-3′; IL-1β (130 bp), forward primer: 5′-TCAGGCAGGCAGTATCACTC-3′, and reverse primer: 5′-AGGATGGGCTCTTCTTCAA-3′; IL-8 (242 bp), forward primer: 5′-CTCTTGGCAGCCTTCCTG-AT-3′, and reverse primer: 5′-ACAACCCTCTGCACC-CAGTT-3′; ICAM-1 (122 bp), forward primer: 5′-CCTCCG-GACTTTCGATCTT-3′, and reverse primer: 5′-GAGCTT-CAGAGGCAGGAAAC-3′; TLR7 (117 bp), forward primer: 5′-ACGCTTTCTTTGCAACTGTG-3′, and reverse primer: 5′-TTTGTGTGCTCCTGGACCTA-3′; MyD88 (136 bp), forward primer: 5′-TGGTGGTTGTTTCTGACGAT-3′, and reverse primer: 5′-GGAAAGTCCTTCTTCATCGC-3′; JNK (128 bp), forward primer: 5′-ATGCAAATCTTTGCCAAG-TG-3′, and reverse primer: 5′-AGGCTTTAAGTCCCG-ATGAA-3′; p38 (195 bp), forward primer: 5′-AAGCCA-TGAGGCAAGAAACT-3′, and reverse primer: 5′-TCA-TCAGGGTCGTGGTACTG-3′. Preincubation was performed at 94°C for 1 min, followed by amplification in 40 cycles at 94°C for 8 s, 60°C for 34 s, and finally, during slow heating up, 72°C for 10 min. Fold changes of expressions relative to vehicle controls were determined after normalization to glyceraldehydes-3-phosphate dehydrogenase (GAPDH) gene. Relative quantification is generally calculated with the $2^{-\Delta\Delta CT}$ formula by the comparative CT method [6]. The ΔCT value is determined by subtracting the average GAPDH CT value from the average target gene CT value (ΔCT = CT target gene − CT GADPH). The calculation of ΔΔCT involves subtraction by the ΔΔCT calibrator value (ΔΔCT = ΔCT each other sample −ΔCT normal control sample). The fold change for each of treated and virus control samples is relative to the normal control sample = $2^{-\Delta\Delta CT}$.

2.6. Western Immunoblotting. All selected RNA samples were the same as the ones from those used in the DNA microarray assay and real-time PCR assay. For smaller samples, homogenization in liquid nitrogen could be done using mortar and pestle. The tissue was placed to the precooling Eppendorf tube and we added 50 μL lysis buffer rapidly in the tube. Then the tube was placed on ice for 20 min and centrifuged at 16,000 ×g at 4°C for 20 min. We transferred the supernatant to a fresh tube kept on ice and discarded the pellet. We added an equal volume of 2 × SDS Sample Buffer and boiled each cell lysate in sample buffer at 100°C for 5 minutes. Protein lysates were denatured, subjected to 4 to 15% SDS-polyacrylamide electrophoresis gradient gels (Bio-Rad), and transferred to nitrocellulose membranes. The samples were then electrotransferred onto the nitrocellulose membrane. Membranes were incubated overnight and probed with rabbit anti-mouse IL-4 (bs0581R) and IFN-γ (bs0480R) polyclonal antibody (Biosynthesis Biotechnology Co., LTD, Beijing), rabbit anti-mouse TNF-α (BC0088) and IL-1β (BA2782) polyclonal antibody (Boster Biological Co., LTD, WuHan), rabbit anti-human JNK (4764S) and p38 (9252S) polyclonal antibody (Cell Signaling Technology, Inc), rabbit anti-mouse MyD88 (bs1047R) monoclonal antibody (Biosynthesis Biotechnology Co., LTD, Beijing), rabbit anti-human TLR7 (bs6601R) polyclonal antibody (Biosynthesis Biotechnology Co., LTD, Beijing), and rabbit anti-GAPDH (Sigma, USA). Membranes were then washed with TTBS four times for 5 min each and incubated with 1 : 2000 dilution of HRP-labeled Goat Anti-Rabbit IgG (H + L) (Zhongshan Golden Bridge Bio-technology, Beijing) for 1 h at room temperature. Immunoreactive bands were detected using ECL reagents (Santa cruz Biotechnology, Inc., USA) and IPP software. Next we also calculated a relative intensity, using our standard as the common point of comparison. Divide the absolute intensity of each sample band by the absolute intensity of your standard (GAPDH) to come up with a relative intensity for each sample band.

2.7. Statistical Analysis. The relative mRNA expression of the target gene was compared between all groups and analyzed by one-way analysis of variance (ANOVA). The differences between two groups were analyzed by Student's t-test, followed by a SPSS Statistics 17.0 Software. A P value of less than 0.05 ($P < 0.05$) was considered to be statistically significant. Results are presented as mean ± standard deviation (SD).

Table 1: Top 10 categorized pathways based on comparison of gene expression between normal and virus control groups.

Pathway name	Gene counts	P value
Cytokine-cytokine receptor interaction	87	$4.1E-18$
Chemokine signaling pathway	58	$6.4E-10$
MAPK signaling pathway	51	$1.3E-2$
Jak-STAT signaling pathway	48	$3.4E-8$
Toll-like receptor signaling pathway	39	$8.8E-10$
Cell adhesion molecules (CAMs)	32	$1.9E-2$
Apoptosis	32	$2.4E-7$
T-cell receptor signaling pathway	31	$5.5E-4$
Leukocyte transendothelial migration	24	$5.9E-2$
Antigen processing and presentation	23	$5.6E-3$

Similar results were obtained in at least three independent experiments.

3. Result

3.1. Total Differentially Expressed Genes Induced by H1N1 Virus and Treatment. The mouse whole genome microarray was used to perform a systematic alternation of the mRNA expression profiles after H1N1 infection and treatment. Hierarchical cluster analysis (HCA) was first conducted within ArrayTrack. A differentially expressed gene was identified following the criteria of a fold-change than 1 (up or down) and a P value less than 0.05 in comparison to the virus control group. Based on these two criteria, we identified virus control group upregulated 2670 genes expression and downregulated 2968 genes expression, compared to normal control group. Among these up-regulations of genes, 2358, 1877, 2659, and 1868 genes were significantly downregulated in response to the Oseltamivir group, the SH group, the SM group, and the SL group, respectively. Based on these downregulated genes in virus control group, up-regulations of 1849, 1302, 2216, and 1570 genes were identified in the Oseltamivir group, the SH group, the SM group, and the SL group, respectively, as shown in Figure 1.

3.2. Pathway Analysis of the Differentially Expressed Genes. In order to determine the correlation between the affected gene expression and the top 10 significant biological pathways induced by H1N1, the genes were grouped into functional categories and pathways based on the Kyoto Encyclopedia of Genes and Genomes (KEGG) database in Table 1. According to KEGG description, the results showed that the main pathways modulated T cell-mediated immunity during H1N1 infection, including Toll-like receptor signaling pathway, antigen processing and presentation, T cell receptor signaling pathway, and effector T cells activation and cytokines involved in T cell mediated immunity.

3.2.1. Exploration into Toll-Like Receptor Signaling Pathway. Some key Toll-like receptor signaling pathway-related target genes were identified in the present study. A comprehensive examination of gene expression form lung tissues of normal and H1N1-infected mice showed 12 upregulated genes to be differentially expressed in the infective mice, such as *Tlr7*, *MyD88*, *Mapk8*, *Mapk13*, *Tnf*, *Il1b*, *Cxcr2*, *Ccl5*, *Csf2*, *Tgfb1*, *Il18*, and *Il12a*. All of these virus-altered genes were significantly reversed following the SM treatment. The prominent genes in these significantly changed networks were *Tnf* and *Il1b,* exhibiting 5.03- and 4.27-fold decreased expression exposed to the SM group, respectively. Except *Tlr7*, the other 11 genes above (i.e., *MyD88*, *Mapk8*, *Mapk13*, *Tnf*, *Il1b*, *Csf2*, *Cxcr2*, *Ccl5*, *Tgfb1*, *Il18*, and *Il12a*) were downregulated in response to Oseltamivir group. The SL and SH only could down-regulate 9 genes (*MyD88*, *Mapk8*, *Mapk13*, *Tnf*, *Il1b*, *Csf2*, *Cxcr2*, *Ccl5*, and *Il12a*) and 8 genes (*MyD88*, *Mapk8*, *Mapk13*, *Tnf*, *Il1b*, *Csf2*, *Cxcr2*, and *Il12a*), respectively, as shown in Figure 2 and Table 2.

3.2.2. Exploration into Antigen Processing and Presentation. Some key antigen processing and presentation pathway-related target genes were identified in the present study. Twenty-three genes were identified as differentially expressed genes between virus-infected and normal mice, such as *Tap1*, *Tap2*, *Cd74*, *Ctsb*, *Ctss*, *Hspa5*, *Hspa1a*, *Hspa1b*, *H2-M2*, *H2-M3*, *H2-Oa*, *H2-Q10*, *H2-Dma*, *H2-Eb1*, *H2-Ab1*, *Lgmn*, *Lta*, *Psme1*, *H2-T24*, *Cd8a*, *Cd4*, *Cd8b1*, and *Psme2*. Compared with the virus control group, the gene expression result of the SM-treated mice was that a total of 18 antigen processing presentation-associated genes were differentially downregulated, among which 13 genes (*Tap1*, *Tap2*, *Hspa1a*, *Hspa1b*, *H2-M2*, *H2-M3*, *H2-Q10*, *Lta*, *Psme1*, *Cd8a*, *Cd8b1*, *H2-T24*, and *Psme2*) and 5 genes (*Ctss*, *H2-Dma*, *Lgmn*, *H2-Eb1*, and *Cd4*) belong to MHC-I and MHC-II family, respectively. In comparison with the virus control group, the result of the SL group was that a total of 5 antigen processing presentation-associated genes were differentially expressed, among which 4 genes (*H2-M2*, *H2-Q1*, *Cd8b1*, and *Psme2*) and 1 gene (*H2-Eb1*) belong to MHC-I and MHC-II family, respectively. Compared with the virus control group, in the SH group, *H2-Q10* and *Psme2* belonging to MHC-I were differentially expressed in antigen processing presentation-associated genes as shown in Figure 2 and Table 3.

3.2.3. Exploration into Process of T Cell Receptor Signaling Pathway. Some key T cell receptor signaling pathway-related target genes were identified in the present study. Sixteen differential genes were affected by H1N1 infection through comparison with the normal control group, such as *Cd3g*, *Cd247*, *Ptprc*, *Rasgrp1*, *Ctla4*, *Ikbkb*, *Mapk1*, *Map3k8*, *Nfkbie*, *Nfkbib*, *Nfkbia*, *Zap70*, *Pik3r5*, *Pik3cg*, *Map2k,* and *Pik3cd*. Fourteen genes (including *Ctla4*, *Cd247*, *Ptprc*, *Rasgrp1*, *Mapk1*, *Map3k8*, *Nfkbie*, *Nfkbib*, *Nfkbia*, *Zap70*, *Pik3r5*, *Pik3cg*, *Map2k1,* and *Pik3cd*) were downregulated by the SM treatment, of which 13 genes (*Ctla4*, *Cd247*, *Rasgrp1*, *Mapk1*, *Ikbkb*, *Map3k8*, *Nfkbie*, *Nfkbib*, *Nfkbia*, *Zap70*, *Pik3r5*, *Pik3cg,* and *Map2k1*) were also downregulated by the Oseltamivir group. The SL and SH group only could down-regulate 7 genes (*Rasgrp1*, *Map3k8*, *Nfkbie*, *Nfkbib*, *Nfkbia*, *Pik3r5,* and *Pik3cg*) and 4 genes (*Map3k8*, *Nfkbie*, *Nfkbib,* and *Pik3r5*), respectively, as shown in Figure 2 and Table 4.

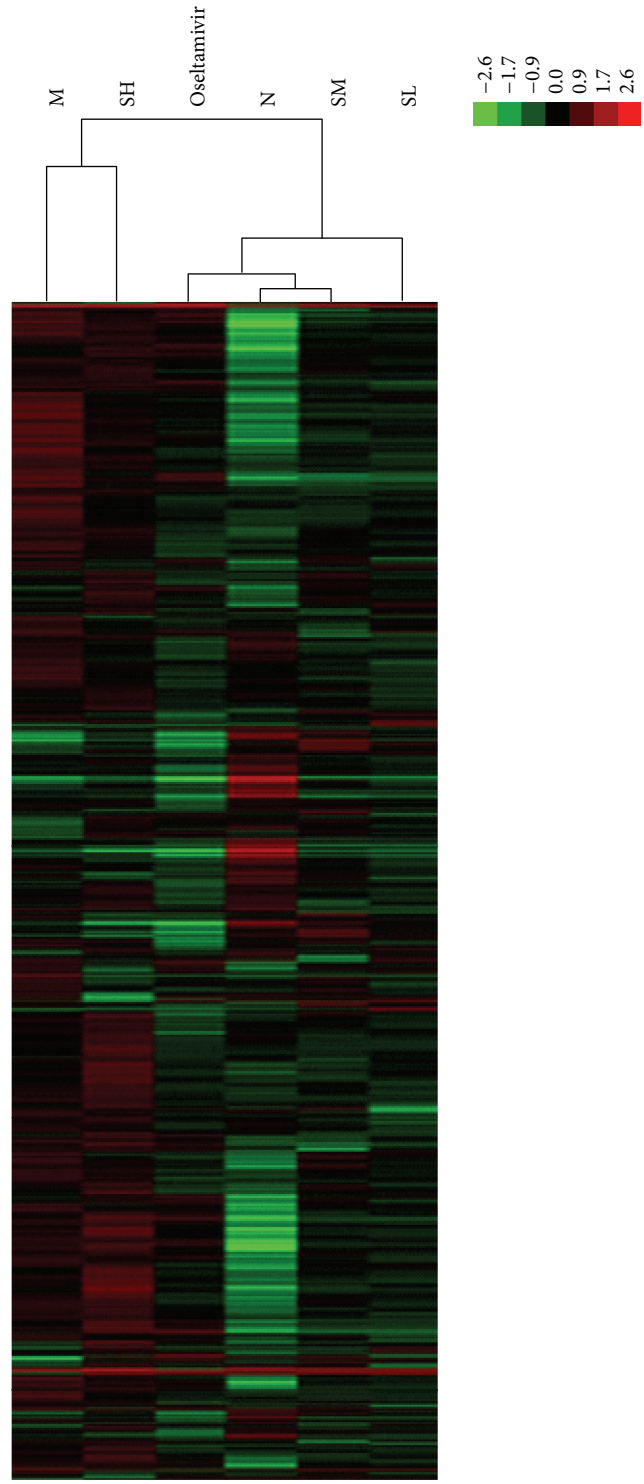

Figure 1: Two-way hierarchical clustering of selected genes in T cell recognition, activation, and proliferation activities was performed to visualize the correlations among the replicates and varying sample conditions. Up- and downregulated genes are represented in red and green colors, respectively. From left to right are virus control group, high-dose SFXF group, Oseltamivir group, normal control group, medium-dose SFXF group, and low-dose SFXF group.

Table 2: Genes associated with Toll-like receptor signaling pathway.

Symbol	GenBank accession	Gene description	$\log_2$ FC[a]				
			M/N	SH/M	SM/M	SL/M	Oseltamivir/M
Tlr7	mMC009252	Toll-like receptor 7, TLR7	1.39	0.02	−2.02	−0.43	−0.92
MyD88	PH_mM_0009196	Myeloid differentiation primary response gene 88	2.22	−1.18	−2.63	−1.36	−1.62
Mapk8	PH_mM_0009123	Mitogen-activated protein kinase 8, JNK	1.82	−1.14	−1.22	−1.04	−1.24
Mapk13	PH_mM_0004240	Mitogen-activated protein kinase 13, P38	1.39	−2.27	−1.89	−2.10	−1.50
Tnf	mMC016605	Tumor necrosis factor, TNF-α	5.47	−3.86	−5.03	−4.58	−4.60
Il1b	mMC010962	Interleukin 1 beta, IL-1β	3.69	−2.92	−4.27	−2.33	−2.47
Cxcr2	PH_mMC_0000540	Chemokine (C-X-C motif) receptor 2, IL-8	1.93	−2.80	−3.25	−2.25	−2.22
Ccl5	mMC0118383	Chemokine (C-C motif) ligand 5, RANTES	3.51	−0.93	−3.39	−1.95	−2.26
Tgfb1	PH_mMC_0001301	Transforming growth factor, beta 1	1.46	−0.84	−1.25	−0.92	−1.35
Csf2	mMC014357	Colony stimulating factor 2	2.41	−1.40	−2.03	−1.43	−2.19
Il18	mMC021817	Interleukin 18, IL-18	2.02	−0.66	−1.10	−0.76	−1.26
Il12a	PH_mM_0009192	Interleukin 12a, IL-12	3.38	−3.32	−2.92	−2.91	−3.05

[a]Fold change. The intensity ratio of probe signal criteria for differential expressions was defined as a twofold change (up or down) ($\log_2$ FC ≥ 1 or ≤ -1) in gene expression compared with virus control group and a P value less than 0.05 in at least one time point as a minimum requirement to select. For instance, $\log_2$ (M/N) ≥ 1 means that the comparison between normal control group and virus control group was scattered, indicating that a large number of genes in virus control group were up-regulated in response to H1N1 infection. $\log_2$ (SH/M) ≤ -1, $\log_2$ (SM/M) ≤ -1, $\log_2$ (SL/M) ≤ -1, and $\log_2$ (Oseltamivir/M) ≤ -1 means that down-regulation in gene expression attributable to the high-dose SFXF group treatment, medium-dose group SFXF treatment, low-dose SFXF group treatment, and Oseltamivir group treatment was done by comparing genes in virus control group, respectively (P value data not shown).

3.2.4. Exploration into Effector T Cells Activation and Cytokines Involved in T Cell Mediated Immunity. Some key effector T cells activation and cytokines-related target genes were identified in the present study. Influenza virus led to significant changes in the expression of 6 genes in virus control group, of which 5 genes (*Prf1*, *Gzmb*, *Fas*, *Fasl,* and *Il4*) were upregulated and 1 gene (*Ifng*) was downregulated in comparison with the normal control group. All of altered genes above were reversed by the SM group and Oseltamivir group. The notable genes in these significantly changed networks were *Gzmb* and *Il4,* exhibiting 4.79- and 5.19-fold decreased expression exposed to the treatment of the SM group, respectively. *Fasl*, *Fas*, *Il4,* and *Ifng* were found to be significantly altered by the SH group. Also down-regulation of *Il4,* as well as up-regulation of *Ifng*, was observed in the SL group as shown in Figure 2 and Table 5.

3.3. Confirmation of Microarray Data by Real-Time PCR. Real-time PCR was adopted to validate some selected genes whose expression changes were seen using microarrays, including the up-regulation of IL-1β, TNF-α, IL-4, TLR7, MyD88, JNK, p38, IL-8, and RANTES gene expressions and the down-regulation of IFN-γ gene expression. All selected RNA samples were the same as the ones from those used in the DNA microarray assay. Compared with normal control group, in virus control group, the expression of IFN-γ mRNA was significantly downregulated, while the expression of IL-1β, TNF-α, IL-4, TLR7, MyD88, JNK, p38, IL-8, and RANTES mRNA was markedly upregulated (all $P < 0.05$). Compared with virus control group, in all the treatment groups except the SH group, the expressions of IFN-γ mRNA were significantly upregulated, while IL-1β, TNF-α, IL-4, TLR7, MyD88, JNK, p38, IL-8, and RANTES mRNA were markedly downregulated. These differential genes in virus control group were the most significantly altered by the medium SFXF treatment. The regulation of the SM group in IL-1β, TNF-α, IL-4, TLR7, MyD88, JNK, p38, IL-8, and RANTES was superior to Oseltamivir, the high- and low-dose SFXF. As expected, real-time PCR data were consistent with the results of microarray assay as shown in Figures 3, 4, and 5.

3.4. Determination of IL-4, IFN-γ, IL-1β, TNF-α, TLR7, MyD88, JNK, and p38 Proteins in Lung Tissues by Western Immunoblotting. The levels of IL-1β, TNF-α, IL-4, TLR7, MyD88, JNK, and p38 were low and IFN-γ was high in the lung tissue of the normal control group. The protein levels of IL-1β, TNF-α, IL-4, TLR7, MyD88, JNK, and p38 in the H1N1 infection group were higher than those in normal control group ($P < 0.05$). In infected mice, the protein level of IFN-γ was lower than that in uninfected mice. The majority of upregulated IL-1β, TNF-α, IL-4, TLR7, MyD88, JNK, and p38 were significantly suppressed, while the level of IFN-γ was also converted to increase with treatment of SFXF in all doses and Oseltamivir group, which meant that significant difference was found between the virus control group and all treatment groups. After the treatment of the SM, all variants had turned to baseline levels, which showed no statistical difference from Oseltamivir group as shown in Figures 3 and 4.

4. Discussion

Chinese compound medicine has become one of the most popular choices on therapeutic treatment of influenza in the Orient, because it has such advantages as multiple pathways, multitargets, and low side effect, for example, Xiaoqing-long-tang [3]. Unfortunately, the interaction of complicated composition, the important signaling pathways, and the efficacy of Chinese traditional medicine at the transcriptional

Table 3: Genes associated with antigen processing presentation.

Symbol	GenBank accession	Gene description	$\log_2$ FC[a]				
			M/N	SH/M	SM/M	SL/M	Oseltamivir/M
Tap1	PH_mM_0000666	Transporter 1, ATP-binding cassette, subfamily B (MDR/TAP)	2.24	−0.30	−2.83	−0.41	−1.00
Tap2	mMC017161	Transporter 2, ATP-binding cassette, subfamily B (MDR/TAP)	2.29	−0.02	−2.27	−0.20	−1.05
Cd74	PH_mM_0016294	CD74 antigen (invariant polypeptide of major histocompatibility complex, class II antigen-associated), also as CLIP	1.74	0.47	0.60	0.13	−0.75
Ctsb	PH_mM_0013880	Cathepsin B	1.47	−0.27	−0.95	−0.24	−0.54
Ctss	PH_mM_0009536	Cathepsin S	1.99	0.29	−1.39	−0.28	−0.90
Hspa5	mMC021274	Heat shock protein 5	1.27	0.78	0.22	0.29	−0.16
Hspa1a	PH_mM_0000552	Heat shock protein 1A	2.05	−0.17	−2.39	−0.67	−0.75
Hspa1b	PH_mM_0001288	Heat shock protein 1B	1.53	0.63	−1.08	−0.47	−0.18
H2-M2	PH_mM_0002687	Histocompatibility 2, M region locus 2	2.27	−0.64	−2.16	−1.89	−1.47
H2-M3	PH_mM_0009138	Histocompatibility 2, M region locus 3	2.37	−0.24	−2.10	−0.55	−1.39
H2-Oa	PH_mM_0000005	Histocompatibility 2, O region alpha locus	1.15	−0.38	−0.44	−0.55	−0.67
H2-Q10	PH_mM_0005188	Histocompatibility 2, Q region locus 10	5.62	−2.04	−2.72	−3.84	−4.12
H2-Dma	PH_mM_0005361	Histocompatibility 2, class II, locus DMa	1.49	−0.17	−1.11	−0.43	−1.14
H2-Eb1	PH_mM_0006643	Histocompatibility 2, class II antigen E beta	1.30	−0.31	−1.87	−1.31	−1.33
H2-Ab1	PH_mM_0006906	Histocompatibility 2, class II antigen A, beta 1	1.17	0.26	−0.05	0.33	−0.10
Lgmn	mMC007543	Legumain	2.27	0.08	−1.10	−0.24	−0.83
Lta	mMC008431	Lymphotoxin A, TNF-β	1.34	−0.14	−1.17	−0.18	−1.19
Psme1	PH_mM_0004486	Proteasome (prosome, macropain) 28 subunit, alpha	1.00	−0.40	−1.16	−0.53	−0.50
H2-T24	PH_mM_0007562	Histocompatibility 2, T region locus 24	2.82	−0.15	−2.19	0.21	−1.72
Psme2	PH_mM_0012374	Proteasome (prosome, macropain) 28 subunit, beta	1.99	−1.00	−1.55	−1.58	−1.00
Cd8a	PH_mM_0015300	CD8 antigen, alpha chain	2.27	1.20	−1.65	−0.42	−1.05
Cd8b1	mMC017400	CD8 antigen, beta chain 1	2.49	1.31	−1.18	−1.58	−0.73
Cd4	mMC002333	CD4 antigen	1.05	−0.32	−1.11	−0.92	−1.00

[a]Fold change. The intensity ratio of probe signal criteria for differential expressions was defined as a twofold change (up or down) ($\log_2$ FC ≥ 1 or ≤ -1) in gene expression compared with virus control group and a P value less than 0.05 in at least one time point as a minimum requirement to select. For instance, $\log_2$ (M/N) ≥ 1 means that the comparison between normal control group and virus control group was scattered, indicating that a large number of genes in virus control group were up-regulated in response to H1N1 infection. $\log_2$ (SH/M) ≤ -1, $\log_2$ (SM/M) ≤ -1, $\log_2$ (SL/M) ≤ -1, and $\log_2$ (Oseltamivir/M) ≤ -1 means that down-regulation in gene expression attributable to the high-dose SFXF group treatment, medium-dose group SFXF treatment, low-dose SFXF group treatment, and Oseltamivir group treatment was done by comparing genes in virus control group, respectively (P value data not shown).

level all challenge our biotechnique to identify precise molecular therapeutic targets. Therefore, the whole-genome DNA microarray has been proved to be an unbiased and high-throughput approach to thoroughly analyze virus infection and antiviral treatment by monitoring gene changes in deletion variants.

In this study, we studied the gene transcription profiles of the lung tissue of mice infected with H1N1 virus for 4 consecutive days. The major pathways involved in T-cell mediated immunity in response to H1N1 infection were mostly upregulated, such as Toll-like receptor signaling pathway, antigen processing and presentation, and T-cell receptor signaling pathway, as well as effector T cells activation and cytokines in cell-mediated immunity.

Since the largest number of differentially expressed genes was detected in the medium-dose SFXF treatment, we focused further analyses on gene functions and pathways primarily for the medium-dose SFXF treatment. In terms of Toll-like receptor signaling pathway, TLR7 (*Tlr7*) senses single-stranded RNA from influenza virus within the endosomes and induces the downstream signaling pathway involving MyD88 (*Myd88*)/IRAK/TRAF6, which activated the p38 (*Mapk13*) and JNK (*Mapk8*), causing proinflammatory cytokines (i.e., TNF-α, IL-1β, IL-8, IL-12, IL-18, GM-CSF, and RANTES) production to control and potentially eradicate virus infections [7]. In T cells, TLR7 activation mediates inflammation, cross presentation of cell-associated antigens, and cross priming of CD8+ T cells upon lung IVA infection

Table 4: Genes associated with T-cell receptor signaling pathway.

Symbol	GenBank accession	Gene description	$\log_2$ FC[a]				
			M/N	SH/M	SM/M	SL/M	Oseltamivir/M
Cd3g	PH_mM_0008250	CD3 antigen, gamma polypeptide, CD3γ	1.26	1.43	−0.50	0.17	−0.49
Cd247	PH_mM_0012514	CD247 antigen, CD3ζ	1.56	0.38	−1.59	−0.65	−1.10
Ptprc	PH_mM_0012802	Protein tyrosine phosphatase, receptor type, C. CD45	1.65	0.32	−1.41	−0.11	−0.52
Rasgrp1	PH_mM_0009315	RAS guanyl releasing protein 1	2.43	−0.93	−1.94	−1.25	−1.60
Ctla4	mMC018651	Cytotoxic T-lymphocyte-associated protein 4	1.59	0.67	−1.94	−0.49	−1.01
Ikbkb	mMR027870	Inhibitor of kappaB kinase beta	1.33	−0.65	−0.87	−0.67	−1.19
Mapk1	mMC024552	Mitogen-activated protein kinase 1, Erk	2.23	−0.90	−1.04	−0.47	−1.50
Map3k8	mMC012006	Mitogen-activated protein kinase kinase kinase 8, COT	3.59	−2.86	−3.98	−2.92	−3.09
Nfkbie	PH_mM_0006219	Nuclear factor of kappa light polypeptide gene enhancer in B cells inhibitor, epsilon. IκBε	4.26	−1.84	−3.75	−2.32	−3.13
Nfkbib	mMC008604	Nuclear factor of kappa light polypeptide gene enhancer in B cells inhibitor, beta. IκBβ	3.34	−2.35	−2.68	−2.12	−2.88
Nfkbia	mMC012597	Nuclear factor of kappa light polypeptide gene enhancer in B cells inhibitor, alpha. IκBα	1.66	−0.92	−1.95	−1.33	−1.52
Zap70	mMC019091	Zeta-chain associated protein kinase, ZAP-70	1.53	0.38	−1.36	−0.58	−1.49
Pik3r5	PH_mM_0003125	Phosphoinositide-3-kinase, regulatory subunit 5, p101. PI3K	3.12	−2.52	−3.90	−2.95	−2.88
Pik3cg	mMC005200	Phosphoinositide-3-kinase, catalytic, gamma polypeptide. PI3K	1.64	−0.75	−1.49	−1.25	−1.21
Map2k1	PH_mM_0006215	Mitogen-activated protein kinase kinase 1	1.76	−0.53	−1.00	−0.81	−1.06
Pik3cd	PH_mM_0001034	Phosphatidylinositol 3-kinase catalytic delta polypeptide. PI3K	1.42	−0.27	−2.08	−0.74	−0.96

[a]Fold change. The intensity ratio of probe signal criteria for differential expressions was defined as a twofold change (up or down) ($\log_2$ FC ≥ 1 or ≤ -1) in gene expression compared with virus control group and a P value less than 0.05 in at least one time point as a minimum requirement to select. For instance, $\log_2$ (M/N) ≥ 1 means that the comparison between normal control group and virus control group was scattered, indicating that a large number of genes in virus control group were up-regulated in response to H1N1 infection. $\log_2$ (SH/M) ≤ -1, $\log_2$ (SM/M) ≤ -1, $\log_2$ (SL/M) ≤ -1, and $\log_2$ (Oseltamivir/M) ≤ -1 means that down-regulation in gene expression attributable to the high-dose SFXF group treatment, medium-dose group SFXF treatment, low-dose SFXF group treatment and Oseltamivir group treatment was done by comparing genes in virus control group, respectively (P value data not shown).

Table 5: Genes associated with effector T cells activation and cytokines involved in T-cell-mediated immunity.

symbol	GenBank accession	Gene description	$\log_2$ FC[a]				
			M/N	SH/M	SM/M	SL/M	Oseltamivir/M
Gzmb	PH_mM_0001308	Granzyme B	4.36	1.17	−4.79	−0.13	−1.54
Prf1	mMC017608	Perforin 1	2.43	0.31	−2.71	−0.55	−1.55
Fas	mMC008894	Tumor necrosis factor receptor superfamily member 6	1.70	−1.13	−1.83	−0.88	−1.70
FasL	mMC013655	Fas ligand	1.91	−1.49	−2.13	−0.08	−1.07
Il4	PH_mM_0000958	Interleukin 4, IL-4	5.43	−1.00	−5.19	−1.33	−2.64
Ifng	PH_mM_0001407	Interferon-gamma, IFN-γ	−1.02	1.28	1.23	1.38	1.35

[a]The intensity ratio of probe signal criteria for differential expressions was defined as a twofold change (up or down) ($\log_2$ ratio ≥ 1 or ≤ -1) in gene expression compared with virus control group and a P value less than 0.05 in at least one time point as a minimum requirement to select. For instance, $\log_2$ (M/N) ≥ 1 means that the comparison between normal control group and virus control group was scattered, indicating that a large number of genes in virus control group were up-regulated in response to H1N1 infection. $\log_2$ (SH/M) ≤ -1, $\log_2$ (SM/M) ≤ -1, $\log_2$ (SL/M) ≤ -1, and $\log_2$ (Oseltamivir/M) ≤ -1 means that down-regulation in gene expression attributable to the high-dose SFXF group treatment, medium-dose SFXF group treatment, low-dose SFXF group treatment, and Oseltamivir group treatment was done by comparing genes in virus control group, respectively (P value data not shown).

[8]. MyD88 is crucial for Th1 cell responses against primary IVA infection [9]. JNK is required for polarized differentiation of T-helper cells into Th1 cells. TCR-activated p38α and p38β are important and redundant positive regulators of T-cell proliferation and Th skewing [10]. Once infected with influenza virus, proinflammatory cytokines are released from airway epithelial cells to trigger inflammatory responses, as the body's first line of defense against infection or injury. Otherwise, overexpression of cytokine storms in the host can cause significant pathology and ultimately death. In the present study, overexpression of cytokines, including TNF-α (*Tnf*), IL-1β (*Il1b*), IL-8 (*Cxcr2*), and RANTES (*Ccl5*), led to inflammation-induced tissue pathology in virus control group. SFXF in medium-dose significantly decreased the

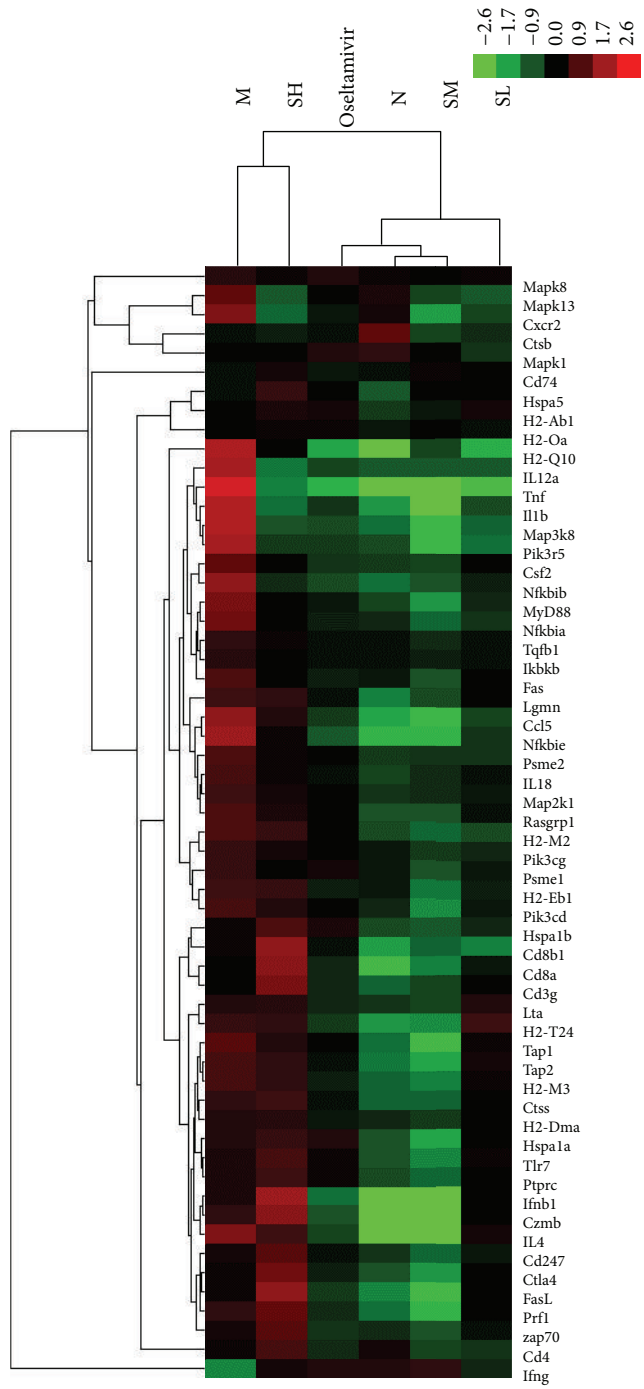

Figure 2: Two-way hierarchical clustering of selected genes in T cell recognition, activation, and proliferation activities was performed to visualize the correlations among the replicates and varying sample conditions. Up- and downregulated genes are represented in red and green colors, respectively. From left to right are virus control group, high-dose SFXF group, Oseltamivir group, normal control group, medium-dose SFXF group, and low-dose SFXF group.

TLR7, MyD88, p38, JNK, TNF-α, IL-1β, IL-8, and RANTES mRNA expression ($P < 0.05$ or $P < 0.01$), compared with the virus control group. The medium-dose SFXF may provide evidence that pathway-specific in Toll-like inhibition is possible. SFXF formula may prevent the overexuberant activation of cytokines, contribute to the resolution of inflammation, and inhibit inflammatory immunopathogenesis from influenza-induced injury.

Following infection with H1N1, viral proteins were synthesized in the infected cell for the virus control group. The significantly changed genes after the medium-dose SFXF administration were that a total of 13 genes (*Tap1*, *Tap2*,

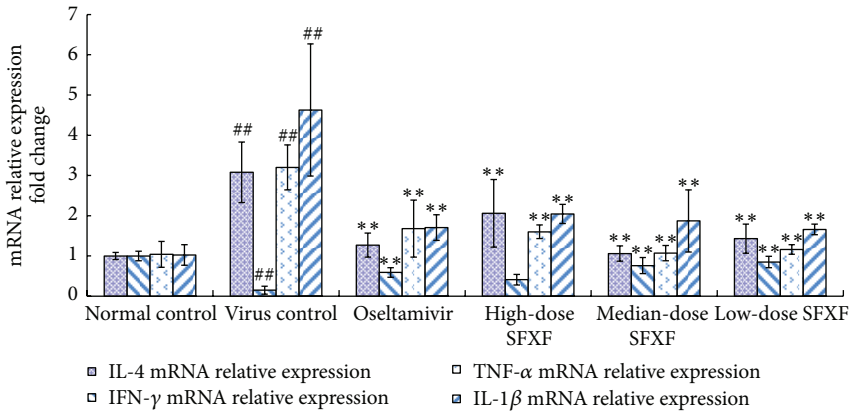

(a)

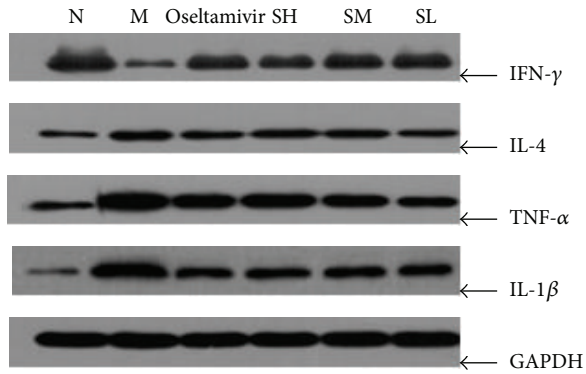

(b)

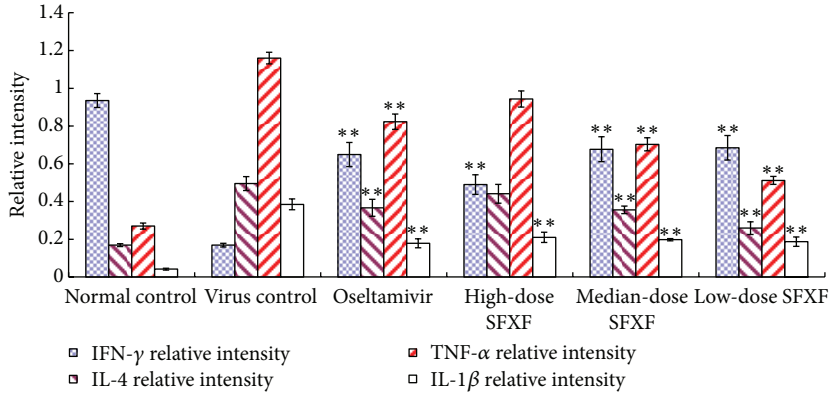

(c)

Figure 3: Mice were anesthetized and then infected intranasally by dropping 0.05 mL of influenza virus suspension ($4LD_{50}$) except normal control group. High-dose SFXF (3.76 mg/kg), medium-dose SFXF (1.88 mg/kg), low-dose SFXF (0.94 mg/kg), or Oseltamivir (11.375 mg/kg) was administrated daily starting at 2 hours before the first viral infection until 4 days post-infection (4 dpi). Then total RNA was isolated from lung tissues of normal control, virus control, and Oseltamivir- and SFXF-treated mice and was analyzed by real-time PCR and western immunoblotting. (a) Relative quantification of the IL-4, IFN-γ, TNF-α, and IL-1β mRNA expressed in the mice lung tissue of six groups, with 12 mice in each group. The quantity of mouse IL-4, IFN-γ, TNF-α, and IL-1β mRNA expression was normalized to the mRNA expression of mouse GAPDH (a housekeeping gene). The quantities are shown as mean ± standard deviation (SD) and two indicated groups as determined by the Newman-Keuls multiple comparison test following one-way ANOVA. Compared with the normal control group: $^{\#\#}P < 0.01$ and compared with the virus control group: $^{*}P < 0.05$, $^{**}P < 0.01$. (b) Western immunoblottings of IL-4, IFN-γ, TNF-α, and IL-1β protein expressions in the mice lung tissue of six groups, with 12 mice in each group. In normal control group, mice were blank and not infected with H1N1 virus (N). Mice were infected with H1N1 virus but not treated with any drugs (M). And mice were infected with H1N1 virus with treatment of high-dose SFXF (SH), medium-dose SFXF (SM), low-dose SFXF (SL), and Oseltamivir. The total gray value of each band was determined using ECL reagents and IPP software. (c) Western immunoblottings of relative quantification of IL-4, IFN-γ, TNF-α, and IL-1β protein levels. The relative intensity data were shown as the ratios of the target gene intensity to GAPDH intensity. Data shown were the mean ± SD of three independent experiments. $^{*}P < 0.05$ and $^{**}P < 0.01$ versus the virus control group (virus only).

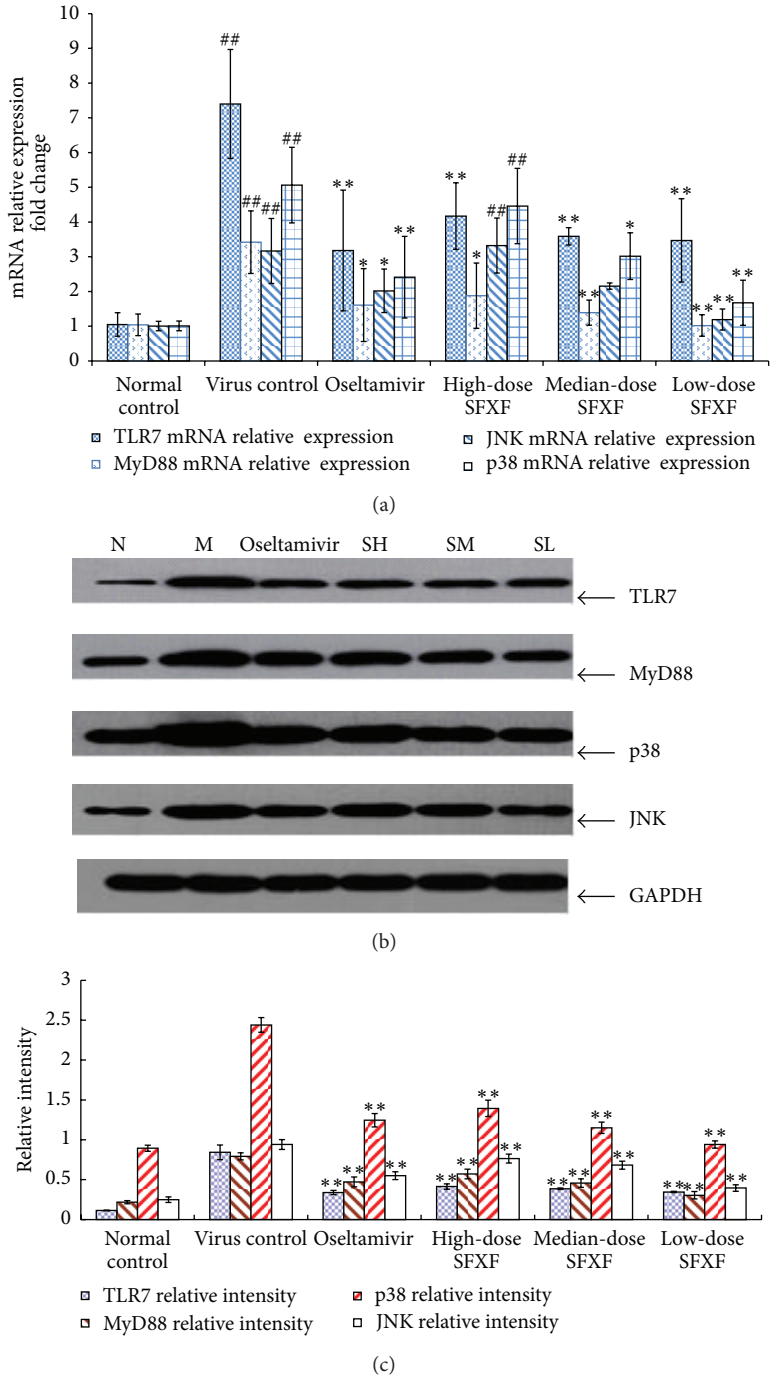

Figure 4: Mice were anesthetized and then infected intranasally by dropping 0.05 mL of influenza virus suspension ($4LD_{50}$) except normal control group. High-dose SFXF (3.76 mg/kg), medium-dose SFXF (1.88 mg/kg), low-dose SFXF (0.94 mg/kg), or Oseltamivir (11.375 mg/kg) was administrated daily starting at 2 hours before the first viral infection until 4 days post-infection (4 dpi). Then total RNA was isolated from lung tissues of normal control, virus control, and Oseltamivir- and SFXF-treated mice and was analyzed by real-time PCR and western immunoblotting. (a) Relative quantification of the TLR7, MyD88, JNK, and p38 mRNA expressed in the mice lung tissue of six groups, with 12 mice in each group. The quantity of mouse TLR7, MyD88, JNK, and p38 mRNA expression was normalized to the mRNA expression of mouse GAPDH (a housekeeping gene). The quantities are shown as mean ± standard deviation (SD) and two indicated groups as determined by the Newman-Keuls multiple comparison test following one-way ANOVA. Compared with the normal control group: $^{\#\#}P < 0.01$ and compared with the virus control group: $^{*}P < 0.05$, $^{**}P < 0.01$. (b) Western immunoblottings of TLR7, MyD88, JNK, and p38 protein expressions in the mice lung tissue of six groups, with 12 mice in each group. In normal control group, mice were blank and not infected with H1N1 virus (N). Mice were infected with H1N1 virus but not treated with any drugs (M). And mice were infected with H1N1 virus with treatment of high-dose SFXF (SH), medium-dose SFXF (SM), low-dose SFXF (SL), and Oseltamivir. The total gray value of each band was determined using ECL reagents and IPP software. (c) Western immunoblottings of relative quantification of TLR7, MyD88, JNK, and p38 protein levels. The relative intensity data were shown as the ratios of the target gene intensity to GAPDH intensity. Data shown were the mean ± SD of three independent experiments. $^{*}P < 0.05$ and $^{**}P < 0.01$ versus the virus control group (virus only).

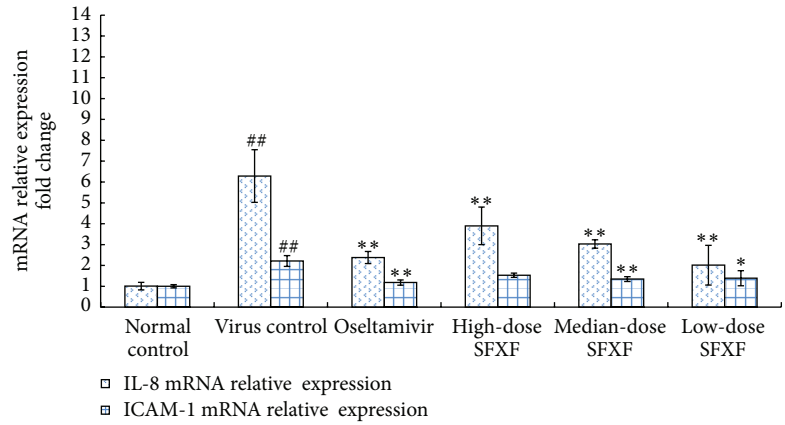

Figure 5: Mice were anesthetized and then infected intranasally by dropping 0.05 mL of influenza virus suspension ($4LD_{50}$) except normal control group. High-dose SFXF (3.76 mg/kg), medium-dose SFXF (1.88 mg/kg), low-dose SFXF (0.94 mg/kg), or Oseltamivir (11.375 mg/kg) was administrated daily starting at 2 hours before the first viral infection until 4 days postinfection (4 dpi). Then total RNA was isolated from lung tissues of normal control, virus control, and Oseltamivir- and SFXF-treated mice and was analyzed by real-time PCR. Relative quantification of the IL-8 and RANTES mRNA had expressions in the mice lung tissue of six groups, with 12 mice in each group. The quantity of mouse IL-8 and RANTES mRNA expression was normalized to the mRNA expression of mouse GAPDH (a housekeeping gene). The quantities are shown as mean ± standard deviation (SD) and two indicated groups as determined by the Newman-Keuls multiple comparison test following one-way ANOVA. Compared with the normal control group: $^{\#\#}P < 0.01$ and compared with the virus control group: $^{*}P < 0.05$, $^{**}P < 0.01$.

Hspa1a, *Hspa1b*, *H2-M2*, *H2-M3*, *H2-Q10*, *Lta*, *Psme1*, *H2-T24*, *Psme2*, *Cd8a,* and *Cd8b1*) were belonging to pathway of MHC-I antigen processing and presentation. The processing of antigens is regulated by two distinct pathways, one requiring PA28 and the other hsp70 [11]. Heterodimer of PA28a (*Psme1*) and PA28b (*Psme2*) induced by membrane Lta (*Lta*) results in proteolysis of intracellular proteins to generate class I binding peptides. Hsp70 (*Hspa1a*, *Hspa1b*) is an effective molecular stimulator in the induction of CD8 T cells to inhibit influenza virus ribonucleoprotein (RNP) complex [12]. Then Tap1 (*Tap1*) and Tap2 (*Tap2*), as transporters of antigenic peptides, together select and pump cytosolic peptides into the lumen of endoplasmic reticulum, where major histocompatibility complex I (MHC- I) genes (*H2-M2*, *H2-M3*, *H2-Q10,* and *H2-T24*) were upregulated. Binding of peptide stabilizes the class I molecule and facilitates its transport to the cell surface. CD8 (*CD8b1* and *Cd8a*) recognizes the virus-specific peptides presented by class I molecules.

The alteration of 5 genes (*Ctss*, *H2-Dma*, *Lgmn*, *H2-Eb1,* and *Cd4*) in MHC-II-associated pathway by the medium-dose SFXF treatment could potentially prevent virus attachment against viral infection, before virus could replicate and cause infection in host cells. Nayak et al. suggested that the characteristics of the CD4 T cell repertoire to any given pathogen, such as influenza, may be highly dependent on the array of MHC class II molecules in a given individual [13]. In our study, major histocompatibility complex II (MHC-II) genes (*H2-Oa*, *H2-Dma*, *H2-Eb1,* and *H2-Ab1*) were significantly upregulated in response to H1N1 infection. Lgmn (*AEP*) has a pivotal role to degrade the endocytosed antigens in the endosomal/lysosomal degradation system. And AEP −/− mice are unable to generate a strong anti-influenza A virus (IAV) response, as TLR7 requires a proteolytic cleavage by AEP to generate a C-terminal fragment competent for signaling [8]. Thus, SFXF may offer new therapeutic potential through AEP activity for targeting TLR7-dependent inflammatory diseases. Class II molecules are synthesized in the endoplasmic reticulum (ER) and bind the invariant chain (*Cd74*). Major histocompatibility complex class II-associated invariant chain is transported to the trans-Golgi, where cellular proteinases including cathepsins B, S (*Ctsb* and *Ctss*) cleave the invariant chain to produce a shorter, residual peptide called corticotrophin-like intermediate lobe peptide (CLIP) (*Cd74*). Then removal of CLIP by HLA-DM (*H2-Dma*) allows endocytically processed peptides to bind and stabilize the MHC proteins. The peptide-MHC class II is transported to the cell surface and recognized by CD4 T cells (*CD4*).

Fourteen genes (including *Ctla4*, *Cd247*, *Ptprc*, *Rasgrp1*, *Mapk1*, *Map3k8*, *Nfkbie*, *Nfkbib*, *Nfkbia*, *Zap70*, *Pik3r5*, *Pik3cg*, *Map2k1,* and *Pik3cd*) were downregulated by medium-dose SFXF treatment. Recognition of peptide-MHC complex by the TCR is the first signal for activation of T cell. The second signal is closely associated with CD28/CTLA-4 costimulatory pathway. Interestingly, we found that CTLA4 (*Ctla4*) expression from lung tissue of H1N1 increased 1.59-fold, but no significant difference was detected for CD28 expression. Our data was consistent with some previous studies as below. First, Ayukawa and others found that the percentages of intracellular CTLA-4-positive CD4 T cells in the patients with influenza virus infection were significantly higher than those in the healthy ($P < 0.01$) [14]. Second, Bour-Jordan and colleagues suggested that CTLA-4 had a critical role in stabilization by increasing the strength of signaling through the T cell receptor [15]. Third, Schneider's finding showed that CTLA-4 increased T cell motility and overrided the T cell receptor (TCR) induced stop signal required for stable conjugate formation between T cells and

antigen-presenting cells [16]. For cytoplasmic signaling, the TCR-induced increase in tyrosine phosphorylation of the TCR zeta-chains (*CD247*) via CD45 (*Ptprc*) can recruit and activate the protein-tyrosine kinase ZAP-70 (*Zap70*), which mediates the downstream signaling cascades. Ras (*Rasgrp1*)/MEK (*Map2k1*)/ERK (*Mapk1*)/MAPK pathway, PI3 K (*Pik3r5*, *Pik3cg* and *Pik3cd*)/Akt signaling pathway, and IKK (*Nfkbie*, *Nfkbib* and *Nfkbia*)/NF-κB signaling pathway then induced the expression of genes involved in the signal transduction of T cell activation in this study. In addition, in IKK/NF-κB signaling pathway, it is recently reported that NS1 is also able to interact with IKKβ and also impairs IκBα phosphorylation and consequent translocation of NF-κB dimers to the nucleus [17]. TLR engagement can control IKK activation for type I IFNs induction [18]. IκBβ acts through p65 : c-Rel dimers to maintain prolonged expression of TNFα [19]. IkBε itself is upregulated at the mRNA level by TNF, whose overexpression is a feature of inflammatory disease [20]. This observation in our study, together with previous studies, may represent a mechanism of contributing to the activation of type I IFNs and TNF-α during infection and inflammatory response.

Then these signalings translocate to the nucleus and make effector T cells activate and proliferate. CTLs maturated from CD8 precursor T-cell can kill target cells by releasing perforins (*Prf1*) and granzymes (*Gzmb*). Meanwhile, CTLs induce apoptosis by triggering the Fas death receptor (*Fas*) on the surface of the target cells and binding to the Fas ligand (*Fasl*). In our study, we indicated that the notable genes in these significantly changed networks were *Gzmb* and *Tnf,* exhibiting 4.79- and 5.03-fold decreased expression exposed to the treatment of the medium-dose SFXF, respectively. As SFXF might have a role in lung tissue repair, it might protect the lung from host or virus-mediated damage. Cell deaths in these two mechanisms are within 4–6 hours. CTLs rely on the binding of TNF-α (*Tnf*) and its receptor to induce apoptosis in 18 hours.

A significant role for CD4 T cell in cross-protection may be supporting and enhancing CTL responses and memory cells, as well as providing help for B-cell responses via cytokine secretion [21, 22]. CD4 T cells can be divided into two different subsets, designated as Th1 and Th2 cells, which are based on the distinct lymphokine expression. IL-4 produced by Th2 cells is required for B cell proliferation and activates enzymes and molecules correlated with CD8+ cytotoxic T cells. IFN-γ made by Th1 cells is performed for clonal expansion of the antigen-specific T cells. So mRNA expression of either IFN-γ or IL-4 is evaluated in terms of Th1 and Th2 differentiation from naïve cells. The balance between Th1 and Th2 cytokine is required for the protection against influenza virus [23]. Recent reports indicated that influenza virus A infection led to Th2-biased immunity by enzyme-linked immunosorbent assay (ELISA) [24]. In our study, influenza virus infection caused Th2 polarization, too. Compared with normal control group, the expressions of IFN-γ mRNA and protein were significantly downregulated in virus control group, while those of IL-4 were markedly upregulated (all $P < 0.05$). The medium-dose SFXF may induce a decrease in the Th2 products with the Th1/Th2 balance and a shift from Th2 to Th1 response. After treatment of the medium-dose SFXF, all cytokines were turned to baseline levels. There was no statistical difference from the medium-dose SFXF and Oseltamivir.

Before this study, based on the guidelines issued by the Chinese Ministry of Health, the data of pyretic patients in fever clinic of Chinese-Japanese Friendship Hospital were collected by rapid influenza diagnostic tests (RIDT) from February to April, 2012. Clinical trials of this herbal granule had demonstrated its efficacy on reducing the duration of fever in patients with influenza A (H3N2) virus infection. Efficacy of a Chinese medicine granule, Shu-Feng-Xuan-Fei, had been demonstrated in reducing the duration of fever among patients with influenza A (H3N2) virus [4]. In our previous experiments *in vivo*, we treated mice with SFXF and Oseltamivir therapy for 4 consecutive days following infection with H1N1. SFXF had also been found efficacious in reducing lung index and pathological lesion (especially for inflammation severity). In three groups of SFXF from high-dose to low-dose, inhibition ratios of pulmonary-index were 15.66%, 33.31%, and 29.76%, respectively. Meanwhile, with histopathologic analyses of lung tissue of mice in virus control group, alveolar walls were diminished and infiltrated by a large number of lymphocytes, monocytes, and neutrophils. The medium-dose SFXF, as well as the Oseltamivir group, had little infiltration of inflammatory cells and tended to have mostly recovered from the primary influenza infection [25]. Moreover, we focused on innate immune response and screened for genes associated with natural killer (NK) cell mediated cytotoxicity in pneumonia mice infected with influenza virus and regulation of SFXF granules in variant doses. NK cells were activated without MHC molecules restricted early in the viral infection and later were taken over by CTLs. Apart from gene coexpression network in the high-dose and the low-dose SFXF, the medium-dose SFXF expressed extra differential genes which the high and the low did not [26]. After treatment of the medium-dose SFXF, main variants had turned to baseline levels, which showed no statistical difference from Oseltamivir. Together with them, the regulation of SFXF granules in medium-dose was the best choice for antivirus treatment in all doses of SFXF. Large amount of Chinese traditional in the high-dose SFXF medicine may delay the pharmaceutic absorption or increase toxicosis in adverse effect. Insufficient curative effect had made the low-dose SFXF undesirable to defend against viral infection.

The major ingredients of SFXF granules are based upon classical Yin-Qiao-San formula, which had been reported that could reduce time to fever resolution in patients with H1N1 influenza virus infection. Following the guidance of monarch, minister, assistant, and guide principle in basic theory of tradition Chinese medicine, the constructions of prescription are divided into principal agents and secondary agents. As principal agents in SFXF granules, indigowoad root, fructus forsythiae, as well as other single Chinese herbs, contain flavonoids, volatile oil, and agglutinin that can lead to a corresponding inhibition of the release of virus particles from infected cells, prevent influenza virus-induced deaths, and regulate immune system [27–29]. Treatment with

classical herb couple of flos lonicerae and fructus forsythiae preparations with an absorption enhancer can prevent MDCK damage after influenza virus propagation [30]. Scutellaria baicalensis inhibits the replication of influenza virus H3N2 at least partly by inhibiting the fusion of viral envelopes with the endosome/lysosome membrane [31]. Monomer from folium isatidis can reduce lung index, pulmonary pathology, and hemagglutination titers over the course of influenza virus [32].

In summary, influenza virus entered and replicates in the host target cell. T cells recognized viral-specific peptides presented by MHC molecules then differentiated, proliferated, and exerted cell-mediated cytotoxic function by CTLs against influenza antigens. So the genes associated with T cell mediated activation, differentiation to CD4 and CD8 T cells, and cytotoxicity in influenza virus infection were almost upregulated, but SFXF granules could down-regulate these genes. The mechanism could be through the reduction of influenza infected cells and activation of T cells. This immunomodulation effects could be realized by regulating gene expressions of T cells activation. Viral replication was found to have been prevented and the viral infection was eliminated with exposure to SFXF granules. Thus, SFXF could help to restore a balance of the host immune system, which may be critical for viral clearance in early phase of influenza virus infection. Further studies are warranted.

5. Conclusion

Recently, DNA microarray analysis has been widely used in detecting the characterization of complex molecular responses in host cells following infection by H1N1 virus. We obtained whole spectrum of gene expression, important bioactivities, and the potential applications of SFXF to regulate T cell-mediated immunity in the treatment of pneumonia infected with influenza virus. Taken together, these results suggested that viral replication was prevented and the viral infection was eliminated because of exposure to SFXF granules. The mechanism could be that the reduction of influenza infected cells and T cells activation were in treatment with SFXF granules. SFXF treatment may induce immunomodulation by regulating gene expressions of T cells activation. Thus, SFXF could help to restore a balance of the host immune system, which may be critical for viral clearance in early phase of influenza virus infection.

Conflict of Interests

The authors declare that there is no conflict of interests regarding the publication of the paper.

Acknowledgment

This research was financially supported by the National Natural Science Foundation of China (Grant no. 81173371).

References

[1] E. A. Govorkova, B. M. Marathe, A. Prevost, J. E. Rehg, and R. G. Webster, "Assessment of the efficacy of the neuraminidase inhibitor oseltamivir against 2009 pandemic H1N1 influenza virus in ferrets," *Antiviral Research*, vol. 91, no. 2, pp. 81–88, 2011.

[2] M. Barbara, V. P. Karolien, V. Veronique, E. Vermeire, and S. Coenen, "The value of neuraminidase inhibitors for the prevention and treatment of seasonal influenza: a systematic review of systematic reviews," *PLoS ONE*, vol. 8, no. 4, Article ID e60348, 2013.

[3] C. Wang, B. Cao, Q. Q. Liu et al., "Oseltamivir compared with the Chinese traditional therapy maxingshigan-yinqiaosan in the treatment of H1N1 influenza: a randomized trial," *Annals of Internal Medicine*, vol. 155, no. 4, pp. 217–225, 2011.

[4] Y. F. Luo, "Clinical research of professor CHAO En-xiang's experience in treating flu with Chinese herbs," *Beijing Journal of Traditional Chinese Medicine*, vol. 31, no. 11, pp. 836–839, 2012.

[5] L. J. Reed and H. J. Muench, "A simple method of estimating fifty per cent endpoints," *The American Journal of Epidemiology*, vol. 27, no. 3, pp. 493–497, 1938.

[6] T. D. Schmittgen and K. J. Livak, "Analyzing real-time PCR data by the comparative C(T) method," *Nature Protocols*, vol. 3, no. 6, pp. 1101–1108, 2008.

[7] M. Michaelis, J. Geiler, P. Naczk et al., "Glycyrrhizin exerts antioxidative effects in H5N1 influenza A virus-infected cells and inhibits virus replication and pro-inflammatory gene expression," *PLoS ONE*, vol. 6, no. 5, Article ID e19705, 2011.

[8] S. Maschalidi, S. Hässler, F. Blanc et al., "Asparagine endopeptidase controls anti-influenza virus immune responses through TLR7 activation," *PLoS Pathogens*, vol. 8, no. 8, Article ID e1002841, 2012.

[9] S. U. Seo, H. J. Kwon, J. H. Song et al., "MyD88 signaling is indispensable for primary influenza A virus infection but dispensable for secondary infection," *Journal of Virology*, vol. 84, no. 24, pp. 12713–12722, 2010.

[10] L. Jirmanova, M. L. G. Torchia, N. D. Sarma, P. R. Mittelstadt, and J. D. Ashwell, "Lack of the T cell-specific alternative p38 activation pathway reduces autoimmunity and inflammation," *Blood*, vol. 118, no. 12, pp. 3280–3289, 2011.

[11] T. Yamano, S. Murata, N. Shimbara et al., "Two distinct pathways mediated by PA28 and hsp90 in major histocompatibility complex class I antigen processing," *Journal of Experimental Medicine*, vol. 196, no. 2, pp. 185–196, 2002.

[12] G. Li, J. Zhang, X. Tong, W. Liu, and X. Ye, "Heat shock protein 70 inhibits the activity of influenza a virus ribonucleoprotein and blocks the replication of virus in vitro and in vivo," *PLoS ONE*, vol. 6, no. 2, Article ID e16546, 2011.

[13] J. L. Nayak, K. A. Richards, F. A. Chaves, and A. J. Sant, "Analyses of the specificity of CD4 T cells during the primary immune response to influenza virus reveals dramatic MHC-linked asymmetries in reactivity to individual viral proteins," *Viral Immunology*, vol. 23, no. 2, pp. 169–180, 2010.

[14] H. Ayukawa, T. Matsubara, M. Kaneko, M. Hasegawa, T. Ichiyama, and S. Furukawa, "Expression of CTLA-4 (CD152) in peripheral blood T cells of children with influenza virus infection including encephalopathy in comparison with respiratory syncytial virus infection," *Clinical and Experimental Immunology*, vol. 137, no. 1, pp. 151–155, 2004.

[15] H. Bour-Jordan, J. L. Grogan, Q. Tang, J. A. Auger, R. M. Locksley, and J. A. Bluestone, "CTLA-4 regulates the requirement for cytokine-induced signals in T(H)2 lineage commitment," *Nature Immunology*, vol. 4, no. 2, pp. 182–188, 2003.

[16] H. Schneider, J. Downey, A. Smith et al., "Reversal of the TCR stop signal by CTLA-4," *Science*, vol. 313, no. 5795, pp. 1972–1975, 2006.

[17] S. Gao, L. Song, J. Li et al., "Influenza A virus-encoded NS1 virulence factor protein inhibits innate immune response by targeting IKK," *Cellular Microbiology*, vol. 14, no. 12, pp. 1849–1866, 2012.

[18] K. Gotoh, Y. Tanaka, A. Nishikimi et al., "Selective control of type I IFN induction by the Rac activator DOCK2 during TLR-mediated plasmacytoid dendritic cell activation," *Journal of Experimental Medicine*, vol. 207, no. 4, pp. 721–730, 2010.

[19] P. Rao, M. S. Hayden, M. Long et al., "IκBβ acts to inhibit and activate gene expression during the inflammatory response," *Nature*, vol. 466, no. 7310, pp. 1115–1119, 2010.

[20] J. M. Clark, K. Aleksiyadis, A. Martin et al., "Inhibitor of κ B epsilon (IκBε) is a non-redundant regulator of c-Rel-dependent gene expression in murine T and B cells," *PLoS ONE*, vol. 6, no. 9, Article ID e24504, 2011.

[21] D. Mucida, M. M. Husain, S. Muroi et al., "Transcriptional reprogramming of mature $CD4^+$ helper T cells generates distinct MHC class II-restricted cytotoxic T lymphocytes," *Nature Immunology*, vol. 14, no. 3, pp. 281–289, 2013.

[22] A. Sundararajan, L. Huan, K. A. Richards et al., "Host differences in influenza-specific CD4 T cell and B cell responses are modulated by viral strain and route of immunization," *PLoS ONE*, vol. 7, no. 3, Article ID e34377, 2012.

[23] S. R. Kumar, S. M. S. Khader, T. K. Kiener, M. Szyporta, and J. Kwang, "Intranasal immunization of baculovirus displayed hemagglutinin confers complete protection against mouse adapted highly pathogenic H7N7 reassortant influenza virus," *PLoS ONE*, vol. 8, no. 6, Article ID e63856, 2013.

[24] X. Gu, P. Li, H. Liu, N. Li, S. Li, and T. Sakuma, "The effect of influenza virus A on th1/th2 balance and alveolar fluid clearance in pregnant rats," *Experimental Lung Research*, vol. 37, no. 7, pp. 445–451, 2011.

[25] Q. Liu, L. G. Gu, N. N. Lu et al., "Protection effect of Shu Feng Xuan Fei Formula and Jie Biao Qing Li Formula on lung injury of mice infected with influenza virus," *China Journal of TCM and Pharmacy*, vol. 27, no. 7, pp. 2132–2134, 2013.

[26] N. N. Lu, L. G. Gu, Q. Liu et al., "Screening for genes associated with natural killer cell-mediated cytotoxicity in pneumonia mice infected with influenza virus and regulation of two herbal anti-virus formulas," *Chinese Critical Care Medicine*, vol. 25, no. 6, pp. 322–326, 2013.

[27] P. Sithisarn, M. Michaelis, M. Schubert-Zsilavecz, and J. Cinatl Jr., "Differential antiviral and anti-inflammatory mechanisms of the flavonoids biochanin A and baicalein in H5N1 influenza A virus-infected cells," *Antiviral Research*, vol. 97, no. 1, pp. 41–48, 2013.

[28] S. Liu, J. Yan, J. Xing, F. Song, Z. Liu, and S. Liu, "Characterization of compounds and potential neuraminidase inhibitors from the n-butanol extract of compound indigowoad root granule using ultrafiltration and liquid chromatography-tandem mass spectrometry," *Journal of Pharmaceutical and Biomedical Analysis*, vol. 59, no. 1, pp. 96–101, 2012.

[29] Z. Liu, Z. Q. Yang, and H. Xiao, "Antiviral activity of the effective monomers from folium isatidis against influenza virus in vivo," *Virologica Sinica*, vol. 25, no. 6, pp. 445–451, 2010.

[30] W. Zhou, H. D. Wang, X. X. Zhu et al., "Improvement of intestinal absorption of forsythoside A and chlorogenic acid by different carboxymethyl chitosan and chito-oligosaccharide, application to Flos Lonicerae-Fructus Forsythiae herb couple preparations," *PLoS ONE*, vol. 8, no. 5, Article ID e63348, 2013.

[31] T. Nagai, Y. Suzuki, T. Tomimori, and H. Yamada, "Antiviral activity of plant flavonoid 5,7,4′-trihydroxy-8-methoxyflavone, from the roots of *Scutellaria baicalensis* against influenza A (H3N2) and B virus," *Biological and Pharmaceutical Bulletin*, vol. 18, no. 2, pp. 295–299, 1995.

[32] E. K. Shin, D. H. Kim, H. Lim, H. K. Shin, and J. K. Kim, "The anti-inflammatory effects of a methanolic extract from radix isatidis in murine macrophages and mice," *Inflammation*, vol. 33, no. 2, pp. 110–118, 2010.

Hindawi Publishing Corporation
Evidence-Based Complementary and Alternative Medicine
Volume 2013, Article ID 538673, 5 pages
http://dx.doi.org/10.1155/2013/538673

Research Article

The Drinking Effect of Hydrogen Water on Atopic Dermatitis Induced by *Dermatophagoides farinae* Allergen in NC/Nga Mice

Rosa Mistica C. Ignacio,[1] Hyun-Suk Kwak,[2] Young-Uk Yun,[2] Ma. Easter Joy V. Sajo,[1] Yang-Suk Yoon,[1] Cheol-Su Kim,[3] Soo-Ki Kim,[3] and Kyu-Jae Lee[1]

[1] *Department of Environmental Medical Biology, Wonju College of Medicine, Yonsei University, Wonju, Gangwon 220-701, Republic of Korea*
[2] *ECO Solution Team, Digital Media and Communications R&D Center, Samsung Electronics Co., Ltd., Suwon, Gyeonggi 443-742, Republic of Korea*
[3] *Department of Microbiology, Wonju College of Medicine, Yonsei University, Wonju, Gangwon 220-701, Republic of Korea*

Correspondence should be addressed to Kyu-Jae Lee; medbio9@gmail.com

Received 13 September 2013; Revised 28 October 2013; Accepted 5 November 2013

Academic Editor: KB Harikumar

Hydrogen water (HW) produced by electrolysis of water has characteristics of extremely low oxidation-reduction potential (ORP) value and high dissolved hydrogen (DH). It has been proved to have various beneficial effects including antioxidant and anti-inflammatory effects; however, HW effect on atopic dermatitis (AD), an inflammatory skin disorder, is poorly documented. In the present study, we examined the immunological effect of drinking HW on *Dermatophagoides farinae*-induced AD-like skin in NC/Nga mice. Mice were administered with HW and purified water (PW) for 25 days. We evaluated the serum concentration of pro-inflammatory (TNF-α), Th1 (IFN-γ, IL-2, and IL-12p70), Th2 (IL-4, IL-5, and IL-10), and cytokine expressed by both subsets (GM-CSF) to assess their possible relationship to the severity of AD. The serum levels of cytokines such as IL-10, TNF-α, IL-12p70, and GM-CSF of mice administered with HW was significantly reduced as compared to PW group. The results suggest that HW affects allergic contact dermatitis through modulation of Th1 and Th2 responses in NC/Nga mice. This is the first note on the drinking effect of HW on AD, clinically implying a promising potential remedy for treatment of AD.

1. Introduction

Atopic dermatitis (AD) is an allergic inflammatory skin disorder characterized by impaired immunological responses [1]. AD usually affects 10% to 20% infants and young children, but it can persist into adulthood (1%–3%) since it is often a long-lasting skin disease [2]. AD has a complex etiology involving interrelationship of several factors such as genetic, environmental, pharmacologic, psychological, immunologic and skin barrier dysfunction [3]. The altered immune function received special attention as the major factor contributing to the onset, development, and severity of AD. AD is well characterized by having clinical phenotype such as elevated serum IgE levels, peripheral eosinophilia, and eczematous skin lesions infiltrated by inflammatory cells [4, 5]. NC/Nga mice were the first representative animal model for investigating and developing treatment on AD-like skin disease [6, 7]. In conventional surroundings, NC/Nga mice were observed to spontaneously develop skin lesions characterized by scratching behavior, erythema and hemorrhage, edema, scaling, and dryness of the skin comparable to human AD [6]. Under pathogenic-free surrounding, NC/Nga mouse model does not show skin lesions and thus AD-like symptoms are triggered by exposure to a stimulus. *Dermatophagoides farinae* (Df) is a cosmopolitan species of house dust mites and a common contributory cause of AD. The topical application of this allergen Df extract (DfE) produces atopic dermatitis-like skin lesions in NC/Nga mice [8, 9]. Therefore, we adopted

NC/Nga mouse model exposed with DfE mimicking the pathogenesis of human AD.

Hydrogen molecule has been demonstrated to have excellent antioxidant as well as anti-inflammatory properties. Active hydrogen acts as antioxidant and showed protection of oxidative-induced damage *in vitro* [10]. It has also been reported that it can selectively scavenge reactive oxygen species (ROS) [11] and showed positive influence in cytokine imbalance [12]. Hydrogen is known to easily penetrate the skin, diffuses rapidly into tissues and cells, and distributes in the body through blood flow [13]. H_2 can be incorporated in the body through inhalation of H_2 gas, drinking water with dissolved H_2, and injecting saline with dissolved H_2. HW produced by electrolysis of water is included of the drinking water containing high concentration of hydrogen gas and has properties of high dissolved hydrogen (DH), negative oxidation-reduction potential (ORP) level, and neutral pH. Previous studies on electrolyzed reduced water (ERW) and alkaline reduced water, which are also hydrogen-rich water produced by the same reaction with HW, showed various beneficial effects such as reducing the levels of serum triglyceride and blood glucose in OLEFT diabetic rat model [14, 15], prevention of insulin resistance [16], and liver inflammation [17]. In addition, the oral intake of hydrogen-rich water showed antiallergic effect *in vivo* [18]. However, at present, there is no evidence that drinking water rich in DH provides benefits for patients with AD. Thus, the objective of the study was to examine the drinking effect of hydrogen water (HW) with high DH, low ORP, and neutral pH on AD induced by repeated application with DfE ointment in NC/Nga mice. We might expect drinking HW to complement the topical drugs for AD through modulating the Th1 and Th2 responses.

2. Materials and Methods

2.1. Preparation of Control Water (Purified Water). Purified water (PW) was prepared by using tap water (TW) as source water. The TW was purified by reverse osmosis (RO) process (R/O Membrane Filter, Coway Co. Ltd., Gumi, Republic of Korea). In the RO process, the TW is push against a special semipermeable membrane from the pressure on the waterline that causes the molecular squeezing thereby separating the water molecules from the contaminants. The water molecules then pass through to the inside of the membrane. The R/O Membrane Filter rejects contaminants based on their size and it is equipped with an ultrafiltration pore that has a size around 0.001 μm. PW generated was used as a control water given to positive control (PC) group and it had an ORP value of 292 ± 5 mV, DH of 0.002 ± 0.001 ppm, and a pH of 7.01 ± 0.02.

2.2. Preparation of Test Water (Hydrogen Water). HW was prepared by using PW generated through RO and ultrafiltration. The PW was further processed by water-electrolyzing apparatus (Samsung Highly Reactive Hydrogen Reduced Water Maker, Samsung Electronics Co., Ltd., Korea) and was collected from water tank containing cathode platinum plate. ORP value was controlled to −510 ± 6 mV (HM-21P, TOA Electronics Co., Japan), and DH value was controlled to 0.50 ± 0.02 ppm (DH-35A, DKK-TOA Co., Japan) through electrolysis of water. pH of HW was regulated to 7.30 ± 0.02 through neutralization of OH^- generated during electrolysis in cathode water tank. HW generated was used as a test water given to HW group.

2.3. Animals. Four-week-old male NC/Nga mice weighing 25 ± 2 g were purchased from Orient Bio Inc. (Korea) and were maintained for 1 week prior to experiments. Mice were housed in stainless steel cages in a controlled environment with temperature of 22 ± 2°C and 40–60% humidity under a 12 : 12-hour light-dark cycle. The Animal Use and Care Protocol for this Animal Experiment was approved by the Institutional Animal Care and Use Committee (IACUC) at Wonju Campus, Yonsei University, Gangwon, Wonju, Republic of Korea.

2.4. Induction of Atopic Dermatitis in NC/Nga Mice. AD-like skin lesions in NC/Nga mice were performed using mite antigen as described previously [19]. The hair on the back was shaved with depilatory cream (Veet, Oxy Reckitt Benckiser Ltd., France) 1 day before experiments. The exposed dorsal region was treated with 200 μL with DfE ointment (Biostir-AD, Biostir, Kobe, Japan) prepared from house dust mites, a crude extract allergen of *Dermatophagoides farinae* as described previously [9], twice a week for 3 weeks. NC/Nga mice were randomly assigned to two groups: PW (n = 12) and HW (n = 12). Mice received the last water treatment (water administration) on day 25 and were sacrificed on day 26 to evaluate immunological changes.

2.5. Analysis of Th1, Th2, and Proinflammatory Cytokines. Cytokines secreted in the blood were investigated. Serum concentrations of IL-2, IL-4, IL-5, IL-10, IL-12p70, GM-CSF, TNF-α, and IFN-γ were measured using Multiplex kit (Bio-Rad, San Diego, USA) and run on Luminex technology (Bio-Plex Multiplex Bead Array System, Bio-Rad Hercules, CA, USA) according to the manufacturer's instruction. Raw fluorescence data were analyzed by the software using a 5-parameter logistic method.

2.6. Statistical Analysis. Data values were expressed as the mean ± SEM. The mean values among groups were analyzed and compared by one-way analysis of variance followed by subsequent multiple comparison test (Tukey) with Graph Prism version 5.0 software packages (GraphPad Software, USA). Differences were considered statistically significant at $P < 0.05$, $P < 0.01$, and $P < 0.001$.

3. Results and Discussion

At present, there is no evidence for the drinking effect of HW on AD. Here, we investigated the relationship between drinking HW and AD through examination of various cytokines closely related to AD and examined therapeutic possibility of HW. Repeated application of DfE to NC/Nga mice leads to atopic dermatitis-like skin lesions characterized by impaired immune response. Previous studies have pointed out the importance of Th1 and Th2 cytokines, which are

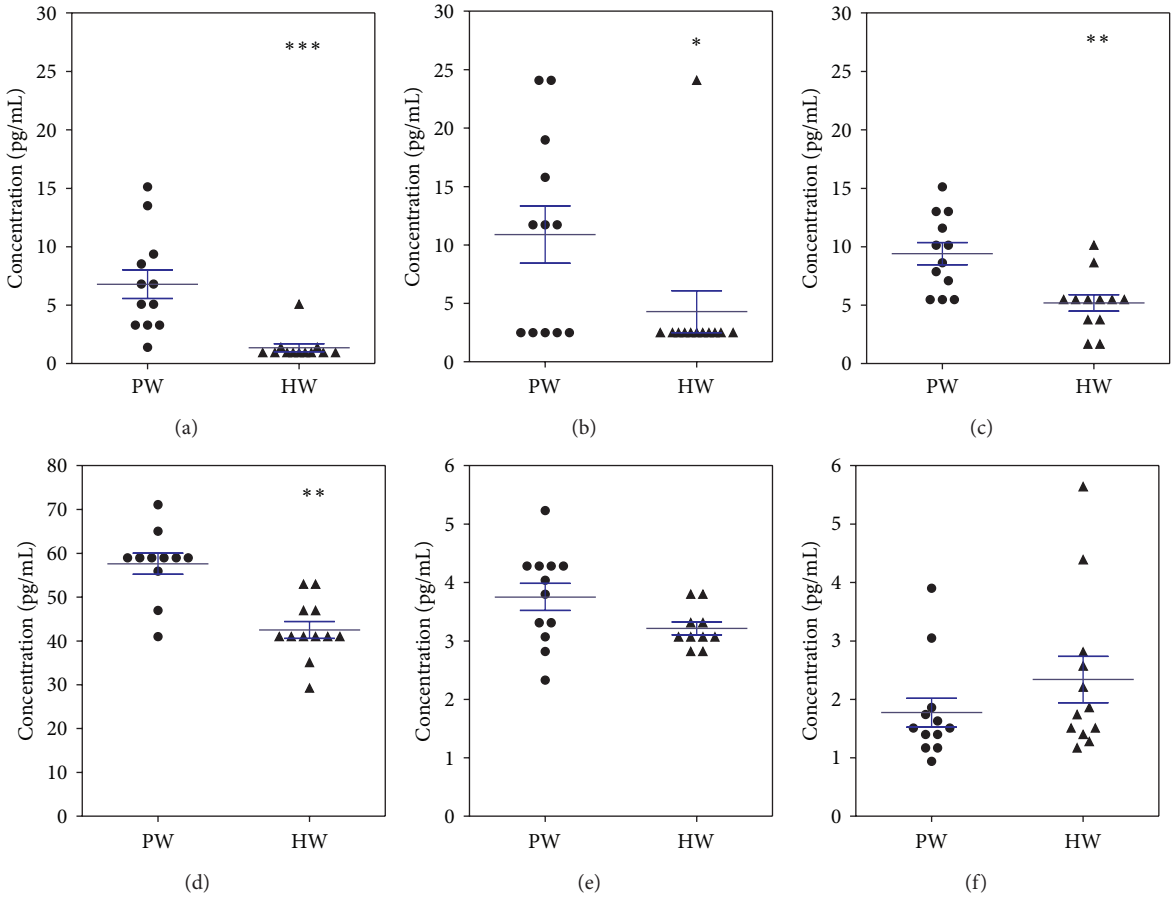

Figure 1: Effect of drinking hydrogen water (HW) on proinflammatory, T helper (Th) 1, and Th2 cytokines. Mice administered with HW significantly decreased *Dermatophargoides farinae* extract had (DfE-)induced cytokines IL-10 (a), GM-CSF (b), IL-12p70 (c) and TNF-α (d) levels. IL-2 (e) and IL-4 (f) did not differ significantly between HW and purified water (PW) groups. Data are mean ± SD, $n = 12$. $^{*}P < 0.05$, $^{**}P < 0.01$, and $^{***}P < 0.001$ indicate significant differences tested with ANOVA. Tukey's test was used for *post hoc* tests.

found to be overexpressed on the skin as means of inflammatory response on experimental models of allergen-induced allergic inflammation in mice [5]. Moreover, after the DfE application, Th1, Th2, and proinflammatory cytokines were increased in concentration as demonstrated by the study of Sung and colleagues [20]. Here, we investigated the effect of drinking HW on serum cytokines (Th1, Th2 and pro-inflammatory) using Luminex-bead array system known for its high sensitivity and precision. The supplementation of HW significantly decreased DfE-induced cytokines IL-10 (Figure 1(a)), GM-CSF (Figure 1(b)), IL-12p70 (Figure 1(c)), and TNF-α (Figure 1(d)) levels. IL-10 produced mainly by Treg cells participates in the immune dysregulation that is characteristic of human AD and IL-10 is suggested that it inhibits cell-mediated immunity, which may account for the reduced allergic contact reactivity in AD cases [21]. IL-10, which is one of the traditional cytokines involved in AD, has been regarded to have a conflicting role. Production of IL-10 by CD4+ T cells varies depending on the severity of AD, fewer on severe AD as compared to mild AD [22]. Thorough understanding of the effect of IL-10 will help in the interpretation of the pathogenesis of AD. As noted by Niwa [23]; plasma levels of IL-10 seem to correlate inversely with the severity of AD. However, increased production of IL-10 has been demonstrated by other studies [21, 24]. T cells stimulated with IL-12 showed induction of IL-10 *in vitro* [25]. The lower level of IL-10 in our study might be correlated with the decreased level of IL-12p70. IL-12, which consists of p35 and p40 subunits, enhances Th1 cytokine production [26]. These results suggest that HW suppresses the development of AD by suppressing the cytokines level. In contrast, levels of IL-2 (Figure 1(e)) and IL-4 (Figure 1(f)) did not differ significantly between HW and PW (control) groups. Additionally, IL-5 and IFN-γ were undetectable in the serum of NC/Nga mice (data not shown). These results could be, in part, explained by the variability in the source of the samples (blood or skin), the time the sample was collected, and also by the different assay methods employed.

The repeated application of the allergen induced the increased production of Th2 cytokines [27]. The supplementation of HW suppressed this cytokine production. The chemical properties of HW that we used in this study are high DH, low ORP, and neutral pH. The abrogating effect of HW on Th1, Th2, and pro-inflammatory cytokines in AD model is

attributable to the rich hydrogen content of HW. As discussed by Xie et al. [28], hydrogen gas has anti-inflammatory properties in zymosan-induced generalized inflammation model partly by reducing the levels of pro-inflammatory cytokines in the serum. In our previous studies related to immunological effect of hydrogen-rich ERW, bathing was found to restore cytokine imbalance in mice model with induced UVB skin injury [12] and drinking ERW ameliorated obesity through restoring adipokine and inflammatory cytokines network [29]. Given these reported data, the beneficial effect of DH in HW might be due, in part, to the anti-inflammatory property of hydrogen [30], such as the downregulation of Th1, Th2, and pro-inflammatory cytokines.

Hydrogen represents an emerging safe and potent medical gas that promises to provide a treatment and preventive control of various diseases. Hydrogen can be administered into the body through drinking water rich in H_2 such as HW, inhaling H_2 gas, injecting saline with dissolved H_2, and taking a hydrogen bath. Among these accepted methods of administration of hydrogen in the body, drinking or oral intake of hydrogen-rich water is the most convenient and suitable for continuous consumption for therapeutic use. Not only hydrogen has anti-inflammatory effects, but also several studies had demonstrated that hydrogen exhibits antioxidative stress effects [11, 13, 30, 31]. Of note, H_2 has several advantages as potential antioxidant since it is mild enough not to disturb any metabolic oxidation-reduction reactions, thus sparing the mammalian cells in initiating defense mechanism leading to the production of ROS [11]. Our HW might be a feasible candidate as antioxidant not only that it has a high DH, also it has low (negative) ORP. "As discussed elsewhere [32]"; decreased ORP means increased reducing capacity. In the water ionizer industry, ORP is equivalent to antioxidant potential, and the negative implies the reduction power of the water. This study is the first to provide evidence for the drinking effect of HW on AD. To uncover the profound mechanism of HW on inflammatory response, further studies targeting signaling pathways and ROS production would be necessary, as AD is a type of oxidative stress-related and inflammatory disease. This study opens a new insight into the new therapeutic and preventive treatment of AD, applying safer fluid such as HW. In addition, our results give attention and advance understanding to those traditional cytokines that could possibly affect the severity of AD. Together these data, although conflicting, suggest that the role of traditional cytokines involved in AD needs to be examined scrupulously and further studies on how HW works on molecular level still await an answer. Lastly, the potential of HW as antioxidant is underway.

4. Conclusions

To conclude, drinking HW suppressed the levels of inflammation-related mediators such as Th1, Th2, and pro-inflammatory cytokines which are number one players in the pathogenesis of human AD. In addition, this study provides a new insight of the relevance of certain cytokines in AD. HW represents a potentially alternative therapeutic and preventive treatment of AD.

Abbreviations

H_2: Molecular hydrogen
AD: Atopic dermatitis
HW: Hydrogen water
Df: *Dermatophargoides farinae*
DfE: Df extract
ORP: Oxidation reduction potential
DH: Dissolved hydrogen
PW: Purified water
TW: Tap water
RO: Reverse osmosis
IACUC: Institutional Animal Care and Use Committee
ERW: Electrolyzed reduced water
ROS: Reactive oxygen species.

Conflict of Interests

The authors declare that there is no conflict of interests.

Acknowledgment

This research was supported by a Grant (YUWCM-2011-17) from Wonju College of Medicine, Yonsei University, Republic of Korea.

References

[1] M. Auriemma, G. Vianale, P. Amerio, and M. Reale, "Cytokines and T cells in atopic dermatitis," *European Cytokine Network*, vol. 24, no. 1, pp. 37–44, 2013.

[2] L. Schneider, S. Tilles, P. Lio et al., "Atopic dermatitis: a practice parameter update 2012," *The Journal of Allergy and Clinical Immunology*, vol. 131, no. 2, pp. 295–299, 2013.

[3] M. Udompataikul and D. Limpa-o-vart, "Comparative trial of 5% dexpanthenol in water-in-oil formulation with 1% hydrocortisone ointment in the treatment of childhood atopic dermatitis: a pilot study," *Journal of Drugs in Dermatology*, vol. 11, no. 3, pp. 366–374, 2012.

[4] D. Y. M. Leung and T. Bieber, "Atopic dermatitis," *The Lancet*, vol. 361, no. 9352, pp. 151–160, 2003.

[5] D. Y. M. Leung, M. Boguniewicz, M. D. Howell, I. Nomura, and Q. A. Hamid, "New insights into atopic dermatitis," *The Journal of Clinical Investigation*, vol. 113, no. 5, pp. 651–657, 2004.

[6] H. Matsuda, N. Watanabe, G. P. Geba et al., "Development of atopic dermatitis-like skin lesion with IgE hyperproduction in NC/Nga mice," *International Immunology*, vol. 9, no. 3, pp. 461–466, 1997.

[7] Y. Y. Sung, Y. S. Kim, and H. K. Kim, "Illicium verum extract inhibits TNF-α- and IFN-γ-induced expression of chemokines and cytokines in human keratinocytes," *Journal of Ethnopharmacology*, vol. 144, no. 1, pp. 182–189, 2012.

[8] H. Matsuoka, N. Maki, S. Yoshida et al., "A mouse model of the atopic eczema/dermatitis syndrome by repeated application of a crude extract of house-dust mite *Dermatophagoides farinae*," *Allergy*, vol. 58, no. 2, pp. 139–145, 2003.

[9] M. Yamamoto, T. Haruna, K. Yasui et al., "A novel atopic dermatitis model induced by topical application with *Dermatophagoides farinae* extract in NC/Nga mice," *Allergology International*, vol. 56, no. 2, pp. 139–148, 2007.

[10] S. Shirahata, Y. Li, T. Hamasaki et al., "Redox regulation by reduced waters as active hydrogen donors and intracellular ROS scavengers for prevention of type 2 diabetes," in *Cell Technology For Cell Products*, E. Smith, Ed., vol. 3, pp. 99–101, 2007.

[11] I. Ohsawa, M. Ishikawa, K. Takahashi et al., "Hydrogen acts as a therapeutic antioxidant by selectively reducing cytotoxic oxygen radicals," *Nature Medicine*, vol. 13, no. 6, pp. 688–694, 2007.

[12] K. S. Yoon, X. Z. Huang, Y. S. Yoon et al., "Histological study on the effect of electrolyzed reduced water-bathing on UVB radiation-induced skin injury in hairless mice," *Biological and Pharmaceutical Bulletin*, vol. 34, no. 11, pp. 1671–1677, 2011.

[13] S. Ohta, "Recent progress toward hydrogen medicine: potential of molecular hydrogen for preventive and therapeutic applications," *Current Pharmaceutical Design*, vol. 17, no. 22, pp. 2241–2252, 2011.

[14] D. Jin, S. H. Ryu, H. W. Kim et al., "Anti-diabetic effects of electrolyzed reduced water on OLEFT rats," *Bioscience, Biotechnolgy, and Biochemistry*, vol. 70, no. 1, pp. 31–37, 2006.

[15] M.-J. Kim and H. K. Kim, "Anti-diabetic effects of electrolyzed reduced water in streptozotocin-induced and genetic diabetic mice," *Life Sciences*, vol. 79, no. 24, pp. 2288–2292, 2006.

[16] S. Kajiyama, G. Hasegawa, M. Asano et al., "Supplementation of hydrogen-rich water improves lipid and glucose metabolism in patients with type 2 diabetes or impaired glucose tolerance," *Nutrition Research*, vol. 28, no. 3, pp. 137–143, 2008.

[17] B. Gharib, S. Hanna, O. M. S. Abdallahi, H. Lepidi, B. Gardette, and M. De Reggi, "Anti-inflammatory properties of molecular hydrogen: Investigation on parasite-induced liver inflammation," *Comptes Rendus de l'Academie des Sciences III*, vol. 324, no. 8, pp. 719–724, 2001.

[18] T. Itoh, Y. Fujita, M. Ito et al., "Molecular hydrogen suppresses FcεRI-mediated signal transduction and prevents degranulation of mast cells," *Biochemical and Biophysical Research Communications*, vol. 389, no. 4, pp. 651–656, 2009.

[19] Y.-Y. Sung, T. Yoon, J. Y. Jang, S.-J. Park, G.-H. Jeong, and H. K. Kim, "Inhibitory effects of Cinnamomum cassia extract on atopic dermatitis-like skin lesions induced by mite antigen in NC/Nga mice," *Journal of Ethnopharmacology*, vol. 133, no. 2, pp. 621–628, 2011.

[20] Y. Y. Sung, W. K. Yang, A. Y. Lee et al., "Topical application of an ethanol extract prepared from *Illicium verum* suppresses atopic dermatitis in NC/Nga mice," *Journal of Ethnopharmacology*, vol. 144, no. 1, pp. 151–159, 2012.

[21] J. D. Ohmen, J. M. Hanifin, B. J. Nickoloff et al., "Overexpression of IL-10 in atopic dermatitis: contrasting cytokine patterns with delayed-type hypersensitivity reactions," *The Journal of Immunology*, vol. 154, no. 4, pp. 1956–1963, 1995.

[22] S. L. Seneviratne, L. Jones, A. S. Bailey, A. P. Black, and G. S. Ogg, "Severe atopic dermatitis is associated with a reduced frequency of IL-10 producing allergen-specific $CD4^+$ T cells," *Clinical and Experimental Dermatology*, vol. 31, no. 5, pp. 689–694, 2006.

[23] Y. Niwa, "Elevated RANTES levels in plasma or skin and decreased plasma IL-10 levels with subsets of patients with severe atopic dermatitis," *Archives of Dermatology*, vol. 136, no. 1, pp. 125–126, 2000.

[24] D. Simon, L. R. Braathen, and H.-U. Simon, "Increased lipopolysaccharide-induced tumour necrosis factor-α, interferon-γ and interleukin-10 production in atopic dermatitis," *British Journal of Dermatology*, vol. 157, no. 3, pp. 583–586, 2007.

[25] Y. Yoshizawa, H. Nomaguchi, S. Izaki, and K. Kitamura, "Serum cytokine levels in atopic dermatitis," *Clinical and Experimental Dermatology*, vol. 27, no. 3, pp. 225–229, 2002.

[26] H. Tanaka, M. Narita, S. Teramoto et al., "Role of interleukin-18 and T-helper type 1 cytokines in the development of *Mycoplasma pneumoniae* pneumonia in adults," *Chest*, vol. 121, no. 5, pp. 1493–1497, 2002.

[27] E. B. Brandt and U. Sivaprasad, "Th2 cytokines and atopic dermatitis," *Journal of Clinical and Cellular Immunology*, vol. 2, no. 3, pp. 1–25, 2011.

[28] K. Xie, Y. Yu, Z. Zhang et al., "Hydrogen gas improves survival rate and organ damage in zymosan-induced generalized inflammation model," *Shock*, vol. 34, no. 5, pp. 495–501, 2010.

[29] R. C. Ignacio, T. Y. Kang, C. S. Kim et al., "Anti-obesity of alkaline reduced water in high fat-fed obese mice," *Biological and Pharmaceutical Bulletin*, vol. 36, no. 7, pp. 1052–1059, 2013.

[30] C.-S. Huang, T. Kawamura, Y. Toyoda, and A. Nakao, "Recent advances in hydrogen research as a therapeutic medical gas," *Free Radical Research*, vol. 44, no. 9, pp. 971–982, 2010.

[31] S. Ohta, "Molecular hydrogen is a novel antioxidant to efficiently reduce oxidative stress with potential for the improvement of mitochondrial diseases," *Biochimica et Biophysica Acta*, vol. 1820, no. 5, pp. 586–594, 2012.

[32] K. C. Nam and D. U. Ahn, "Effects of ascorbic acid and antioxidants on the color of irradiated ground beef," *Journal of Food Science*, vol. 68, no. 5, pp. 1686–1690, 2003.

Hindawi Publishing Corporation
Evidence-Based Complementary and Alternative Medicine
Volume 2013, Article ID 748123, 9 pages
http://dx.doi.org/10.1155/2013/748123

Research Article

Immunosuppression of the Trimellitic Anhydride-Induced Th2 Response by Novel Nonanatural Products Mixture in Mice

Min-Jung Bae,[1,2] Hee Soon Shin,[1] and Dong-Hwa Shon[1]

[1] *Korea Food Research Institute, 1201-62 Anyangpangyo-ro, Bundang-gu, Seognam-si, Kyeonggi-do 463-746, Republic of Korea*
[2] *Institute for Basic Science, School of Biological Sciences, Seoul National University, 599 Gwanak-ro, Gwanak-gu, Seoul 151-742, Republic of Korea*

Correspondence should be addressed to Dong-Hwa Shon; dhs95@kfri.re.kr

Received 29 July 2013; Accepted 26 September 2013

Academic Editor: V. R. Vineesh

Many natural dietary products prevent or cure allergic inflammation; however, the ability of mixtures of these natural medicinals to suppress allergic skin inflammation is unknown. We examined the inhibitory effects of nonanatural products mixture (NPM-9), which provides immunoregulatory activation, on Th2-mediated skin allergic inflammation. Oral administration of NPM-9 in mice reduced ear thickness and specific IgE production in trimellitic anhydride- (TMA-)induced contact hypersensitivity (CHS). NPM-9 also suppressed IL-4 and IL-1β production in splenocytes but prevented only TMA-induced IL-1β production in inflamed ears. To characterize the mechanism of this effect, we examined NPM-9 immunosuppression on an OVA-induced Th2 allergic state. Oral administration of NPM-9 inhibited Th2-mediated serum IgE overproduction. NPM-9 also downregulated the polarized Th2 response, whereas it upregulated Th1 response in splenocytes. These data suggest that NPM-9 may be a useful therapeutic agent for allergic inflammatory diseases through its suppression of the Th2-mediated allergic response.

1. Introduction

Allergic dermatitis (AD) is characterized by allergic skin inflammation. Among the various types of AD, contact dermatitis is induced by an allergic response to a multitude of chemical substances associated with environmental contamination. Dysregulated type 1 helper T cell (Th1) and Th2 responses are pathogenic in allergic dermatitis via Th2 production of IL-4, IL-5, and IL-13 [1, 2]. Th2 cytokines promote mast cell development. Mast cells are key effectors in immunoglobulin (Ig) E-associated Th2-type immune responses because they are activated by cross linking of FcεRI. Allergen-provoked mast cells trigger release of allergic inflammatory mediators including histamine via degranulation [3]. IFN-γ suppresses IgE production by B cells, as well as IL-4 production from Th2 cells [4]. Therefore, the development of dermatitis is thought to be caused primarily by overproduction of Th2-mediated cytokines [5, 6].

Many therapeutic trials have evaluated agents that may modulate dermatitis, but prolonged use of these compounds causes a variety of side effects. Natural herbs, with their improved safety profiles and immune-regulatory effects, have been suggested as alternative therapeutics for the treatment of dermatitis and have been the subject of many studies [7–9]. It is unclear, however, whether natural products function synergistically to produce antiallergic effects on Th2 differentiation-induced contact dermatitis.

We previously investigated the anti-allergic effects of natural product extracts derived from herbs and foods using various methods such as allergen permeation, Th2-related cytokines, and mast cell degranulation (Figure 1). We identified 4 food-derived extracts with high anti-allergenic potential, including black pepper (*Piper nigrum*), green tea (*Camellia sinensis*), turmeric (*Curcuma longa*), and fermented soybean paste (cheonggukjang), as well as herb-derived extracts of licorice (*Glycyrrhiza uralensis*), hawkweed (*Hieracium albiflorum*), beefsteak plant (*Perilla frutescens*), fenugreek (*Trigonella foenum-graecum*), and skullcap (*Scutellariae baicalensis*) (Table 1). Their curative properties have been demonstrated in many studies. Licorice, hawkweed,

Table 1: The activity of food- and herb-derived species.

Sample extract	Scientific name	Division	Relative activity		
			Inhibitory activity on allergen permeation	Inhibitory activity on IL-4 production	Inhibitory activity on degranulation
Licorice	*Glycyrrhiza uralensis*	Herb	+++	+	+
Hawkweed	*Hieracium albiflorum*	Herb	++	++	++
Beefsteak plant	*Perilla frutescens*	Herb	++	++	+
Fenugreek	*Trigonella foenum-graecum*	Herb	++	+++	++
Skullcap	*Scutellariae baicalensis*	Herb	+++	++	++
Black pepper	*Piper nigrum*	Food		++	+++
Green tea	*Camellia sinensis*	Food	+++	+++	++
Turmeric	*Curcuma longa*	Food	+	+	+++
Fermented soybeans paste (cheonggukjang)		Food	++	++	++

+++: very strong; ++: strong; +: mild.

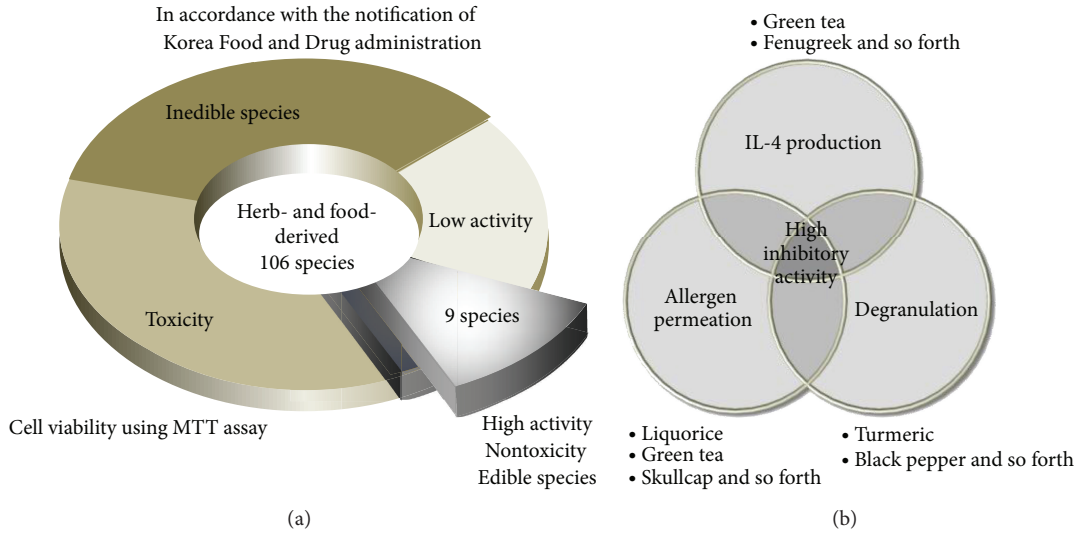

Figure 1: Flowchart representing selected criteria for NPM-9 from food- and herb-derived extracts. (a) The selection of food- and herb-derived species (edible, highly active, and nontoxic). (b) Selected food- and herb-derived species have a potent inhibitory activity against allergen permeation of human epithelial cells, IL-4 production in splenocyte T cells, and degranulation in mast cells.

and skullcap suppress inflammation by regulating immune function in antigen-activated macrophages [10–12]. Beefsteak plant and green tea inhibit mast cell activation by suppressing histamine release and inflammatory cytokine and chemokine production [13–15]. Fenugreek, black pepper, and fermented soybean paste extracts and major constituents may serve as immunoregulatory mediators [16–19]. Turmeric produces an immunomodulatory response by stimulating dendritic cell function [20].

These 9 extracts were mixed to produce an effective treatment for allergic disorders after verifying their efficacy by assessing allergen permeation into the intestinal epithelium, Th2-related cytokine production in splenocytes, and mast cell degranulation. The mixture was named nona natural product mixture (NPM-9) and has been patented in Korea (Patent number 10-1141191).

The aim of this study was to investigate the anti-allergic effect of NPM-9 in trimellitic anhydride- (TMA-) induced contact hypersensitive (CHS) mice.

2. Materials and Methods

2.1. Animals. Female BALB/c mice, weighing 18 to 20 g, were purchased from OrientBio Inc. (Kyeonggi, Korea). The 4-week-old mice were housed in an air-conditioned room (23 ± 2°C) with a 12 h light/dark cycle. They were allowed free access to food and tap water. All animal experiments were performed according to the guidelines for animal use and care at the Korea Food Research Institute.

2.2. Sample Preparation. Herb- and food-derived elements were purchased from Kyungdong Oriental Medicine Market

Table 2: Extraction yield for food- and herb-derived species.

Extraction yield (w/w, %)								
Licorice	Hawkweed	Beefsteak plant	Fenugreek	Skullcap	Black pepper	Green tea	Turmeric	Fermented soybeans paste (cheonggukjang)
21.15	20.22	45.68	17.50	13.50	33.08	30.27	48.47	19.69

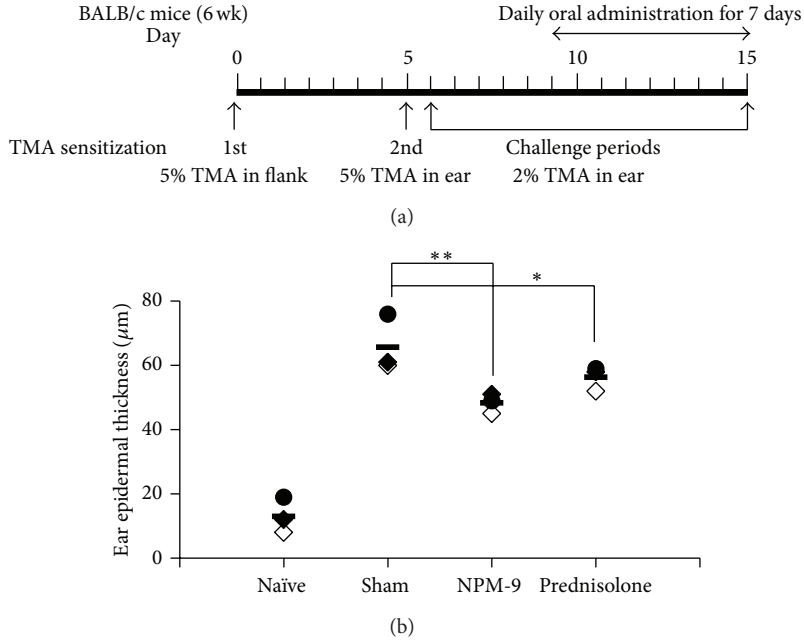

Figure 2: Experimental protocol and ear thickness in TMA-induced CHS mouse model. (a) Experimental protocol. (b) BALB/c mice were divided into naïve, sham (TMA), NPM-9 (250 mg/kg BW), and prednisolone groups (30 mg/kg BW). Ear epidermal thickness was measured by histological analysis (H&E staining). Values are presented as mean ± SD ($n = 4$ in each group). Data were analyzed by ANOVA followed by Student's t test. $^{*}P < 0.05$, $^{**}P < 0.01$, significantly different from the saline value.

(Seoul, Korea) or a local market (Kyeonggi, Korea). Herbals were identified by Professor Y. Bu, Department of Herbal Pharmacology, Kyung Hee University. The specimens have been maintained by the functional materials research group, Korea Food Research Institute. Samples of each product (100 g) were reflux extracted twice in 1 L 70% ethanol using a Soxwave100 apparatus. Ethanol extracts were dried under a vacuum in a rotary evaporator. Concentrated extracts were lyophilized, yielding a dried powder that was stored at 4°C. The yield (%) of each product is provided in Table 2. Dried ethanol extracts were dissolved in saline (Sigma-Aldrich, St. Louis, MO) prior to use. NPM-9 (250 mg/kg) was mixed with the same volume of herbal (licorice, hawkweed, beefsteak plant, fenugreek, and skullcap) and food extracts (black pepper, green tea, turmeric).

2.3. Schedules for Mouse Sensitization, TMA Challenges, and Sample Treatment. TMA induction of CHS was performed as described in [21]. A schematic of the experimental procedure is shown in Figure 2(a). To induce CHS, mice were divided into naïve, sham, NPM-9, and prednisolone groups. Mice were sensitized with 50 μL of 5% TMA (Sigma-Aldrich, St. Louis, MO) in solvent on shaved flank skin on day 0. Challenges with 10 μL of 5% TMA in solvent on the dorsum of both ears were performed on day 5. In the chronic model, animals received challenges on the ears with 10 μL of 2% TMA in solvent on days 6–15. A solvent control group was exposed to acetone and isopropyl myristate (4 : 1, v/v) throughout the duration of the experiment. In the treatment groups, NPM-9 (250 mg/kg body weight (BW)) and prednisolone (30 mg/kg BW), which served as a positive control, were administered orally 1 h before challenge. Each treatment was performed on days 9–15. Body weight and water intake were measured daily. Ear thickness was determined with a custom-built micrometer (Schering AG, Germany). Ears were mechanically homogenized in 2 mL PBS (Sigma-Aldrich, St. Louis, MO), centrifuged at 25,000 g for 30 min at room temperature, and cultured in the presence of 5 μg/mL ConA. Cytokines were measured in the supernatant. Blood samples were obtained from the brachial plexus to estimate the immunoglobulin titer by ELISA 24 h after the final treatment. Spleens were removed and incubated with 5 μg/mL ConA for 72 h. Cytokine production was measured by ELISA.

2.4. Sensitization with OVA and Preparation of Splenocyte Cultures. Mice were sensitized with 20 μg OVA (Grade

VI; Sigma-Aldrich, St. Louis, MO) adsorbed in 2 mg/mL Imject Alum (Pierce, Rockford, USA) and administered by intraperitoneal (i.p.) injection on days 7 and 14. Splenocytes were prepared by aseptically removing the spleen from each mouse. Homogenized single spleen cells were collected and treated with red blood cell- (RBC-) lysing buffer (Sigma-Aldrich). The splenocytes were adjusted to 5×10^6 cells/mL in RPMI medium using the trypan blue dye exclusion method. The splenocytes (200 μL/well) were then cultured in the presence or absence of OVA (100 μg/mL/well) and each herb and food extract. The plates were incubated at 37°C for 72 h in a humidified incubator with 5% (v/v) CO_2 and 95% (v/v) air. Cytokines in the supernatant were measured by ELISA.

2.5. Oral NPM-9 Treatment in OVA-Sensitized Mice. To investigate NPM-9 inhibition of the OVA-induced allergic response *in vivo*, mice were divided into normal (naïve), untreated (sham), and NPM-9-treated groups. Mice were sensitized with 20 μg OVA adsorbed in 2 mg/mL Imject Alum i.p. injection on days 7 and 21. The solvent control group was administered saline and 2.5% ethanol throughout the experiment. In the treatment groups, 250 mg/kg NPM-9 was administered orally. NPM-9 treatments were performed on days 14–28. A schematic of the experimental procedure is shown in Figure 4(a). Twenty-four hours after the last treatment, blood samples were obtained from the brachial plexus. Splenocytes were prepared from each mouse.

2.6. Measurement of Serum IgE. IgE antibody levels in sera were measured by ELISA. Aliquots (200 μL per well) of IgE capture antibody (BD PharMingen, San Diego, CA, USA) or OVA (10 μg/mL dissolved in 0.1 mol/L $NaHCO_3$ (Wako Pure Chemical Industries), pH 8.2) were pipetted into 96-microwell plates (Nunc, Thermo Fisher Scientific, Roskilde, Denmark). The plates were incubated overnight at 4°C and then carefully washed 3 times with washing buffer (0.5 g/L Tween 20 in PBS). Serum samples were diluted 1 : 5 for specific IgE determinations. Aliquots (100 μL) of diluted serum samples were added to the wells. Pooled sera from nonssensitized and sensitized mice were included as negative and positive controls. The levels were determined using biotin-conjugated rat anti-mouse IgE (BD PharMingen, San Diego, CA, USA) according to manufacturer protocols. The plates were read using an ELISA plate reader (Molecular Devices, Inc.) at 450 nm.

2.7. Measurement of Cytokine Levels Using ELISA. A cytokine assay kit (BD PharMingen, San Diego, CA, USA) was used to measure cytokine levels (IFN-γ, IL-12, IL-4, and IL-10), according to manufacturer protocols. Briefly, supernatants and standard solution were transferred to 96-well plates precoated with monoclonal antibodies to each of the target cytokines and then incubated at room temperature for 2 h. After thorough washing with the washing buffer included in the kit, a horseradish peroxidase- (HRP-) conjugated secondary antibody was added to each well, and incubation was continued at room temperature for 2 h. After removal of the secondary antibody, the substrate solution for the enzymatic reaction was added, and samples were incubated for another 30 min in the dark. The reaction was terminated by addition of stop solution, and absorbance was measured at 450 nm in a microplate reader (Molecular Devices, Inc.). The IC_{50} value of IL-4 was calculated from the reduction of IL-4 by different concentrations of test substance using linear regression analysis.

2.8. Statistical Analysis. Each result is expressed as the mean ± SD. Differences were assessed by ANOVA followed by Student's *t*-test.

3. Results and Discussion

3.1. Oral Administration of NPM-9 Attenuates TMA-Induced Infiltration of Inflammatory Cells in the Ear Dermis. In the BALB/c model of TMA-induced CHS, mice are sensitized on the flank skin, and T-cell-dependent inflammation of the ear skin is induced by topical challenges with TMA (Figure 2(a)). The TMA-induced response increased production of Th2 cytokines and immune cell infiltration, such as by mast cells [21]. The severity of inflammation can be assessed using ear thickness [22]. In all but the naïve group, 5% TMA challenge on days 0 and 5 and subsequent daily low-dose challenges with 2% TMA for 10 days induced a significant increase in ear thickness; this increase was inhibited by prednisolone (30 mg/kg BW), which served as the positive control [18]. Daily NPM-9 gavage (250 mg/kg BW) also produced an incremental decline in ear thickness (Figure 2(b)). We also measured epidermal thickness, infiltration of eosinophils and lymphocytes, and the number of mast cells in the dermis of the ears and found that NPM-9 inhibited the effects of TMA (data not shown). We also observed the body weight of each mouse in days 5~20 on Th2-mediated skin allergic inflammation to examine toxicity or side effect of NPM-9. As a result, body weight of NPM-9 group did not differ from that of sham or prednisolone group (data not shown).

3.2. Oral Administration of NPM-9 Suppressed IgE Levels in TMA-Induced CHS Mice. TMA-sensitized and -challenged mice received orally administered NPM-9 (250 mg/kg) daily for 14 days. Serum was collected from each group for serum IgE measurements (Figure 3(a)). The TMA-induced CHS model displays characteristics of AD such as increased IgE. Allergen-specific IgE triggers local inflammatory responses, eventually generating various allergic responses [23]. In this study, serum IgE levels in TMA-treated CHS mice were higher than in nontreated mice, and oral NPM-9 administration suppressed this effect (Figure 3(a)). The capability of NPM-9 to reduce serum TMA-specific IgE was compared to that of prednisolone.

3.3. NPM-9 Administration Suppresses TMA-Induced Cytokine Expression in Ear Tissue and Splenocytes. We examined whether NPM-9 inhibits the production of Th2 cytokine IL-4 and inflammatory cytokine IL-1β in inflamed ear tissue and splenocytes. Oral administration of NPM-9 reduced the level of inflammatory cytokine IL-1β in inflamed ear tissue

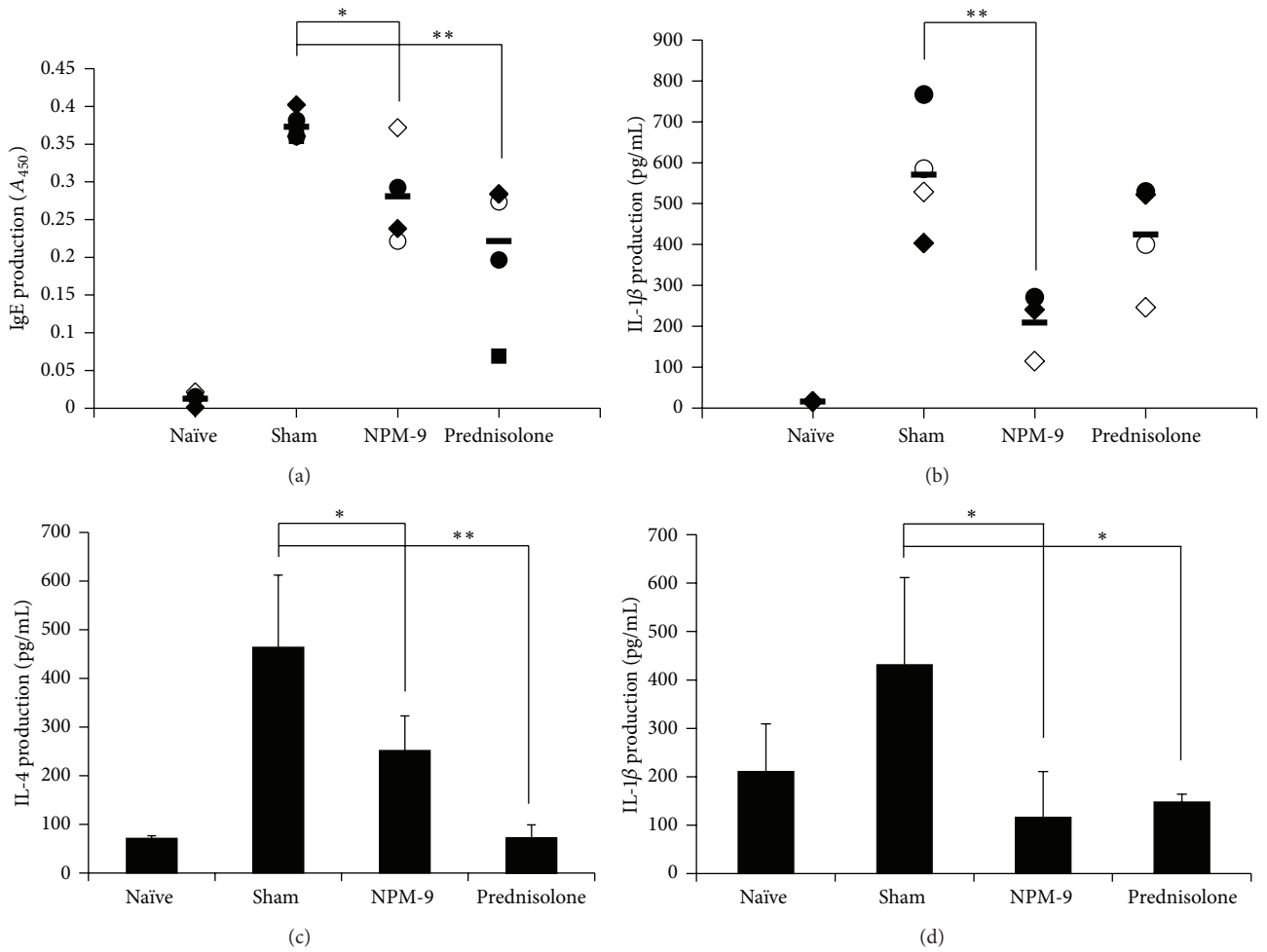

Figure 3: Inhibitory effect of NPM-9 in inflamed regions and splenocytes from TMA-induced allergic mice. (a) IgE levels in serum were measured by ELISA. To measure IgE, collected sera were diluted 1 : 50. (b) IL-1β was quantified by ELISA after homogenization in PBS-T using inflamed ear skin from TMA-induced BALB/c mice. Secreted (c) IL-4 and (d) IL-1β were quantified by ELISA after 72 h culture using splenocytes from TMA-induced BALB/c mice. Values are presented as mean ± SD ($n = 4$ per group). Data were analyzed by ANOVA followed by Student's t test. $^{*}P < 0.05$, $^{**}P < 0.01$, significantly different from the saline value.

but not IL-4 (Figure 3(b)). In splenocytes, NPM-9 reduced IL-4 and IL-1β without cytotoxicity (Figures 3(c) and 3(d)). It is possible that NPM-9 had not yet induced Th2 migration to the inflamed regions but was sufficiently potent to downregulate Th2 in splenocytes. These results show that oral administration of NPM-9 constricted TMA-induced dermal inflammation; the biological basis of this inhibition appears to involve the balance of Th2 cells in the immune system. It is also important to demonstrate IFN-γ production in skin inflammation. There are distinct types of TMA-induced skin inflammation mouse models: acute TMA-induced CHS in Balb/c mice with subacute and chronic models of TMA-induced ear inflammation. In comparison to the acute model, the chronic TMA-induced CHS model exhibits a mixed type 1 and 2 T-cell differentiation and activation pattern [21]; however, the TMA-induced CHS mouse model used in this study is acute or subacute, characterized by eosinophil and T-cell infiltration, Th2 cytokine production, and IgE expression [21]. Moreover, oral administration of NPM-9 suppressed early-phase Th2 skewing, prohibiting the development of chronic inflammation. Therefore, we examined the Th2-dependent immune responses (IgE and IL-4) and proinflammatory cytokine IL-1β as indicators of Th2-mediated skin inflammation; however, the effect of NPM-9 on IFN-γ production in both Th1-s and Th2-dependent chronic skin inflammation requires further study.

3.4. Synergistic Inhibition of IL-4 Production in Ex Vivo Splenocytes from OVA-Sensitized BALB/c Mice. To determine how skin inflammation is inhibited by suppression of skewing to Th2 cells, we examined how each extract inhibited Th2 polarization *ex vivo*. Levels of IL-4 in splenocytes were determined using the OVA-induced Th2 allergic mouse as an *ex vivo* model. Inhibition of Th2 polarization was measured as the IC_{50} with IL-4. IC_{50} values were calculated and compared as illustrated in Table 3. IL-4 production was inhibited by fenugreek > black pepper > chonggugjang > licorice > green tea > skullcap > turmeric > hawkweed > beefsteak plant.

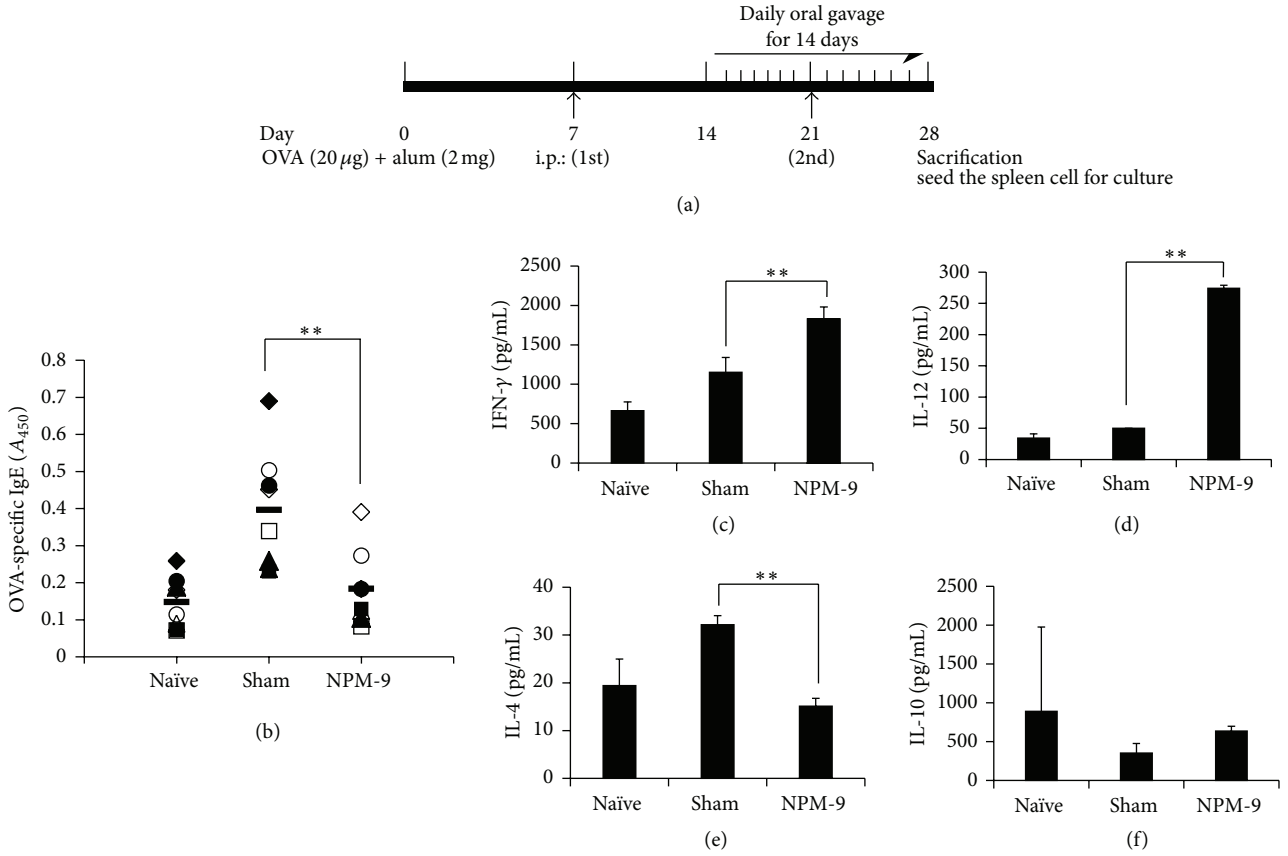

Figure 4: NPM-9 suppression of OVA-specific IgE and IL-4 production in OVA-sensitized BALB/c mice. (a) Experimental protocol for OVA-induced allergic response in mice. (b) OVA-specific IgE levels in serum were measured by ELISA. To determine total and OVA-specific antibody titers, the collected sera were diluted 1 : 50 for IgE detection. Secreted (c) IFN-γ, (d) IL-12, (e) IL-4, and (f) IL-10 were quantified by ELISA after 72 h culture using splenocytes from OVA-sensitized BALB/c mice. Values are presented as mean ± SD ($n = 7$ per group). Data were analyzed by ANOVA followed by Student's t test. $^{*}P < 0.05$, $^{**}P < 0.01$, significantly different from the saline value.

Each extract produced an antiallergic effect by inhibiting IL-4 production; food extracts were more effective than herb extracts. Splenocytes cultured with NPM-9 produced IL-4 levels 1.6- to 16-fold lower than that with each extract alone (Table 3). The IC_{50} ratio of IL-4 versus IFN-γ in the presence of NPM-9 was 1.6- to 48-fold higher than that with each extract alone. These results indicate that NPM-9 exerts potent synergistic suppression of the allergic response by inhibiting IL-4 secretion and inducing IFN-γ secretion.

3.5. Oral Administration of NPM-9 Suppressed the Serum IgE in OVA-Induced Allergic Mice. We also examined how oral administration of NPM-9 inhibits the OVA-induced Th2-mediated allergic response. OVA-sensitized mice received orally administered NPM-9 (250 mg/kg) daily for 14 days (Figure 4(a)). Serum from each group was collected for measurement of OVA-specific IgE (Figure 4(b)). Th2 cells play an important role in the OVA-induced mouse model by their influence on IL-4 and IL-5 production [24]. IL-4 is the major inducer of class switching of Ig to B lymphocyte IgE biosynthesis associated with allergic responses [23]. In this study, NPM-9-treated mice exhibited a significant reduction in serum OVA-specific IgE than nontreated mice in the Th2-mediated allergic state.

Table 3: IC_{50} of NPM-9 for IL-4 and IFN-γ.

Sample extract	IC_{50} for IL-4 (ug/mL)	Ratio of IFN-γ/IL-4
Licorice	62.7	3.00
Hawkweed	208	0.15
Beefsteak plant	213	0.10
Fenugreek	15.4	2.50
Skullcap	86.7	0.98
Black pepper	31.3	1.45
Green tea	80.3	0.23
Turmeric	148	0.15
Fermented soybeans paste (cheonggukjang)	54.3	0.82
NPM-9	12.7	4.80

IC_{50} of IFN-γ and IL-4 were quantified by ELISA after cells were cultured for 72 h with splenocytes from OVA-induced allergic mice in the presence of each extract or NPM-9, Natural Nonaproduct Mixture.

3.6. Oral Administration of NPM-9 Inhibits the Production of Th2 Cytokines in Splenocytes from OVA-Induced Th2-Mediated Allergic Mice. To determine how NPM-9 administration in OVA-sensitized mice modulates the Th1 and Th2 pathways, splenocyte levels of IL-4 and IFN-γ were determined using the OVA-induced allergic mouse described above. IFN-γ and IL-12 levels were greater in the splenocytes of NPM-9-treated OVA-stimulated mice than in untreated mice. IL-4 was suppressed in the splenocytes of NPM-9-treated versus the untreated OVA-stimulated group. However, IL-10 secretion was not enhanced by NPM-9 treatment (Figures 4(c)–4(f)). The effect of NPM-9 on IL-12 and IL-10 is interesting in the context of macrophages. IL-12, a product of activated macrophages, induces the Th1 cytokine pattern [25], and IL-10 inhibits macrophage-dependent cytokine synthesis by Th1 cells [26]. That is, Th1 cells can be inhibited by IL-10 but induced by IL-12 through the regulation of macrophages. Consistent with this model, we speculated that NPM-9 suppression of Th2-mediated allergic responses such as skin inflammation may occur through the induction of Th1 via macrophages.

Based on the immunomodulatory effects of NPM-9 in the TMA-induced dermatitis model, we conclude that the diverse active compounds of NPM-9 have synergistic effects on allergic responses. The main chemical constituents in each compound include coumarin, luteolin, and caffeic and chlorogenic acids in hawkweed [27]; rosmarinic acid in beefsteak plant [28]; baicalein and wogonin in skullcap [29]; glycyrrhizin in licorice [30]; poly γ-glutamic acid and isoflavone in fermented soybean paste (Cheonggukjang) [13]; alkylamides and piperine in black pepper [12]; saponin and flavonoid in fenugreek [31]; curcumin in turmeric [14]; and catechin in green tea [32]. Many studies have reported that flavonoids such as curcumin or catechin have immunomodulatory activities. Glycyrrhizin enhances LPS-induced IL-12 production by peritoneal macrophages independent of IFN-γ and GM-CSF [33]. Saponin and poly γ-glutamic acid have immunostimulatory effects on the immune function of lymphocytes or the immune responses to vaccine immunizations [14, 34, 35]. Oral administration of NPM-9 (250 mg/kg/d) for 2 weeks had no adverse effects in mice, demonstrating that NPM-9 is safe even at high concentrations. The safety and immunomodulatory effects of NPM-9 may result from the interaction of active ingredient in each extract. Thus, NPM-9 may be a safe, natural therapy for allergic diseases such as atopic dermatitis, allergic coryza, and asthma.

4. Conclusion

We have demonstrated that NPM-9 suppresses allergic skin inflammation in a TMA-induced CHS mouse model and exerts its effect by inhibiting a skewed Th2 response. NPM-9 inhibits the polarized Th2 response through Th1 skewing that is dependent on IFN-γ and IL-12 secretion in an OVA-induced Th2 allergic state. Our results provide scientific proof of the prevention and treatment of skin allergic inflammation by the synergistically inhibitory effects of food and herb extracts on Th2-polarized allergic responses.

Abbreviations

AD: Allergic dermatitis
APC: Antigen-presenting cells
CHS: Contact hypersensitivity
DNP: Dinitrophenyl
ELISA: Enzyme-linked immunosorbent assay
HRP: Horseradish peroxidase
IFN: Interferon
Ig: Immunoglobulin
IL: Interleukin
NPM-9: Nonanatural products mixture
OVA: Ovalbumin
Th: T-helper
TMA: Trimellitic anhydride.

Conflict of Interests

The authors have no conflict of interests to declare.

Authors' Contribution

Min-Jung Bae and Hee Soon Shin contributed equally to this work.

Acknowledgment

This paper was supported by research grants from the Korea Food Research Institute.

References

[1] D. Y. M. Leung and N. A. Soter, "Cellular and immunologic mechanisms in atopic dermatitis," *Journal of the American Academy of Dermatology*, vol. 44, no. 1, pp. S1–S12, 2001.

[2] J. M. Spergel, E. Mizoguchi, H. Oettgen, A. K. Bhan, and R. S. Geha, "Roles of T(H)1 and T(H)2 cytokines in a murine model of allergic dermatitis," *Journal of Clinical Investigation*, vol. 103, no. 8, pp. 1103–1111, 1999.

[3] S. J. Galli, M. Tsai, and A. M. Piliponsky, "The development of allergic inflammation," *Nature*, vol. 454, no. 7203, pp. 445–454, 2008.

[4] F. D. Finkelman, I. M. Katona, T. R. Mosmann, and R. L. Coffman, "IFN-γ regulates the isotypes of Ig secreted during in vivo humoral immune responses," *Journal of Immunology*, vol. 140, no. 4, pp. 1022–1027, 1988.

[5] L. Chen, O. Martinez, L. Overbergh, C. Mathieu, B. S. Prabhakar, and L. S. Chan, "Early up-regulation of Th2 cytokines and late surge of Th1 cytokines in an atopic dermatitis model," *Clinical and Experimental Immunology*, vol. 138, no. 3, pp. 375–387, 2004.

[6] G. Sandoval-López and L. M. Teran, "TARC: novel mediator of allergic inflammation," *Clinical and Experimental Allergy*, vol. 31, no. 12, pp. 1809–1812, 2001.

[7] C. Vestergaard, H. Yoneyama, M. Murai et al., "Anti-tumor metastatic activity of beta-glucan purified from mutated *Saccharomyces cerevisiae*," *International Immunopharmacology*, vol. 8, no. 1, pp. 36–42, 2008.

[8] J. Koo and S. Arain, "Traditional chinese medicine for the treatment of dermatologic disorders," *Archives of Dermatology*, vol. 134, no. 11, pp. 1388–1393, 1998.

[9] M. Kotani, M. Matsumoto, A. Fujita et al., "Persimmon leaf extract and astragalin inhibit development of dermatitis and IgE elevation in NC/NGa mice," *Journal of Allergy and Clinical Immunology*, vol. 106, no. 1 I, pp. 159–166, 2000.

[10] J. K. Kim, S. M. Oh, H. S. Kwon, Y. S. Oh, S. S. Lim, and H. K. Shin, "Anti-inflammatory effect of roasted licorice extracts on lipopolysaccharide-induced inflammatory responses in murine macrophages," *Biochemical and Biophysical Research Communications*, vol. 345, no. 3, pp. 1215–1223, 2006.

[11] K. Schütz, R. Carle, and A. Schieber, "Taraxacum-A review on its phytochemical and pharmacological profile," *Journal of Ethnopharmacology*, vol. 107, no. 3, pp. 313–323, 2006.

[12] S. B. Yoon, Y. J. Lee, S. K. Park et al., "Anti-inflammatory effects of *Scutellaria baicalensis* water extract on LPS-activated RAW 264.7 macrophages," *Journal of Ethnopharmacology*, vol. 125, no. 2, pp. 286–290, 2009.

[13] T. Y. Shin, S. H. Kim, S. H. Kim et al., "Inhibitory effect of mast cell-mediated immediate-type allergic reactions in rats by *Perilla frutescens*," *Immunopharmacology and Immunotoxicology*, vol. 22, no. 3, pp. 489–500, 2000.

[14] Y. Fujimura, D. Umeda, S. Yano, M. Maeda-Yamamoto, K. Yamada, and H. Tachibana, "The 67 kDa laminin receptor as a primary determinant of anti-allergic effects of O-methylated EGCG," *Biochemical and Biophysical Research Communications*, vol. 364, no. 1, pp. 79–85, 2007.

[15] M. Maeda-Yamamoto, K. Ema, and I. Shibuichi, "In vitro and in vivo anti-allergic effects of 'benifuuki' green tea containing O-methylated catechin and ginger extract enhancement," *Cytotechnology*, vol. 55, no. 2-3, pp. 135–142, 2007.

[16] B. Bin-Hafeez, R. Haque, S. Parvez, S. Pandey, I. Sayeed, and S. Raisuddin, "Immunomodulatory effects of fenugreek (*Trigonella foenum graecum* L.) extract in mice," *International Immunopharmacology*, vol. 3, no. 2, pp. 257–265, 2003.

[17] M. J. Bae, H. S. Shin, D. W. Choi, and D. H. Shon, "Antiallergic effect of *Trigonella foenum-graecum* L. extracts on allergic skin inflammation induced by trimellitic anhydride in BALB/c mice," *Journal of Ethnopharmacology*, vol. 144, no. 3, pp. 514–522, 2012.

[18] A. F. Majdalawieh and R. I. Carr, "In vitro investigation of the potential immunomodulatory and anti-cancer activities of black pepper (*Piper nigrum*) and cardamom (*Elettaria cardamomum*)," *Journal of Medicinal Food*, vol. 13, no. 2, pp. 371–381, 2010.

[19] W. K. Tae, Y. L. Tae, C. B. Hyun et al., "Oral administration of high molecular mass poly-γ-glutamate induces NK cell-mediated antitumor immunity," *Journal of Immunology*, vol. 179, no. 2, pp. 775–780, 2007.

[20] G. Y. Kim, K. H. Kim, S. H. Lee et al., "Curcumin inhibits immunostimulatory function of dendritic cells: MAPKs and translocation of NF-κB as potential targets," *Journal of Immunology*, vol. 174, no. 12, pp. 8116–8124, 2005.

[21] C. Schneider, W. D. F. Döcke, T. M. Zollner, and L. Röse, "Chronic mouse model of TMA-induced contact hypersensitivity," *Journal of Investigative Dermatology*, vol. 129, no. 4, pp. 899–907, 2009.

[22] D. M. Sailstad, M. D. W. Ward, E. H. Boykin, and M. K. Selgrade, "A murine model for low molecular weight chemicals: differentiation of respiratory sensitizers (TMA) from contact sensitizers (DNFB)," *Toxicology*, vol. 194, no. 1-2, pp. 147–161, 2003.

[23] L. K. Poulsen and L. Hummelshoj, "Triggers of IgE class switching and allergy development," *Annals of Medicine*, vol. 39, no. 6, pp. 440–456, 2007.

[24] L. L. Carter and R. W. Dutton, "Type 1 and Type 2: a fundamental dichotomy for all T-cell subsets," *Current Opinion in Immunology*, vol. 8, no. 3, pp. 336–342, 1996.

[25] J. Frostegård, A. K. Ulfgren, P. Nyberg et al., "Cytokine expression in advanced human atherosclerotic plaques: dominance of pro-inflammatory (Th1) and macrophage-stimulating cytokines," *Atherosclerosis*, vol. 145, no. 1, pp. 33–43, 1999.

[26] D. F. Fiorentino, A. Zlotnik, T. R. Mosmann, M. Howard, and A. O'Garra, "IL-10 inhibits cytokine production by activated macrophages," *Journal of Immunology*, vol. 147, no. 11, pp. 3815–3822, 1991.

[27] C. Zidorn, B. Schubert, and H. Stuppner, "Altitudinal differences in the contents of phenolics in flowering heads of three members of the tribe Lactuceae (Asteraceae) occurring as introduced species in New Zealand," *Biochemical Systematics and Ecology*, vol. 33, no. 9, pp. 855–872, 2005.

[28] E. S. Lin, H. J. Chou, P. L. Kuo, and Y. C. Huang, "Antioxidant and antiproliferative activities of methanolic extracts of *Perilla frutescens*," *Journal of Medicinal Plant Research*, vol. 4, no. 6, pp. 477–483, 2010.

[29] H. S. Shin, M. J. Bae, S. Y. Jung, and D. H. Shon, "Inhibitory effect of skullcap (*Scutellaria baicalensis*) extract on ovalbumin permeation in vitro and in vivo," *Food Chemistry*, vol. 140, pp. 22–30, 2013.

[30] J. Cinatl, B. Morgenstern, G. Bauer, P. Chandra, H. Rabenau, and H. W. Doerr, "Glycyrrhizin, an active component of liquorice roots, and replication of SARS-associated coronavirus," *Lancet*, vol. 361, no. 9374, pp. 2045–2046, 2003.

[31] A. Mandegary, M. Pournamdari, F. Sharififar, S. Pournourmohammadi, R. Fardiar, and S. Shooli, "Alkaloid and flavonoid rich fractions of fenugreek seeds (*Trigonella foenum-graecum* L.) with antinociceptive and anti-inflammatory effects," *Food and Chemical Toxicology*, vol. 50, no. 7, pp. 2503–2507, 2012.

[32] H. S. Youn, J. Y. Lee, S. I. Saitoh et al., "Suppression of MyD88- and TRIF-dependent signaling pathways of toll-like receptor by (-)-epigallocatechin-3-gallate, a polyphenol component of green tea," *Biochemical Pharmacology*, vol. 72, no. 7, pp. 850–859, 2006.

[33] J. H. Dai, Y. Iwatani, T. Ishida et al., "Glycyrrhizin enhances interleukin-12 production in peritoneal macrophages," *Immunology*, vol. 103, no. 2, pp. 235–243, 2001.

[34] J. Liu, S. Wang, H. Liu, L. Yang, and G. Nan, "Stimulatory effect of saponin from *Panax ginseng* on immune function of lymphocytes in the elderly," *Mechanisms of Ageing and Development*, vol. 83, no. 1, pp. 43–53, 1995.

[35] L. Zhai, Y. Li, W. Wang, Y. Wang, and S. Hu, "Effect of oral administration of ginseng stem-and-leaf saponins (GSLS) on the immune responses to Newcastle disease vaccine in chickens," *Vaccine*, vol. 29, no. 31, pp. 5007–5014, 2011.

Hindawi Publishing Corporation
Evidence-Based Complementary and Alternative Medicine
Volume 2013, Article ID 871648, 12 pages
http://dx.doi.org/10.1155/2013/871648

Research Article

Effects of Korean Red Ginseng and HAART on *vif* Gene in 10 Long-Term Slow Progressors over 20 Years: High Frequency of Deletions and G-to-A Hypermutation

Young Keol Cho,[1] Ba Reum Kim,[1] Mee Soo Chang,[2] and Jung Eun Kim[1]

[1] *Department of Microbiology, University of Ulsan College of Medicine, 88 Olympic-ro 43-gil, Songpa-gu, Seoul 138-736, Republic of Korea*
[2] *Department of Pathology, Seoul National University Boramae Hospital, Seoul 156-707, Republic of Korea*

Correspondence should be addressed to Young Keol Cho; ykcho2@amc.seoul.kr

Received 12 June 2013; Accepted 3 September 2013

Academic Editor: K. B. Harikumar

To investigate if Korean red ginseng (KRG) affects *vif* gene, we determined *vif* gene over 20 years in 10 long-term slowly progressing patients (LTSP) who were treated with KRG alone and then KRG plus HAART. We also compared these data with those of 21 control patients who did not receive KRG. Control patient group harbored only one premature stop codon (PSC) (0.9%), whereas the 10 LTSP revealed 78 defective genes (18.1%) ($P < 0.001$). The frequency of small in-frame deletions was found to be significantly higher in patients who received KRG alone (10.5%) than 0% in the pre-KRG or control patients ($P < 0.01$). Regarding HAART, *vif* genes containing PSCs were more frequently detected in patients receiving KRG plus HAART than patients receiving KRG alone or control patients ($P < 0.01$). In conclusion, our current data suggest that the high frequency of deletions and PSC in the *vif* gene is associated with KRG intake and HAART, respectively.

1. Introduction

Panax ginseng has a long history of medicinal use in Asia. At present, ginseng is the best-selling herbal medicine in the world [1]. About 200 constituents of Korean ginseng have been isolated and characterized. Its major components include ginseng saponins and polysaccharides. The major pharmacological effects of ginseng include adaptogenic effects [2]; that is, ginseng nonspecifically increases the resistance to physical, chemical, and biological stress by immunomodulation of the hypothalamic-pituitary-adrenal axis [3]. Recent studies have also demonstrated ginseng's potential use in adjuvant and immunotherapies [4–8].

Persistent immune activation and inflammation despite sustained antiretroviral therapy (ART)-mediated viral suppression have emerged as a major challenge in the modern era of HIV treatment [9]. In particular, the saponin fraction of ginseng downregulates proinflammatory mediators in LPS-stimulated cells and protects mice against endotoxic shock [10–12]. The absence of microbial translocation and immune activation in well-adapted, natural hosts with simian immunodeficiency virus [13] is a very important mechanism in our understanding of the slow progression of HIV-1-infected patients who have been treated with Korean red ginseng (KRG) [14].

We previously reported that KRG induces gross deletions in the *nef* gene [14] and frequent genetic defects in the 5′ LTR/*gag* gene [15]. Interestingly, the detection of genetic defects was inhibited during the administration of highly active antiretroviral therapy (HAART) [16]. However, there are only a few studies that have reported the gross deletion of the *vif* gene because it is the second most highly conserved gene after *pol* [17–19]. Hence, to determine if KRG affects the *vif* gene, as shown for the *nef* and *gag* genes [14–16], we amplified *vif* gene in peripheral blood mononuclear cells (PBMCs) obtained over 20 years from 10 long-term slowly progressing (LTSP) patients. It appears from our analyses that KRG intake might induce gross and small in-frame deletions.

Table 1: Characteristics of 10 long-term slow progressors.

Patient code	Year of diagnosis	Date of AIDS diagnosis	CD4+ T cells/μL[a]	Viral load (copy/mL)[a]	Follow-up from Dx[b] to HAART (Mo)	HAART[c]	Duration of HAART
87-05	1987	NA	256	115,000	314	None	None
89-17	1989	Jul 02	106	162,000	188	Mar 05	62
90-05	1990	May 08	103	94,376	221	July 08	58
90-18	1990	Mar 04	112	124,000	167	Apr 04	104
90-50	1990	Mar 07	116	244,000	197	May 07	68
91-20	1991	Aug 07	55	3,886	214	Aug 07	65
92-13	1992	June 07	47	5,800	181	Jun 07	45
93-04	1993	NA	297	656,000	166	Nov 06	9
93-60	1993	NA	109	121,000	182	May 08	47
96-51	1996	NA	169	386,543	164	Dec 09	36

[a]CD4+ T cell count and viral load measured just before the initiation of HAART.
[b]Dx: diagnosis.
[c]HAART: highly active antiretroviral therapy.

In addition, we found that HAART increases the frequency of premature stop codons (PSCs) in the *vif* gene.

2. Materials and Methods

2.1. Patients. Ten patients whose annual decrease in CD4+ T cells was <20 cells/μL were diagnosed as LTSP patients [14]. Their clinical characteristics, including changes in CD4+ T-cell count and RNA copy number, KRG therapy, and frequent genetic defects in the *nef* and 5′ LTR/*gag* genes, have been previously described [14, 15]. However, the follow-up period of the present study was extended to include the KRG plus HAART period. The control patients ($n = 21$) were selected from 169 patients [20] who had not been exposed to KRG or any antiretroviral therapies (e.g., AZT) at the time of sampling and whose PBMCs were available for gene amplification. This study was approved by the Institutional Review Board of the Asan Medical Center.

2.2. KRG Intake. KRG powder was manufactured by the Korea Ginseng Corporation (Daejeon, Korea) from the roots of a 6-year-old *Panax ginseng* Meyer red ginseng and harvested in the Republic of Korea. KRG was made by steaming fresh ginseng at 90–100°C for three hours and drying at 50–80°C. KRG powder was prepared from ground red ginseng (500 mg KRG/capsule) and analyzed using high-performance liquid chromatography.

2.3. Amplification of the vif Gene. Nested PCR was used to amplify the proviral *vif* gene from the patients' PBMCs, as previously described [14–16, 19]. Total RNA was extracted from 300 μL serum using the QIAamp Ultra Sense Viral RNA kit (Qiagen, Hilden, Germany), as previously described [20].

2.4. Determination of G-to-A Hypermutation. Sequences were analyzed using the Hypermut 2.0 program (http://www.hiv.lanl.gov/content/sequence/HYPERMUT/hypermut.html), which compares each patient's sequence to a patient-specific consensus in order to determine the frequency and context of the G-to-A mutations [21].

2.5. Statistical Analysis. Data are expressed as the means ± 2 standard deviations (for continuous variables) or as counts and percentages (categorical variables). Comparing the proportions between groups was analyzed by using the Chi-squared test or Fisher exact test. In this study, $P < 0.05$ was considered statistically significant.

2.6. Accession Numbers of the Nucleotide Sequence. The investigated sequences were previously assigned the following GeneBank accession numbers: DQ072735, JF957893, JQ067069-76, AY581367, JF957902, JQ248188-201, AY581377, AY581378, JQ248228-50, JF957922, AY581382-5, DQ072750-51, JF957924, JQ248256-92, DQ072759-60, AY581386-89, JF957933, JQ248313-29, AY581394-95, JF957940, JQ248339-55, AY581398-AY581399, JQ327719, JQ327794-97, JF958044-45, JQ066879-927, AY581341-44, JF957976, JQ268920-39, AY581412-15, JQ268940-61, AF462782, JF957977, AY581416-18, JQ269006-32, JF957983, AY581419-20, KC247158-315, and KF270357-459.

3. Results

3.1. Effects of KRG during the Follow-Up Period prior to HAART Administration. Ten LTSP patients received follow-up without HAART for 199 ± 45 months (16.6 years; range: 164–314 months) following HIV-1 diagnosis (Table 1). During this period, KRG therapy was administered for 173 ± 34 months and, thereafter, KRG plus HAART was administered for 55 ± 26 months. The amounts of KRG administered during these periods were 14,398 ± 5,775 and 5,648 ± 3,677 g, respectively. Patient 89-17's compliance with KRG was poor, and the amount supplied prior to HAART therapy was the least (5,076 g) of the 10 enrolled LTSP patients. Patient 87-05 began to take KRG in December 1991, though his compliance was also poor. He has taken KRG since June 1994, but his

CD4+ T-cell count remained low (Figure 1). The remaining nine patients progressed to AIDS, demonstrating CD4+ T-cell counts of <200 cells/μL (Table 1).

3.2. Effects of HAART on PSC. The 10 LTSP patients we included in our present study were untreated before December 1991, were treated with only KRG between 2004 and 2009, and have been treated with KRG plus HAART since 2009 (Figure 1). We analyzed 432 *vif* genes over 20 years in these 10 LTSP patients. Among these, 15 *vif* genes (3.5%) demonstrated PSC. In total, 275 and 157 *vif* genes were obtained during KRG and KRG plus HAART, respectively. Each group demonstrated 3 (1.1%) and 12 (7.6%) *vif* genes with PSCs, respectively. When receiving only KRG, three patients (90-50, 93-04, and 93-60) demonstrated PSC at 14 years, 1 year and 9 months, and 7 years after starting to receive KRG, respectively. The frequency was significantly higher when receiving KRG plus HAART than KRG alone ($P < 0.01$; Table 2). This suggests that HAART itself might induce G-to-A hypermutation, thereby resulting in PSC and, possibly, lethal hypermutations. This is consistent with the findings of other studies [22]. However, we found no difference in the frequency of PSCs between our KRG (3 of 275 genes) and control groups (1 of 106 genes). Interestingly, of the 15 *vif* genes that demonstrated PSCs in our present analysis, eleven did not satisfy the criteria of Hypermut 2.0 in comparison with the earliest sequences obtained from each patient ($P < 0.05$; Figure 3).

3.3. Effects of KRG and HAART on Genetic Defects. We detected 11 gross deletions in 432 amplicons obtained from our 10 LTSP patients (Table 2; Figure 2). No deleted genes, including gross deletions, were detected in the control patients. In total, five patients demonstrated gross deletions after >19 months of KRG intake. Four patients demonstrated gross deletions during KRG intake prior to HAART, although the frequency was very low (1.5%). Specifically, a sequence containing a gross deletion and duplication/recombination (KC247159) was identified in patient 87-05. A 362-base pair (bp) deletion and 1 bp insertion (KC247195), 309 bp deletion (JQ327719), and 870 bp deletion (JQ327722) were detected as short bands together with the wild-type genotype after 139 months, 115 months, and 125 months of KRG intake in patients 90-05, 91-20, and 93-60, respectively (patient 90-05 demonstrated 9 bp insertions in 16 amplicons after 104 months of KRG intake, including KC247191, JQ248236, DQ295192, and JQ248237-50). In addition, two patients demonstrated gross deletions during KRG plus HAART. Specifically, patient 93-04 demonstrated 386 bp deletions in one-third of amplicons after 14 years of KRG intake. Patient 93-60 demonstrated six deletions (including 374 bp [JQ327723] and 401 bp deletions [KC247314]; Figure 2 and Table 2). Each deletion was one (JQ327723) of 3 amplicons and one (KC247314) of 2 amplicons obtained between August 2008 and October 2010 and all 4 amplicons, respectively (Figure 1). This frequency is the highest among the related studies to date, although we found no significant differences in terms of the frequencies of gross deletions between patients who received KRG (1.5%) or KRG plus HAART (4.5%; Table 2) in our present study. If both PSCs and gross deletions are only defined as nonfunctional *vif* genes, the proportion of nonfunctional genes is 2.5% (7 of 275 genes) during KRG and 12.1% (19 of 157 genes) during KRG plus HAART ($P < 0.01$).

3.4. Position and Frequency of PSCs in the vif Gene. There are 8 tryptophan residues in the Vif protein. In this study, 15 *vif* genes from 5 patients (90-05, 90-18, 90-50, 93-04, and 93-60; Figure 3) demonstrated PSCs. The frequencies of the PSCs in 5 tryptophan residues (21, 38, 70, 89, and 174) were 3, 7, 13, 2, and 7, respectively. In the control group, one patient demonstrated stop codons at residues 21, 70, and 174 (JQ066980).

3.5. Small in-Frame Deletions Are Associated with KRG Intake. We did not find any specific changes in the nucleotide or amino acid sequences due to KRG intake. However, interestingly, two of our patients demonstrated small deletions during KRG intake; one patient (90-18) demonstrated a 9 bp in-frame deletion (detected in 15 of 26 amplicons) at amino acid positions 182–184 in April 1998, and another patient (92-13) demonstrated a 12 bp deletion (detected in 14 of 16 amplicons) at positions 186–189 in May 2005 (Figure 2). The frequencies of these deletions were similar between patients who received KRG (10.5%; 29 of 275 genes) and KRG plus HAART (15.9%; 25 of 157 genes). However, the frequency of these deletions was zero (0 of 52 genes, as determined using RT-PCR) during pre-KRG and 10.5% (29 of 275) during KRG only without HAART ($P < 0.01$). These deletions manifested after 6.3 and 12.0 years of KRG intake in patients 90-18 and 92-13, respectively. Interestingly, patient 90-18 also demonstrated a 6 bp deletion in the *nef* gene after 11 years of KRG intake with HAART, although we did not categorize this as a gross deletion [14]. Deletions were conserved during KRG plus HAART therapy (Figure 2) and comprised a higher proportion than wild-type alleles. In particular, three amplicons containing PSC also demonstrated small deletions in patient 90-18. The presence of both wild-type and mutant alleles in the same samples differed from the findings for the samples obtained from patients who were not treated with KRG, in which all amplicons contained deletions in five patients (data not shown). In addition, there were no such deletions in the control group (0 of 106 genes).

3.6. Overall Rate of Defective Genes. When we included small in-frame deletions of defective genes, the overall proportions of defective genes were 13.1% (36 of 275 genes) when receiving only KRG and 26.8% (42 of 157 genes) when receiving KRG plus HAART ($P < 0.01$). In our current study, the frequency of defective genes identified in PBMCs obtained from HIV-1-infected patients prior to receiving HAART was similar to the results of previous reports by Wieland et al. (10%) [23] and Sova et al. (13%) [24], although exceptional cases have been reported by Yamada and Iwamoto (20.5%) [25] and Tominaga et al. (31%) [26]. Overall, the proportions of defective genes identified in our present study were significantly lower than the proportions of defective *nef* (94 of 479 genes, including

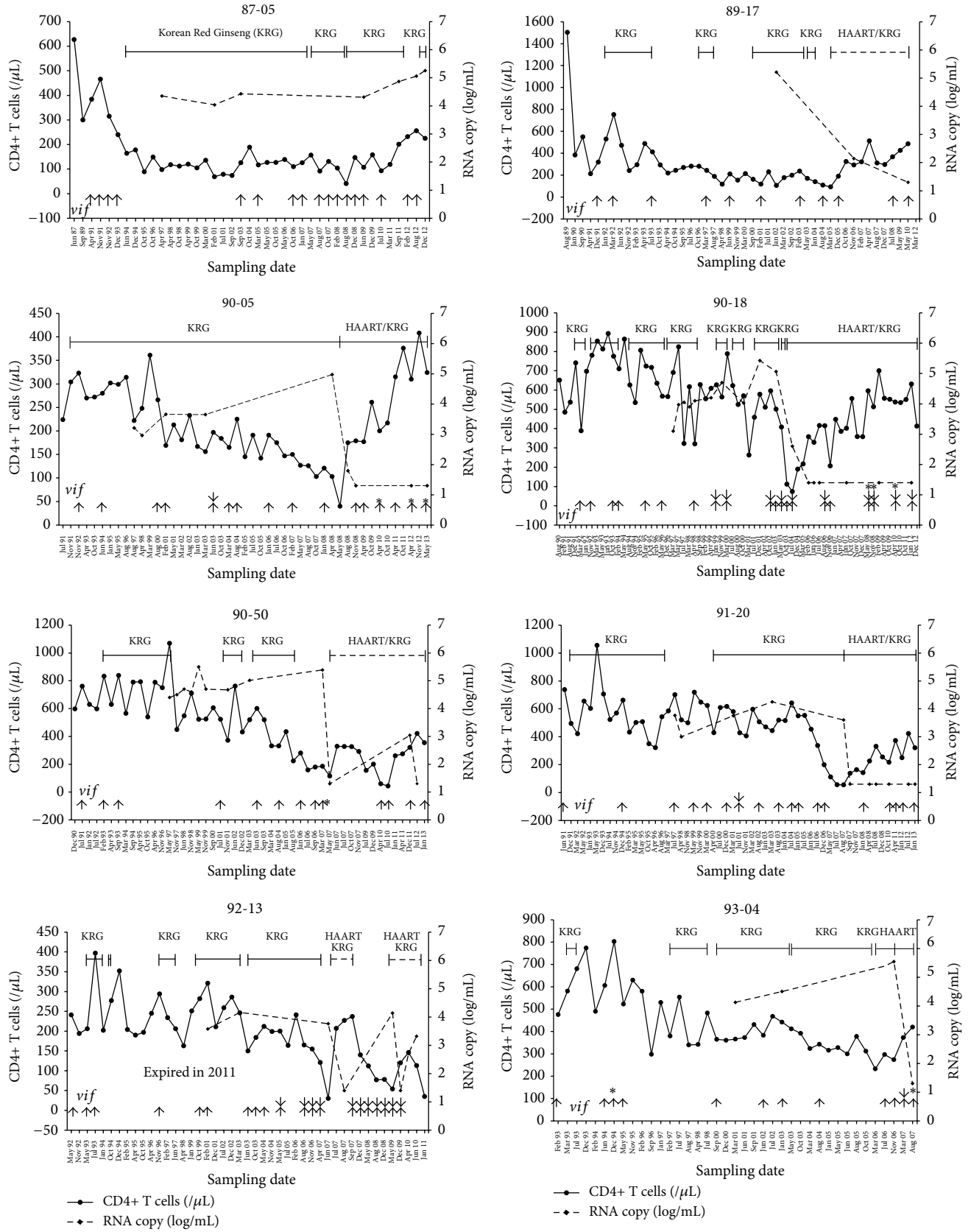

Figure 1: Continued.

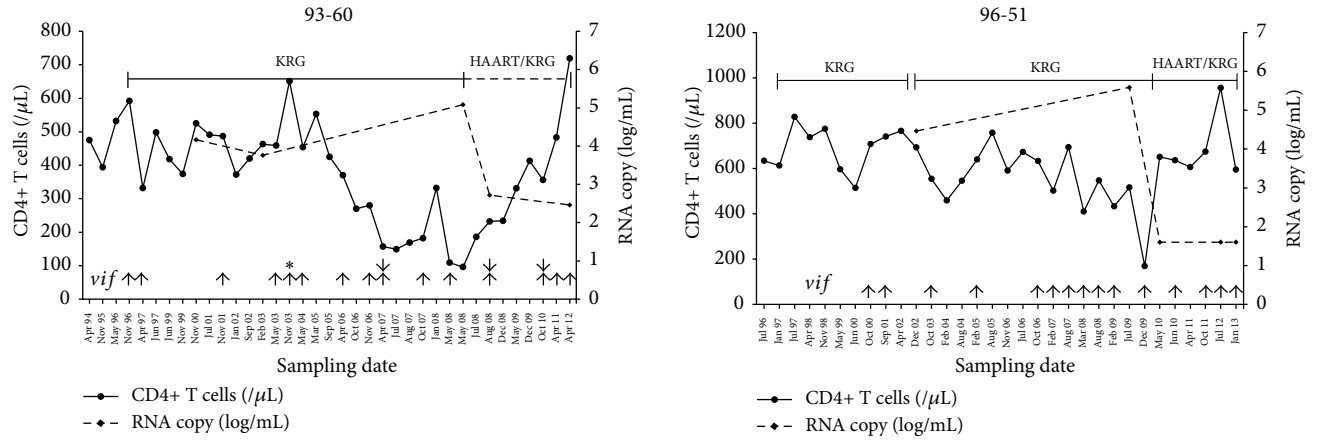

Figure 1: Changes in the CD4+ T-cell count, plasma viral load, and genetic defects in terms of Korean red ginseng (KRG) intake and highly active antiretroviral therapy (HAART). The durations of KRG intake and HAART are indicated by the bars. Solid and dotted lines denote good (>90%) and poor (<90%) compliance according to self-administered responses, respectively. The upward arrow (↑), downward arrow (↓), plus sign (+), and asterisk (∗) denote the sequences of the *vif* gene, gross deletions, 3- and- 6-base pair (bp) in-frame insertions, and stop codons, respectively.

Table 2: Distribution of defective *vif* gene.

Patient	On-KRG				On-HAART/KRG			
	No. of genes	Stop codon	gΔ	sΔ	No. of genes	Stop codon	gΔ	sΔ
87-05	20		1		ND	ND	ND	ND
89-17	9				9	0	0	0
90-05	37		1		18	4	0	0
90-18	35			15	20	3[a]	0	12[a]
90-50	14	1			15	0	0	0
91-20	35		1		20	0	0	0
92-13	53			14	22	0	0	13
93-04	18	1			12	5	1	0
93-60	28	1	1		20	0	6	0
96-51	26				21	0	0	0
Total	275	3[b]	4	29	157	12[b]	7	25

gΔ and sΔ denote gross deletion and in-frame small deletion, respectively.
HAART: highly active antiretroviral therapy; ND: not determined.
[a]Two out of three genes contained both stop codon and sΔ.
[b]$P < 0.01$.
$P < 0.01$ for the sum of 3 kinds of defective genes (36/275 versus 42/157).
Fifty-two *vif* genes at baseline obtained from serum using RT-PCR were all wild types. *Control patients ($n = 21$) revealed premature stop codon in one out of 106 *vif* genes.

stop codons; $P < 0.05$) and 5′ LTR/*gag* genes (71 of 189 genes; $P < 0.001$) identified in the same patients [14, 15].

4. Discussion

To date, we have identified the *vif* gene in 194 Korean patients. Of these, 145 patients were infected with the Korean subclade B of HIV-1 (KSB) and the remaining 49 patients were infected with non-KSB. Of these 194 patients, 10 demonstrated small in-frame deletions (3–15 bp) and all were diagnosed with KSB, whereas no such deletions were detected in non-KSB patients ($P = 0.068$). Of the 10 patients with small deletions, three patients were included in a group of 20 hemophiliacs who were infected with KSB from plasma donors O and P [16, 20]. Interestingly, plasma donors O and P revealed wild-type *vif* only between 1991 and 2002 (AY581320-21, JQ248127-33, JF957909, JF957921, JQ248134, and JF957935-37). In other words, original *vif* gene was wild type without in-frame small deletion. In our current study, only two patients (90-18 and 92-13) demonstrated 9 ($n = 15$) and 12 ($n = 14$) bp in-frame deletions in about two-thirds of the amplicons obtained after 6.3 and 12.0 years of KRG intake, respectively, whereas five patients without KRG intake demonstrated in-frame deletions in all amplicons (data not shown). To our knowledge, these in-frame deletions are very rare and have only been reported in two patients in other countries [26, 27].

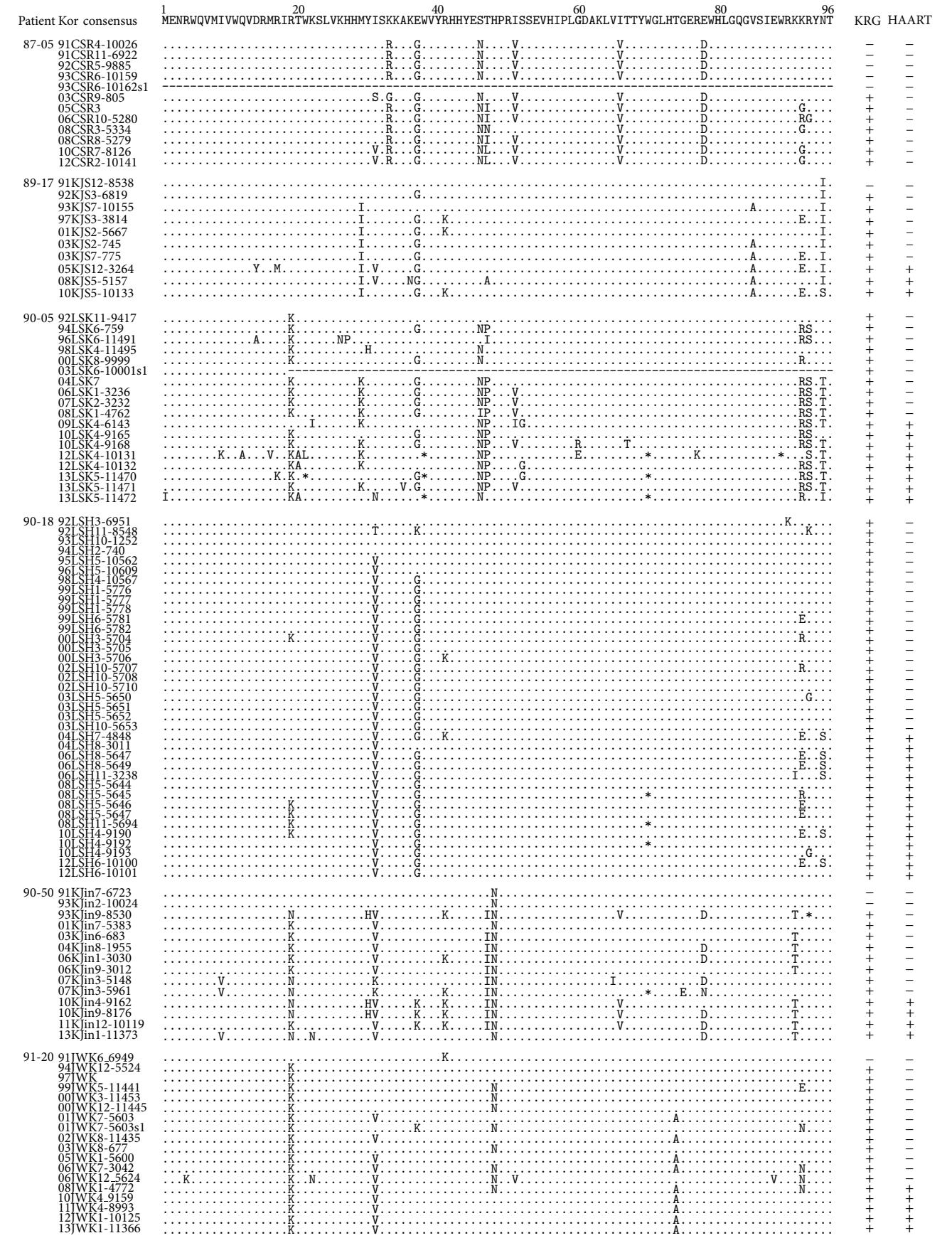

Figure 2: Continued.

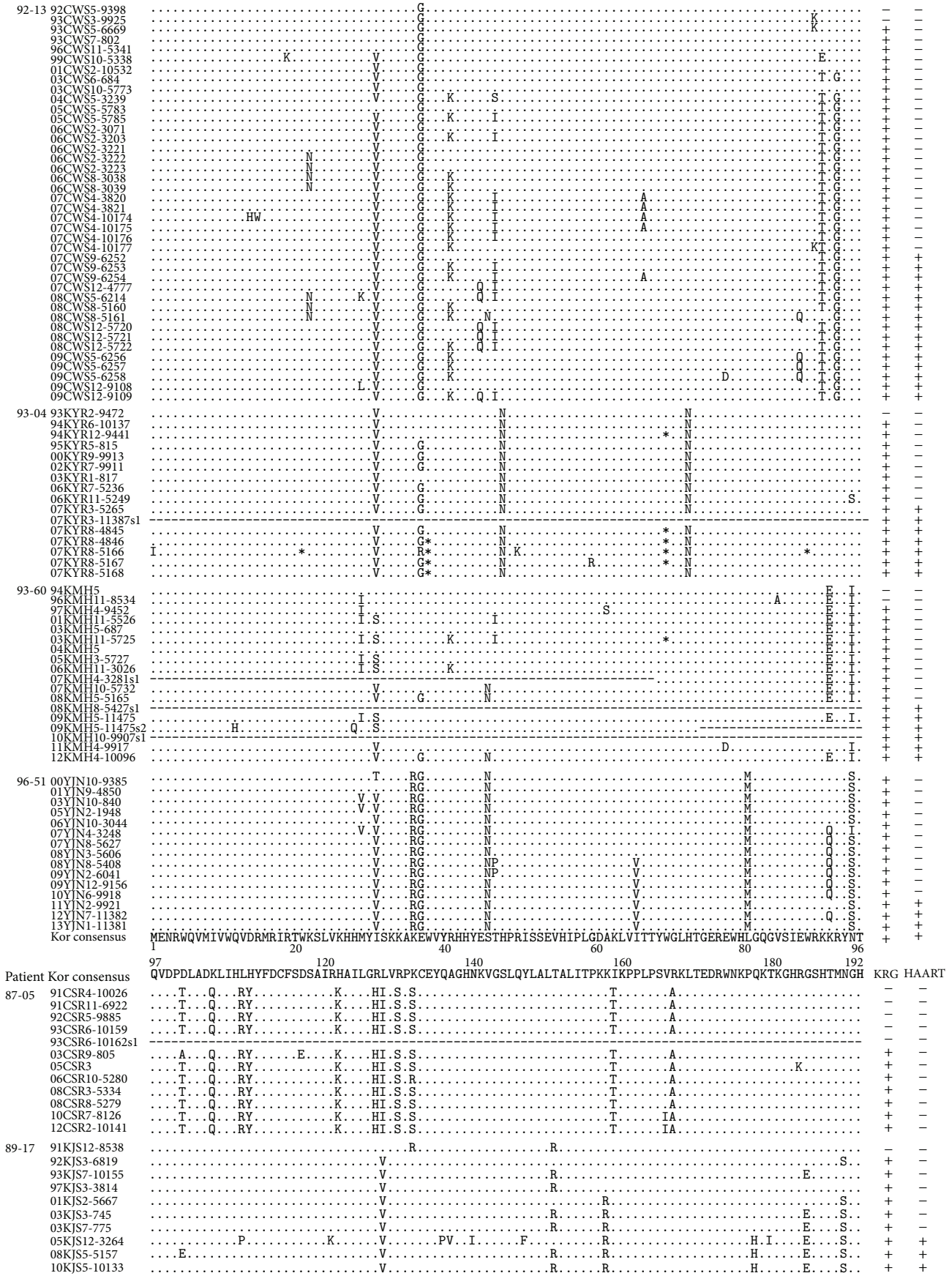

Figure 2: Continued.

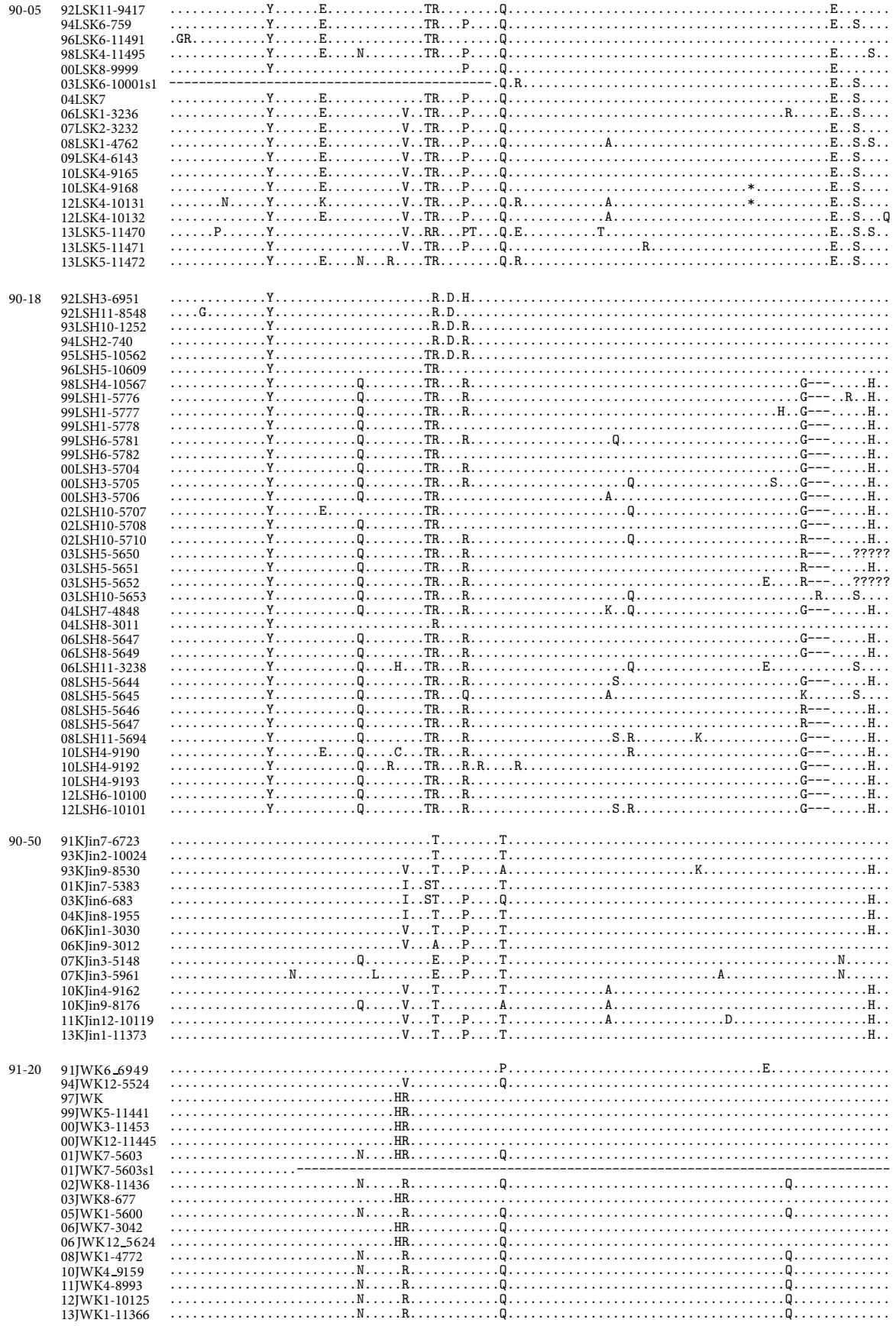

Figure 2: Continued.

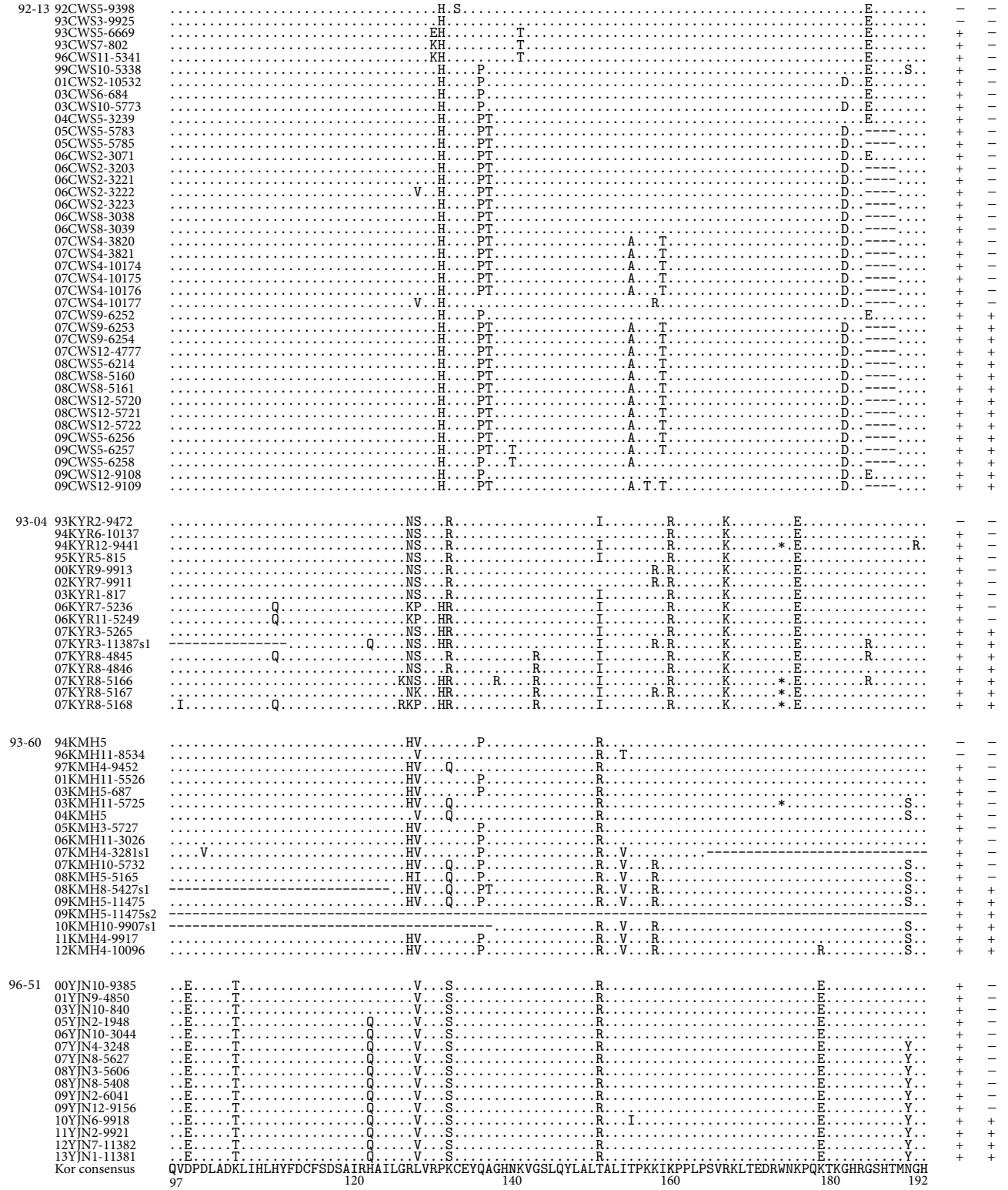

Figure 2: Sequential alignment of the amino acids of the Vif protein over 20 years. All sequences that demonstrated small in-frame deletions, gross deletions, and stop codons are depicted together with the baseline and last sequences of each patient. Patients 90-18 demonstrated a 9 bp deletion (positions 182–184) in April 1998, and patient 92-13 demonstrated a 12 bp deletion (positions 185–188) in May 2005. Patient 90-05 consistently demonstrated a 9 bp insertion (RQTRAR-RAR-NGASRP) at the same position at the terminus of *vpr* beginning in August 2000 (data not shown). The code 92LSH3-6951 (sampling year, initials of the patient, sampling month, and sequence number) denotes that the sampling date is March 1992 and the sequence number is 6951 in patient LSH (90-18). The dot (·), hyphen (-), and asterisk (∗) denote sequence identity, deletions, and premature stop codons, respectively, compared with the Korean consensus [20]. In the right column, the plus (+) and minus (−) signs denote the presence or absence of the corresponding therapy, respectively.

Patient	WT nucleotide sequence no.	61 69 TGGAAAAGT	112 120 TGGGTCTAT	208 216 TGGGGTCTG	264 272 TGGAGGAAA	520 528 TGGAACAAG	Hypermut 2.0 *P* value
90-05	10LSK4-9168	. . . . .	. . . . .	. . . . .	. . . . . G	. A	<0.05
	12LSK4-10131	. A	. A	. A A	. A	. A	<0.001
	13LSK5-11470	. . A	. A	. A	. . . . .	. . . . .	0.15
	13LSK5-11472	. . . . .	. . A	. A A	. . . . .	. . . . .	<0.01
90-18	08LSH5-5645	. . . . .	. . . . .	. A A	. . . . .	. . . . .	0.19
	08LSH11-5694	. . . . .	. . . . .	. . A	. . . . .	. . . . .	0.57
	10LSH4-9192	. . . . .	. . . . .	. A A	. . . . .	. . . . .	0.13
90-54	07KJin3-5961	. . . . .	. . . . .	. . A	. . . . .	. . . . .	0.06
93-04	94KYR12-9441	. . . . .	. . . . .	. A A	. . . . .	. A . . . . G . .	0.09
	07KYR8-5166	. A	. A	. A A	. A	. A . . . . G . .	<0.001
	07KYR8-4846	. . . . .	. A	. A A	. . . . .	. . . . . G . .	0.05
	07KYR8-5167	. . . . .	. A	. . A	. . . . . A . . .	. A . . . . G . .	0.05
	07KYR8-5168	. . . . .	. A	. . . . .	. . . . . A . . .	. A . . . . G . .	0.29
	07KYR8-4845	. . . . .	. . . . .	. A A	. . . . .	. . . . . G . .	0.05
93-60	03KMH11-5725	. . . . .	. . . . .	. A A	. . . . .	. A	0.15
		21 22 23	38 39 40	70 71 72	89 90 91	174 175 176	
	WT amino acid	W K S	W V Y	W G L	W R K	W N K	

Figure 3: Positions of the premature stop codons in the 15 *vif* genes from five patients. All stop codons resulted from GG → GA or GG → AG changes. APOBEC3G exhibits an intrinsic preference for the second cytosine in a 5′CC dinucleotide motif leading to 5′GG-to-AG mutations [38].

In total, five of our patients demonstrated in-frame deletions of the *vif* gene of the 75 KSB-infected patients who were treated with KRG. Also in our present study cohort, five patients, including 90-18 and 92-13, demonstrated deleted *vif* genes (small in-frame and gross deletions) during KRG intake, whereas all of our 10 LTSP patients demonstrated deletions in the *nef* gene ($P < 0.05$) [14]. In addition, compared with the reported deletions of the *nef* and 5′ LTR/*gag* genes, the locations of the deleted *vif* gene were positioned within a narrow range at the terminus [15, 16, 23].

Regarding gross deletions, to date, only two patients have demonstrated gross deletions in the *vif* gene [17, 18] and only one patient has demonstrated the insertion of two amino acids, and these patients were part of a nonprogressing mother-child pair [28]. However, in our present study, of the 10 LTSP patients who were assessed, four patients demonstrated gross deletion in the *vif* gene during KRG intake prior to receiving HAART (1.5%). This frequency is significantly lower than the previously reported incidence of 10 of 10 patients demonstrating gross deletions in the *nef* (18.7%) and 5′ LTR/*gag* genes (37.6%; $P < 0.01$) [27, 28]. The frequency of deletion in the *nef* gene was reported to significantly decrease during KRG plus HAART ($P < 0.01$) [16]. In contrast to previous studies on the *nef* and *gag* genes [16, 29], the detection of in-frame deletions in the *vif* gene was not suppressed in the patients receiving HAART in our present cohort. The reasons for this include the following: (1) the proportion and frequency (approximately two-thirds) of deleted *vif* genes after the first occurrence were much higher than in the *nef* and 5′ LTR/*gag* genes (<20 and 30%, resp.); (2) small deletions in the *vif* gene occurred as a single band, whereas gross deletions in the *nef* and 5′ LTR/*gag* genes were mainly detected as two bands (wild type and short) per PCR reaction; and (3) the number of amplicons indicating PSC due to G-to-A hypermutation was significantly higher in patients receiving KRG plus HAART than patients receiving only KRG. This phenomenon is consistent with our previous data in 5′ LTR/*gag* gene [29]. However, the frequency of G-to-A hypermutation was significantly lower in *vif* gene than that in 5′ LTR/*gag* gene [29]. Thus, for the *vif* gene, the detection of small deletions might be less affected by limit-diluting effects, as has been shown for the *nef* gene [29]. Taken together, these additional defects in the *vif* genes in the same patients might be related to the replicative impairment in *vif* defective HIV-1, which ultimately results in defects in the synthesis of viral DNA [30].

In our present study, it appears that the frequency of hypermutation was higher in patients who maintained good compliance with HAART during HAART plus KRG (90-05, 90-18, and 93-04) than in the patients who demonstrated poor compliance (Figure 1). In our extended data analysis, 12.4% (60/485), 3.1% (5/161), 3.0% (19/617), and 0.9% (1/108) of *vif* genes during KRG plus HAART, HAART alone, KRG alone, and control revealed PSC, respectively. These data indicate the presence of synergistic effect of KRG plus HAART on PSC ($P < 0.01$). There was no case that small deletions were induced by HAART alone. About 6–43% of the integrated proviral *pol* gene is hypermutated by HAART [22, 31, 32], although hypermutated viral genomes are not present in plasma [32].

ApoBec3G-induced hypermutation in LTNPs has been reported previously [33]. Indeed, it has been reported also that LTNP patients harbor PSC-containing *vif* genes more frequently than progressors [25], although the reported frequencies of defective genes vary among studies [34]. In our current analyses, *vif* gene-containing PSC due to G-to-A hypermutation was found to be significantly higher during KRG plus HAART than only KRG intake prior to HAART. This finding is consistent with our previous data obtained from a cohort of the Korean hemophiliacs (2.1% incidence

of G-to-A hypermutation while receiving only KRG versus 9.8% on KRG plus HAART; unpublished data) and other observations regarding the *pol* gene [22].

Previous studies report that certain *vif* mutations, such as L81 M, R132S, S130I, and the insertion of two amino acids, are associated with slow progression or low viral loads [17, 18, 28]. In our present study, L81 M [35] and R132S were consistently detected in patient 96-51 and patients 87-05 and 96-51, respectively, although both mutations were found in only in 2 and 3 of 169 Korean patients, respectively. Although the *vif* gene is highly conserved in HIV-1 genomes, the recovery of hypermutants might be severely underestimated in our present analysis because of the primer mismatching and the difficulties involved in detection following amplification [36, 37]. Overall, our current data suggest that small in-frame deletion and PSCs are associated with KRG intake and HAART, respectively, although further studies are needed.

5. Conclusions

Our data suggest that HAART and KRG intake might induce PSCs and small in-frame deletions, respectively.

Conflict of Interests

The authors have no conflict of interests to declare.

Acknowledgments

This work was supported by a grant from the Korean Society of Ginseng (2010–2012). The authors thank Professor Seung-Chul Yun, the Division of Biostatistics, University of Ulsan College of Medicine, Asan Medical Center, for the statistical consultation.

References

[1] E. Ernst, "*Panax ginseng*: an overview of the clinical evidence," *Journal of Ginseng Research*, vol. 34, no. 4, pp. 259–263, 2010.

[2] K. T. Choi, "Botanical characteristics, pharmacological effects and medicinal components of Korean *Panax ginseng* C A Meyer," *Acta Pharmacologica Sinica*, vol. 29, no. 9, pp. 1109–1118, 2008.

[3] S. J. Fulder, "Ginseng and the hypothalamic-pituitary control of stress," *The American Journal of Chinese Medicine*, vol. 9, no. 2, pp. 112–118, 1981.

[4] V. K. Singh, S. S. Agarwal, and B. M. Gupta, "Immunomodulatory activity of *Panax ginseng* extract," *Planta Medica*, vol. 50, no. 6, pp. 462–465, 1984.

[5] X. Song and S. Hu, "Adjuvant activities of saponins from traditional Chinese medicinal herbs," *Vaccine*, vol. 27, no. 36, pp. 4883–4890, 2009.

[6] D. G. Yoo, M. C. Kim, M. K. Park et al., "Protective effect of ginseng polysaccharides on influenza viral infection," *PLoS ONE*, vol. 7, no. 3, Article ID e33678, 2012.

[7] H. X. Sun, Y. P. Ye, H. J. Pan, and Y. J. Pan, "Adjuvant effect of *Panax notoginseng* saponins on the immune responses to ovalbumin in mice," *Vaccine*, vol. 22, no. 29-30, pp. 3882–3889, 2004.

[8] J. Sun, S. Hu, and X. Song, "Adjuvant effects of protopanaxadiol and protopanaxatriol saponins from ginseng roots on the immune responses to ovalbumin in mice," *Vaccine*, vol. 25, no. 6, pp. 1114–1120, 2007.

[9] P. W. Hunt, "HIV and inflammation: mechanisms and consequences," *Current HIV/AIDS Reports*, vol. 9, no. 2, pp. 139–147, 2012.

[10] T. Yayeh, K. H. Jung, H. Y. Jeong et al., "Korean red ginseng saponin fraction downregulates proinflammatory mediators in LPS stimulated RAW264. 7 cells and protects mice against endotoxic shock," *Journal of Ginseng Research*, vol. 36, no. 3, pp. 263–269, 2012.

[11] A. T. Smolinski and J. J. Pestka, "Modulation of lipopolysaccharide-induced proinflammatory cytokine production in vitro and in vivo by the herbal constituents apigenin (chamomile), ginsenoside Rb1 (ginseng) and parthenolide (feverfew)," *Food and Chemical Toxicology*, vol. 41, no. 10, pp. 1381–1390, 2003.

[12] A. Rhule, S. Navarro, J. R. Smith, and D. M. Shepherd, "*Panax notoginseng* attenuates LPS-induced pro-inflammatory mediators in RAW264.7 cells," *Journal of Ethnopharmacology*, vol. 106, no. 1, pp. 121–128, 2006.

[13] J. M. Brenchley, D. A. Price, T. W. Schacker et al., "Microbial translocation is a cause of systemic immune activation in chronic HIV infection," *Nature Medicine*, vol. 12, no. 12, pp. 1365–1371, 2006.

[14] Y. K. Cho, J. Y. Lim, Y. S. Jung, S. K. Oh, H. J. Lee, and H. Sung, "High frequency of grossly deleted *nef* genes in HIV-1 infected long-term slow progressors treated with Korean red ginseng," *Current HIV Research*, vol. 4, no. 4, pp. 447–457, 2006.

[15] Y. K. Cho and Y. S. Jung, "High frequency of gross deletions in the 5′ LTR and *gag* regions in HIV type 1-infected long-term survivors treated with Korean red ginseng," *AIDS Research and Human Retroviruses*, vol. 24, no. 2, pp. 181–193, 2008.

[16] Y. K. Cho, Y. S. Jung, and H. S. Sung, "Frequent gross deletion in the HIV type 1 *nef* gene in hemophiliacs treated with korean red ginseng: inhibition of detection by highly active antiretroviral therapy," *AIDS Research and Human Retroviruses*, vol. 25, no. 4, pp. 419–424, 2009.

[17] V. Sandonís, C. Casado, T. Alvaro et al., "A combination of defective DNA and protective host factors are found in a set of HIV-1 ancestral LTNPs," *Virology*, vol. 391, no. 1, pp. 73–82, 2009.

[18] H. R. Rangel, D. Garzaro, A. K. Rodríguez et al., "Deletion, insertion and stop codon mutations in *vif* genes of HIV-1 infecting slow progressor patients," *Journal of Infection in Developing Countries*, vol. 3, no. 7, pp. 531–538, 2009.

[19] Y. K. Cho, J. E. Kim, and B. T. Foley, "Phylogenetic analysis of near full-length HIV-1 genomic sequences in 21 Korean individuals," *AIDS Research and Human Retroviruses*, vol. 29, no. 4, pp. 738–743, 2013.

[20] Y. K. Cho, Y. S. Jung, J. S. Lee, and B. T. Foley, "Molecular evidence of HIV-1 transmission in 20 Korean individuals with haemophilia: phylogenetic analysis of the *vif* gene," *Haemophilia*, vol. 18, no. 2, pp. 291–299, 2012.

[21] P. P. Rose and B. T. Korber, "Detecting hypermutations in viral sequences with an emphasis on G → A hypermutation," *Bioinformatics*, vol. 16, no. 4, pp. 400–401, 2000.

[22] S. Fourati, S. Lambert-Niclot, C. Soulie et al., "HIV-1 genome is often defective in PBMCs and rectal tissues after long-term HAART as a result of APOBEC3 editing and correlates with the size of reservoirs," *Journal of Antimicrobial Chemotherapy*, vol. 67, no. 10, pp. 2323–2326, 2012.

[23] U. Wieland, A. Seelhoff, A. Hofmann et al., "Diversity of the vif gene of human immunodeficiency virus type 1 in Uganda," *Journal of General Virology*, vol. 78, no. 2, pp. 393–400, 1997.

[24] P. Sova, M. van Ranst, P. Gupta et al., "Conservation of an intact human immunodeficiency virus type 1 *vif* gene in vitro and in vivo," *Journal of Virology*, vol. 69, no. 4, pp. 2557–2564, 1995.

[25] T. Yamada and A. Iwamoto, "Comparison of proviral accessory genes between long-term nonprogressors and progressors of human immunodeficiency virus type 1 infection," *Archives of Virology*, vol. 145, no. 5, pp. 1021–1027, 2000.

[26] K. Tominaga, S. Kato, M. Negishi, and T. Takano, "A high frequency of defective vif genes in peripheral blood mononuclear cells from HIV type 1-infected individuals," *AIDS Research and Human Retroviruses*, vol. 12, no. 16, pp. 1543–1549, 1996.

[27] Y. K. Cho, H. Sung, I. G. Bae et al., "Full sequence of HIV type 1 Korean subtype B in an AIDS case with atypical seroconversion: TAAAA at TATA box," *AIDS Research and Human Retroviruses*, vol. 21, no. 11, pp. 961–964, 2005.

[28] L. Alexander, M. J. Aquino-DeJesus, M. Chan, and W. A. Andiman, "Inhibition of human immunodeficiency virus type 1 (HIV-1) replication by a two-amino-acid insertion in HIV-1 Vif from a nonprogressing mother and child," *Journal of Virology*, vol. 76, no. 20, pp. 10533–10539, 2002.

[29] Y. K. Cho, Y. S. Jung, H. S. Sung, and C. H. Joo, "Frequent genetic defects in the HIV-1 5′LTR/*gag* gene in hemophiliacs treated with Korean red ginseng: decreased detection of genetic defects by highly active antiretroviral therapy," *Journal of Ginseng Research*, vol. 35, no. 4, pp. 413–420, 2011.

[30] M. Nascimbeni, M. Bouyac, F. Rey, B. Spire, and F. Clavel, "The replicative impairment of Vif-mutants of human immunodeficiency virus type 1 correlates with an overall defect in viral DNA synthesis," *Journal of General Virology*, vol. 79, no. 8, pp. 1945–1950, 1998.

[31] J. P. Vartanian, M. Henry, and S. Wain-Hobson, "Sustained G → A hypermutation during reverse transcription of an entire human immunodeficiency virus type 1 strain Vau group O genome," *Journal of General Virology*, vol. 83, no. 4, pp. 801–805, 2002.

[32] T. L. Kieffer, P. Kwon, R. E. Nettles, Y. Han, S. C. Ray, and R. F. Siliciano, "G → A hypermutation in protease and reverse transcriptase regions of human immunodeficiency virus type 1 residing in resting $CD4^+$ T cells in vivo," *Journal of Virology*, vol. 79, no. 3, pp. 1975–1980, 2005.

[33] B. Wang, M. Mikhail, W. B. Dyer, J. J. Zaunders, A. D. Kelleher, and N. K. Saksena, "First demonstration of a lack of viral sequence evolution in a nonprogressor, defining replication-incompetent HIV-1 infection," *Virology*, vol. 312, no. 1, pp. 135–150, 2003.

[34] G. Hassaine, I. Agostini, D. Candotti et al., "Characterization of human immunodeficiency virus type 1 *vif* gene in long-term asymptomatic individuals," *Virology*, vol. 276, no. 1, pp. 169–180, 2000.

[35] F. A. de Maio, C. A. Rocco, P. C. Aulicino, R. Bologna, A. Mangano, and L. Sen, "Unusual substitutions in HIV-1 Vif from children infected perinatally without progression to AIDS for more than 8 years without therapy," *Journal of Medical Virology*, vol. 84, no. 12, pp. 1844–1852, 2012.

[36] M. Janini, M. Rogers, D. R. Birx, and F. E. McCutchan, "Human immunodeficiency virus type 1 DNA sequences genetically damaged by hypermutation are often abundant in patient peripheral blood mononuclear cells and may be generated during near-simultaneous infection and activation of $CD4^+$ T cells," *Journal of Virology*, vol. 75, no. 17, pp. 7973–7986, 2001.

[37] G. H. Kijak, L. M. Janini, S. Tovanabutra et al., "Variable contexts and levels of hypermutation in HIV-1 proviral genomes recovered from primary peripheral blood mononuclear cells," *Virology*, vol. 376, no. 1, pp. 101–111, 2008.

[38] E. W. Refsland, J. F. Hultquist, and R. S. Harris, "Endogenous origins of HIV-1 G-to-A hypermutation and restriction in the nonpermissive T cell line CEM2n," *PLoS Pathogens*, vol. 8, no. 7, Article ID e1002800, 2012.

Hindawi Publishing Corporation
Evidence-Based Complementary and Alternative Medicine
Volume 2013, Article ID 907016, 8 pages
http://dx.doi.org/10.1155/2013/907016

Research Article

Anti-Inflammatory Effect of Qingpeng Ointment in Atopic Dermatitis-Like Murine Model

Yun-Zhu Li, Xue-Yan Lu, Wei Jiang, and Lin-Feng Li

Department of Dermatology, Peking University Third Hospital, 49 North Garden Road, Haidian District, Beijing 100191, China

Correspondence should be addressed to Lin-Feng Li; zoonli@sina.com

Received 27 May 2013; Revised 8 July 2013; Accepted 22 July 2013

Academic Editor: K. B. Harikumar

Qingpeng ointment (QP) is a Chinese medicine which has been used in treatment of atopic dermatitis (AD) in China. AD-like lesions were induced in BALB/c mice by repeated application of 2,4-dinitrofluorobenzene (DNFB) on shaved backs. The mice were then treated for 2 weeks with QP of different concentrations and Mometasone Furoate cream (MF), respectively. Macroscopic and microscopic changes of the skin lesions were observed after the treatment. The levels of serum immunoglobulin (Ig) E, tissue interferon (IFN)-γ, and interleukin (IL)-4 and IL-17A and the levels of involucrin, filaggrin, and kallikrein7 in epidermis were measured. The results show severe dermatitis with immune profiles similar to human acute AD. A significant infiltration of $CD4^+$ T and mast cells was observed in dermis of lesion but inhibited by QP after a 2-week treatment with it. The production of IgE, IL-4 and the mRNA expression of IL-17A were also suppressed, but the level of IFN-γ was increased. MF suppressed all production of these cytokines and IgE. Accordingly, the mechanism of QP on AD might correlate with its ability of modulating the immune dysfunctions rather than suppressing them. It had no effect on expressions of involucrin and filaggrin, except that its vehicle decreased the level of kallikrein7.

1. Introduction

Atopic dermatitis (AD), also known as atopic eczema, is a common inflammatory skin disease. The pathogenesis of AD has been attributed largely to abnormalities in the adaptive immune system. The dysfunction of T helper (Th) cells and IgE production may play key roles on it [1–3]. The haptens such as 2,4-dinitrofluorobenzene (DNFB) are used to induce model of murine contact hypersensitivity (MCH). In certain conditions, MCH can generate AD-like lesions and immune responses with Th1 and/or Th2 type inflammation [4]. Therefore, it is often used to study drug mechanism on AD [5–13]. In this work, we repeated applying DNFB as a hapten to induce AD-like lesions in BALB/c mice for research of drug mechanism on AD.

Qingpeng ointment (QP) is a traditional Chinese medicine which has been used in treatment of AD in China. Clinical studies including a multicentered, randomized, double-blind, placebo-controlled study had shown that QP is effective in the treatment of eczema [14]. However, the mechanism of its action is still unclear. In this study, the inflammation of the lesion was observed macroscopically and microscopically to research the anti-inflammatory effect of QP. Skin barrier function is recently considered to play important roles in the pathogenesis of AD. The skin barrier related factors, including involucrin, filaggrin, and kallikrein7, take part in the procedure of skin keratinocyte proliferation and desquamation and they have been found to have significant abnormalities in AD patients [15–19]. These factors were also checked for evaluating the effect of QP on skin barrier function in this research.

Recent years, IL-17 (IL-17A), a new found cytokine, is reported probably playing a negative role in human AD [20]. In this work, the effect of QP treatment on expression of IL-17A was investigated. In addition, the Th1 type cytokine IFN-γ, Th2 type cytokine IL-4, and serum IgE were also analyzed to study its possible mechanisms on AD. As topical glucocorticosteroid agents were considered the first used medicine on AD in clinic, Mometasone Furoate cream (MF) treated mice were here used as positive controls in this research.

2. Methods and Materials

2.1. Animals. Female 8-week-old BALB/c mice (Vital River, China) were maintained under SPF conditions. Animals were housed in an air-conditioned animal room with a constant temperature of 23 ± 2°C and a relative humidity of 40 ± 5%. A standard diet and water were provided by the lab. The study was approved by the Institutional Animal Care and Use Committee of Peking University and experiments were conducted in accordance with the guidelines issued by the animal committee of Peking University Health Science Center for the care and use of laboratory animals.

2.2. Induction of Dermatitis and Experimental Schedule. The DNFB (Wako, Japan) was diluted in the mixture of acetone and olive oil (4 : 1). Then, the solution of DNFB (100 μL of 0.5% DNFB) was applied to the shaved backs of mice in the first week for sensitization. After that, 100 μL of 0.2% DNFB was applied twice a week for a further 4 weeks to develop lesions. The model was established at the end of 5th week. During the following experiments, the skin lesions would be re-challenged once one week later to maintain the inflammation. The normal group was applied with nothing during the whole procedure of experiment.

All mice were randomly divided into 7 groups (n = 18 for each group) including a normal group, a remained untreated group (model group), and 5 experimental groups. The experimental groups were then treated, respectively, with vehicle of QP, 50% QP in vehicle, 75% QP in vehicle, 100% QP, and Mometasone Furoate cream (MF) (ELOSON, Merck Sharp & Dohme, USA) for 2 weeks after the model was established. The executor had not been told the group names and drug names and the procedure of grouping and treatment with medicines were done in a blind miner. QP (Qingpeng Ruangao) and its vehicle were provided by Cheezheng Tibetan Medicine Company (Gansu, China) and its contents were given in Table 1. Analyses by liquid chromatography and gas chromatography-mass spectrometry at a laboratory in Fudan University (Shanghai, China) showed that no corticosteroid existed in this medicine (data not shown).

All animals were sacrificed at 24 h after the last treatment. Serum was collected and dorsal skin on fixed position of mice was biopsied for histopathology analysis and measurement of tissue cytokines levels.

2.3. Thickness of Skin. Thickness of dorsal skin was measured with a micrometer (Hautine International Co., China) before killed. For each mouse, 3 different sites of the back skin were measured randomly, and an average data was taken.

2.4. Evaluation of the Skin Lesions. Skin status of each group was photographed before and after the treatment. Skin lesions such as (1) erythem, (2) edema, and (3) scaling were scored as 0 (none), 1 (mild), 2 (moderate), and 3 (severe) as previous study reported [21]. The executor had not been told the group names and the procedure was done in a blind miner.

2.5. Histopathology Analysis. The inflammation of the dorsal skin was observed macroscopically and photographed before the mice were sacrificed. The paraffin sections of dorsal skin were dyed with hematoxylin-eosin staining (HE) and were observed under the microscope field of ×100 (Nikon E600).

Table 1: Ingredients of Qingpeng ointment (Cheezheng*).

Name	Dose (g)
Oxytropis falcata Bunge	100
Rheum lhasaense	50
Aconitum pendulum Busch	75
Chebulae Fructus (without core)	100
Terminaliae Belliricae Fructus	100
Phyllanthi Fructus	100
Benzoinum	35
Tinospora sinensis	150
Muscone	25
Vehicle (liquid paraffin, glycerol, emulsifier, water, etc.)	To 5000

*Standard number: Guo Jia Yao Pin Biao Zhun WS3-BC-0319-95-2009; license number: Guo Yao Zhun Zi Z54020140; quality was examined according to Pharmacopoeia of the People's Republic of China (Chinese Pharmacopoeia), Edition 2005, Part I, Appendices I R, VI B, and D.

2.6. $CD4^+$ T and Mast Cell Counts. The paraffin sections of dorsal skin were analyzed with immunohistology to investigate the effect of QP on $CD4^+$ T cell. The primary antibody for $CD4^+$ T cell (BS1617) was purchased from Bioworld Technology (USA). The secondary antibody (PV-6001) and DAB stain were purchased from Zhongshan Golden Bridge Biotechnology Company (Beijing, China). The stained sections were observed under the microscope field of ×200 (Nikon E600). Average $CD4^+$ T cell numbers in skin were measured by counting 5 different areas in each slide of skin (×200).

Mast cells of dermis were stained with toluidine blue and the section were observed under the microscope field of ×100 (Nikon E600). Average mast cell numbers were measured by counting 5 different areas in each slide of skin (×100).

2.7. Enzyme-Linked Immunosorbent Assay (ELISA). Levels of IL-4 and IFN-γ in the skin tissue and serum IgE level were measured with Enzyme-Linked Immunosorbent Assay (ELISA) kits (Dakewei Bio, China) according to the manufacturer's instruction.

2.8. RNA Isolation and Quantitative Real-Time Polymerase Chain Reaction. Total RNA from dorsal skin was extracted with Trizol (TransGen Bio, China), and then the RNA concentration was measured with ultraviolet spectrophotometer (Thermo, Germen). According to the manufacturer's protocol, separated total RNA was reverse transcribed into complementary DNA (cDNA) with EasyScript Frist-Strand cDNA Synthesis SuperMix (TransGen Bio, China). After cDNA samples were diluted 20 times with distilled water, we mixed cDNA sample, primers (Table 2), distilled water, and the SYBR Premix Ex Taq (TaKaRa Bio, Dalian) into

Table 2: Primers of quantitative real-time polymerase chain reaction.

Gene symbol	Primers	GC (%)	T_m (°C)
β-actin	F: 5′-GCT TCT TTG CAG CTC CTT CGT	52.3	59.8
	R: 5′-AGC GCA GCG ATA TCG TCA TC	55	62
IL-17A	F: 5′-CTC ACC CGT TCC ACG TCA CCC T	59.1	63.8
	R: 5′-CCA GCT TTC CCT CCG CAT T	57.9	59.7

a 20 μL reaction system. The quantitative real-time PCR was performed in iQ5 real-time PCR system (Bio Rad, USA). The β-actin gene was used as an endogenous control to normalize the mRNA expression of IL-17A. Primers for IL-17A and β-actin synthesised by Sagon Bio of China were according to previous researches [22]. The results of PCR were calculated and analyzed with method of relative quantification [23]. The results of CT values were transferred into $2^{-\Delta\Delta CT}$.

2.9. Skin Keratinocyte Proliferation and Desquamation-Related Proteins. The expressions of involucrin, filaggrin, and kallikrein7 in epidermis were measured with method of immunohistology. The primary antibodies for involucrin (ad28057) and filaggrin (ad24584) were both purchased from Abcam Company (UK). The primary antibody for kallikrein7 (sc-20381) was purchased from Santa Cruz company (USA). The secondary antibodies (PV-6001, PV-6002, and PV-9003) and DAB stain were all purchased from Zhongshan Golden Bridge Biotechnology company (Beijing, China). The dyed sections were observed under the microscope field of ×100 (Nikon E600). The mean values of optical density (OD) of stained epidermis of each mouse were measured and analyzed with software of Image-Pro Plus 6.0.

2.10. Statistical Analysis. The statistical analysis was performed with SPSS of version 16.0. All data that followed a normal distribution was tested with *T* test or Least Significant difference (LSD) test of one way ANOVA. A *P* value less than 0.05 was considered significant.

3. Results

3.1. Skin Inflammation and Histological Analysis. The inflammation of model group was more obvious than other groups with severe erythema, desquamation, and crusting. The inflammation of all treatment groups was decreased. Similar to MF, the dorsal skin of 100% QP treated group was almost normal. The histopathology of skin lesions showed thickening of the epidermis and inflammatory cell accumulation in model group, but QP administration clearly inhibited DNFB-induced inflammation in a dose-related pattern (Figure 1) (Table 3).

3.2. $CD4^+$ T and Mast Cell Counts. $CD4^+$ T cells in dermis accumulated in model group, but QP administration clearly inhibited the accumulation in a dose-related pattern. Compared with normal group, mast cell counts were also increased in model group ($P < 0.01$), whereas they declined in 50%, 75%, and 100% QP treated groups compared with vehicle treated group and model group. But there were no significant differences between 50%, 75%, and 100% QP treated groups (Figure 2).

Table 3: Evaluation of the skin lesions and the thickness of skin.

	Score of the skin lesions	Thickness of skin (mm)
Normal	$0 \pm 0^{**}$	$0.35 \pm 0.06^{**}$
Model	8.33 ± 0.52	1.07 ± 0.18
Vehicle	7.83 ± 0.41	1.06 ± 0.07
50% QP	$5.50 \pm 1.05^{**}$	$0.95 \pm 0.03^{*}$
75% QP	$3.17 \pm 0.75^{**}$	$0.87 \pm 0.08^{**}$
100% QP	$0.50 \pm 0.55^{**}$	$0.44 \pm 0.06^{**}$
MF	$0.67 \pm 0.52^{**}$	$0.43 \pm 0.01^{**}$

Values are presented as mean ± SEM. $^{*}P < 0.05$, $^{**}P < 0.01$ versus model group. QP: Qingpeng ointment; MF: Mometasone Furoate cream. Skin lesions such as (1) erythema, (2) edema, and (3) scaling were scored as 0 (none), 1 (mild), 2 (moderate), and 3 (severe). Thickness of skin was randomly measured with 3 different sites of the back. Total data was calculated for each mouse, and the average values were taken to be analyzed.

3.3. Enzyme-Linked Immunosorbent Assay. The level of serum IgE was significantly elevated in model group, but decreased gradually in QP treated groups (50%, 75%, and 100% QP treated groups) with the elevation of drug concentration. Serum IgE of MF treated group was lower than model group but higher than 100% QP treated group ($P < 0.01$) (Figure 3(a)).

The level of IFN-γ of skin tissue in model group decreased significantly ($P < 0.01$), while that in QP treated groups increased gradually along with elevation of drug concentration. The levels of IgE and IFN-γ changed significantly between 100% QP group and model group ($P < 0.05$) (Figures 3(a) and 3(b)).

The level of IL-4 in 100% QP treated group was lower than that of model group ($P < 0.01$) but almost similar to normal group and MF treated group ($P > 0.05$). The IL-4 level of QP treated groups decreased gradually with elevation of drug concentration (Figure 3(c)).

3.4. The mRNA Expression of IL-17A. The result of quantitative real-time PCR shows that mRNA level of IL-17A increased in model group but decreased after QP administration ($P < 0.01$). MF can also decrease the IL-17A expression ($P < 0.05$) on DNFB-induced skin lesion (Figure 4).

3.5. Expressions of Involucrin, Filaggrin, and Kallikrein7. Compared with normal skin, the expressions of involucrin and filaggrin of dermis in model group were decreased,

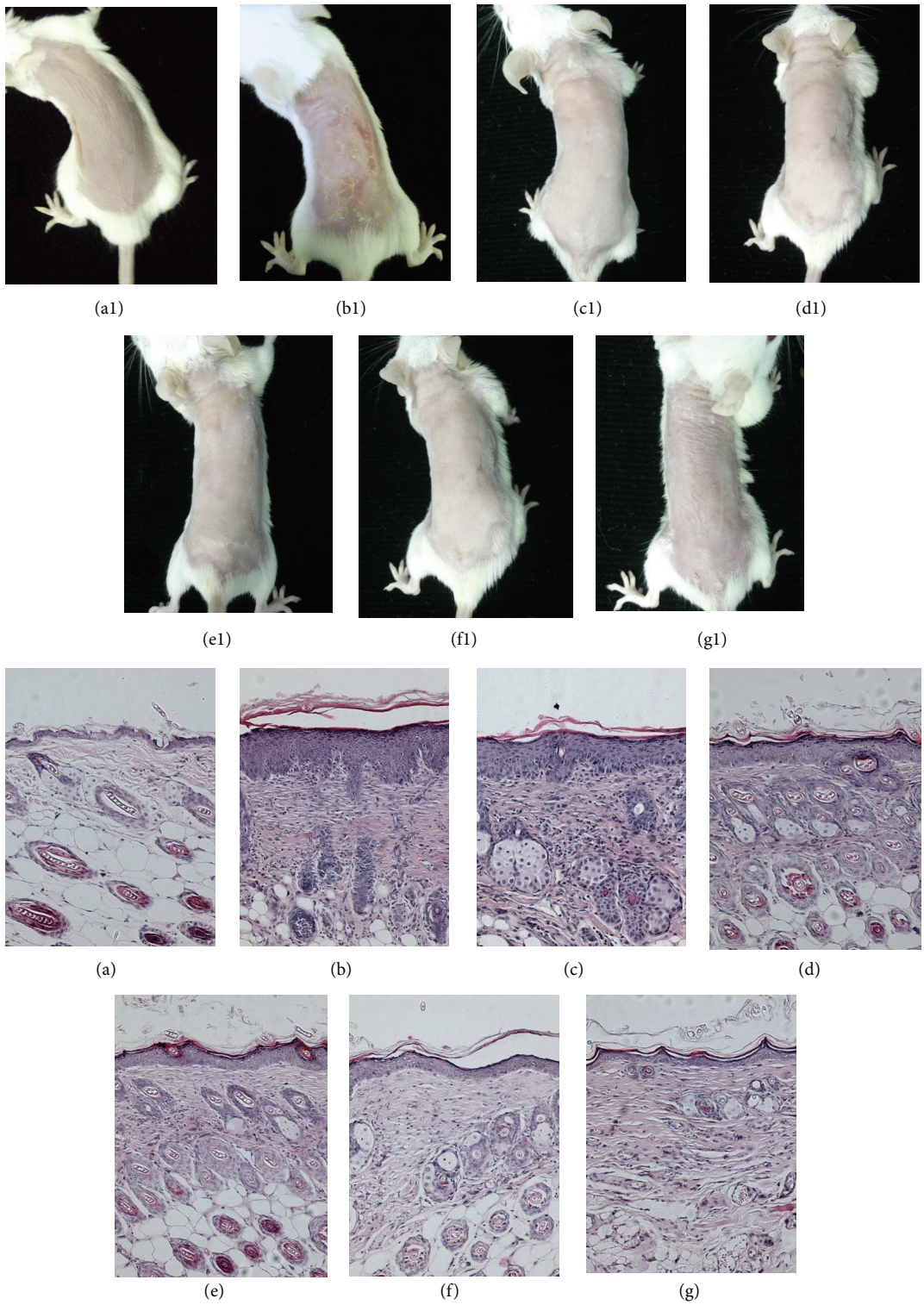

Figure 1: Comparisons of AD-like skin lesions in BALB/c mice after a 2-week treatment. (a1) Normal mouse; (b1) model mouse; (c1) mouse treated with vehicle; (d1) 50% QP-treated mouse; (e1) 75% QP-treated mouse; (f1) 100% QP-treated mouse; (g1) MF-treated mouse. (a)–(g) were histopathology of corresponding skin. Significant erythema, desquamation, and crusting could be seen on the dorsal skin of model group and lessened significantly in all treated groups. Thickening of the epidermis and inflammatory cell accumulation could be seen in model group but was relieved in QP-treated groups in a dose-related pattern. QP: Qingpeng ointment; MF: Mometasone Furoate cream.

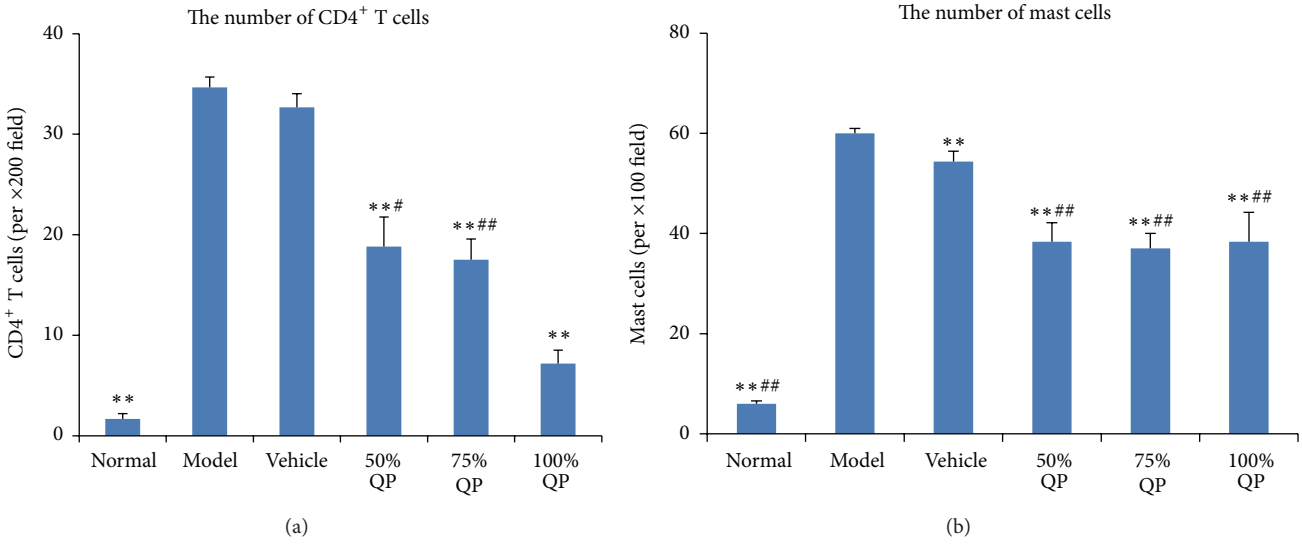

Figure 2: Comparisons of CD4$^+$ T cell counts (×200) and mast cell counts (×100) with the treatment of QP. (a) The number of CD4$^+$T cells; (b) the number of mast cells. $^{**}P < 0.01$ versus model group. QP: Qingpeng ointment. $^{\#}P < 0.05$, $^{\#\#}P < 0.01$ versus QP vehicle.

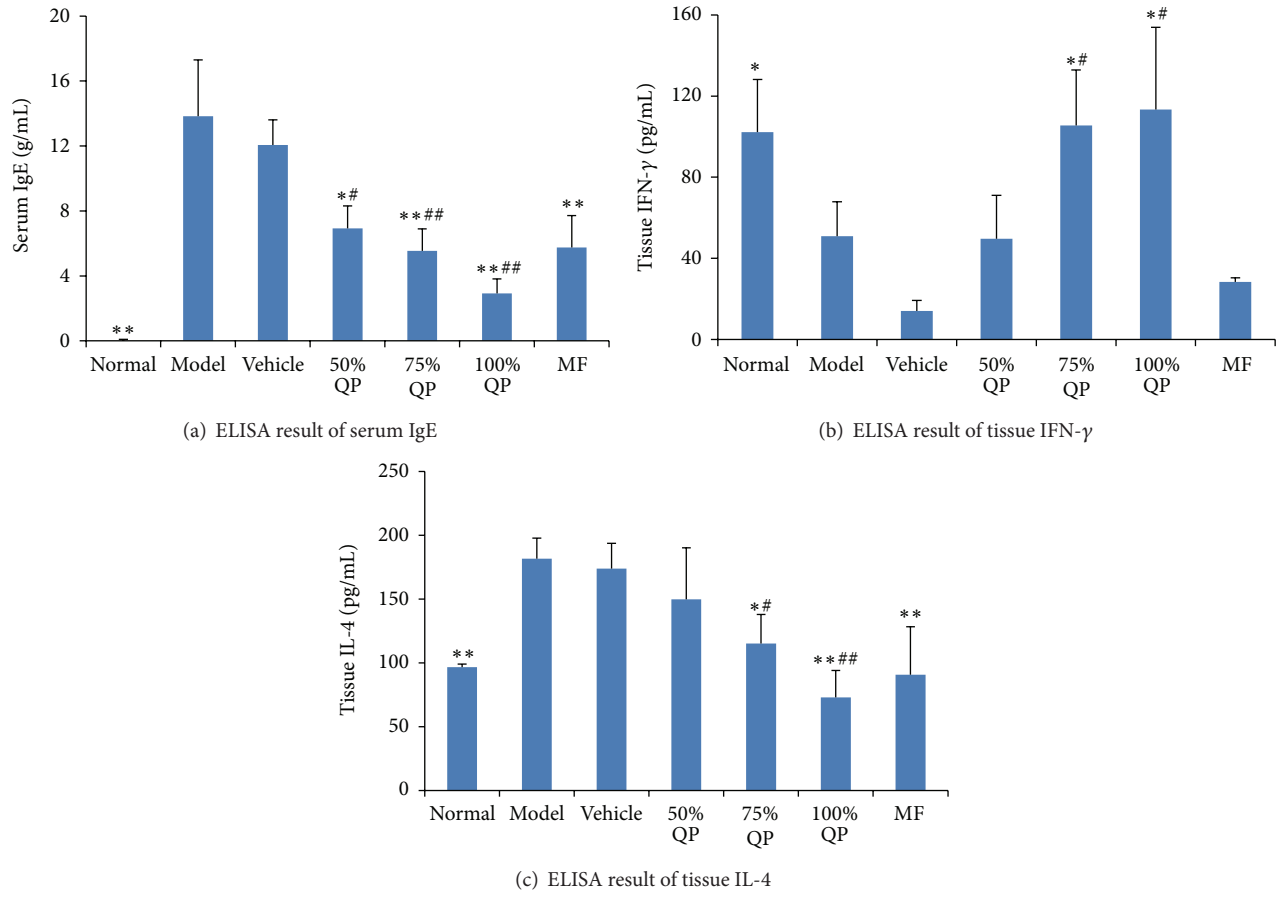

Figure 3: Comparisons of expression of serum IgE, tissue IFN-γ, and IL-4. (a) ELISA result of serum IgE; (b) ELISA result of IFN-γ; (c) ELISA result of IL-4. $^{*}P < 0.05$, $^{**}P < 0.01$ versus model group. QP: Qingpeng ointment; MF: Mometasone Furoate cream. $^{\#}P < 0.05$, $^{\#\#}P < 0.01$ versus QP vehicle.

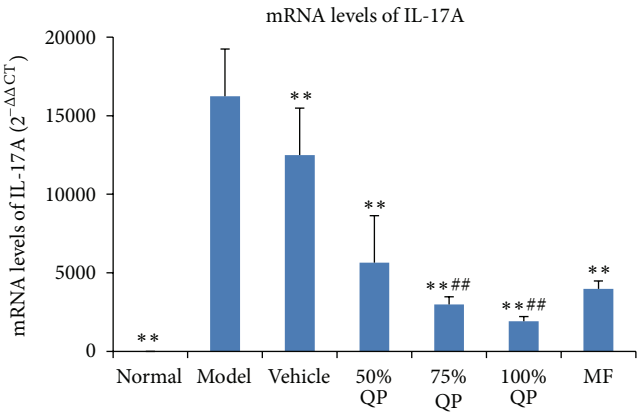

Figure 4: The changes of mRNA levels of IL-17A. The primary value of CT was transferred into $2^{-\Delta\Delta CT}$. $^{**}P < 0.01$ versus model group. MF: Mometasone Furoate cream; QP: Qingpeng ointment. $^{\#\#}P < 0.01$ versus QP vehicle.

Table 4: OD values of involucrin, filaggrin, and kallikrein7 in epidermis.

Groups	Involucrin	Filaggrin	Kallikrein7
Normal	$0.55 \pm 0.05^{*\#}$	$0.71 \pm 0.08^{**\#\#}$	$0.42 \pm 0.02^{*}$
Model	0.52 ± 0.01	0.54 ± 0.03	$0.44 \pm 0.02^{\#}$
Vehicle	0.50 ± 0.01	0.56 ± 0.03	$0.41 \pm 0.02^{*}$
50% QP	0.49 ± 0.02	0.57 ± 0.04	$0.41 \pm 0.01^{**}$
75% QP	0.48 ± 0.03	0.58 ± 0.02	$0.41 \pm 0.01^{**}$
100% QP	0.47 ± 0.02	0.58 ± 0.02	$0.40 \pm 0.02^{**}$

Values are presented as mean ± SEM. $^{*}P < 0.05$, $^{**}P < 0.01$ versus model group; $^{\#}P < 0.05$, $^{\#\#}P < 0.01$ versus vehicle group. QP: Qingpeng ointment; MF: Mometasone Furoate cream.

whereas kallikrein7 was increased. QP treatment in this study showed no significant effects in expressions of involucrin and filaggrin. Although level of kallikrein7 was decreased by vehicle and 50%, 75%, and 100% QP, there was no significant difference between vehicle and QP treated groups (Table 4).

4. Discussion

AD is a chronic recurrent inflammatory skin disease. Dysregulation of function of Th cells and production of IgE are considered the most important factors in the pathogenesis of AD [2, 3]. Th cells are belonged to $CD4^+$ T lymphocytes which include Th1 cells and Th2 cells. The division is based on the pattern of cytokines they secrete. The Th1 is characterized mainly by production of IFN-γ, IL-2, and so forth, whereas the Th2 typically synthesizes IL-4, IL-5, and so forth [24]. These distinct cytokine patterns are associated with specific functions. In particular, some cytokines are not restricted to a specific Th cell subtype such as IL-2 [24]. In this work, we applied DNFB as a hapten to BALB/c mice for 5 weeks and the induced dermatitis showed an immune profile of Th2-dominated inflammation which is similar to early reaction of AD with high level of IgE and Th2 cytokines and low level of Th1 cytokines [25, 26].

Table 5: Changes of IL-1β, IL-2, TNF-α, and IL-5 levels in skin (pg/mL).

Groups	IL-1β	IL-2	TNF-α	IL-5
Normal	$7.94 \pm 0.41^{*\#}$	$7.34 \pm 0.39^{*\#}$	$14.67 \pm 0.74^{*\#}$	$7.56 \pm 0.78^{*\#}$
Model	5.39 ± 0.68	6.62 ± 0.66	9.38 ± 0.82	22.62 ± 1.90
Vehicle	5.30 ± 0.82	6.58 ± 0.61	$11.23 \pm 0.51^{*}$	$18.43 \pm 1.19^{*}$
50% QP	5.28 ± 0.40	6.54 ± 0.24	$11.19 \pm 0.29^{*}$	$17.78 \pm 0.70^{*}$
75% QP	5.44 ± 0.60	6.56 ± 0.19	$11.33 \pm 0.37^{*}$	$16.82 \pm 0.59^{*\#}$
100% QP	5.50 ± 0.72	6.60 ± 0.79	$11.80 \pm 0.39^{*\#}$	$14.23 \pm 1.36^{*\#}$

Values are presented as mean ± SEM. $^{*}P < 0.05$, versus model group, $^{\#}P < 0.05$, versus vehicle group. QP: Qingpeng ointment; MF: Mometasone Furoate cream.

QP has been used in China for treatment of AD for many years but little is known about its mechanism. A previous study on QP with methods of ELISA by Yuan-Yuan and Lin-Feng [27] had demonstrated that 100% QP and 75% QP significantly decrease the levels of IL-5 after 2-weeks treatment in DNFB-induced AD-like lesions. In addition, the 100% QP elevated the levels of TNF-α in skin ($P < 0.05$), which had an unclear relation with mechanism of AD [28, 29]. Resulted from that study, QP showed no effect on IL-1β (produced mainly by macrophagocyte) and IL-2 expression in skin (Table 5). In our research, QP administration significantly inhibited the skin inflammation and the production of IgE and IL-4 as MF, but increased the level of tissue IFN-γ unlike MF. IL-4 and IL-5 are known to be produced by Th2 cells and they can stimulate B cells to differentiate and secret IgE, whereas IFN-γ, secreted mainly by Th1 cell and natural killer (NK) cell, has abilities of activating the neutrophil, NK cell, and Th1 cell and inhibiting the activation of Th2 cell. These results suggested that topical QP might have modulation effects on Th1/Th2 immune deregulations rather than corticosteroids which inhibited the common immune reaction. But as the IFN-γ is related to chronic inflammation, the mechanism of QP on chronic lesion still needs to be researched.

Th17 is a new subtype of $CD4^+$ T cells which was firstly found that it could secrete IL-17A. Recent researches show that IL-17A can be secreted by other innate cells including $CD8^+$ T cells, $\gamma\delta$ T cells and NKT cells [30]. It is found to have pro-inflammatory functions in host defense against extracellular bacteria, fungi, and possibly some viral infections and cancers [31, 32]. Meanwhile, it can also promote inflammation associated with autoimmunity [33, 34]. Besides AD, IL-17A is also reported higher in other skin diseases [35, 36]. Both MF and QP administrations inhibited the mRNA expression in skin lesion which indicates that QP may be also used on treatment of other IL-17A involved skin diseases.

Besides lymphocytes, mast cells are also demonstrated to be involved in the pathogenesis of atopic dermatitis [37, 38]. Intensive degranulation of mast cells is often observed along with the recruitment of these cells in the inflammatory skin region in AD [39]. Moreover, mast cells activation has been shown to be correlated with the severity of AD [40, 41]. In our study, the number of mast cells increased in induced lesions, whereas QP administration suppressed its accumulation

after 2-week treatment. However, the mechanism of this phenomenon needed to be deeply investigated.

More and more studies demonstrated that inherited and/or acquired skin barrier function abnormalities are correlated with the pathogenesis of AD [26, 42]. Involucrin and filaggrin are involved in keratinocyte differentiation while kallikrein7 is a desquamation related enzyme. They all contribute to the permeability barrier function of skin. The extent of its abnormality parallels the severity of the disease phenotype in AD [42]. Our mouse model of AD-like dermatitis showed declined levels of involucrin and filaggrin but an increased level of kallikrein7 which are similar to human AD [17, 19]. But QP treatment on induced AD-like lesions showed little effect on expressions of them in our study except the vehicle of QP which showed a possible ability of suppressing the expression of kallikrein7.

Accordingly, besides its effects on IL-5 and TNF-α, the probable mechanism of QP on treatment of AD might also correlate with its functions of inhibiting the infiltration of $CD4^+$ T cells and mast cells, reducing expressions of IL-4 and IgE, mRNA expression of IL-17A, and increasing the level of IFN-γ on induced Th2-type inflammation in mice.

5. Conclusions

Traditional Chinese medicine has been used in the treatment of eczema for a long history in China. In this work, the pathology and molecular biology analyses showed that QP administration inhibited DNFB-induced AD-like dermatitis and infiltration of $CD4^+$ T cells and mast cells on lesions of BALB/c mice. The levels of IgE, IL-4, and IL-17A were decreased as MF, but the level of IFN-γ was increased which was different from MF. This study therefore provides biological evidence supporting the use of QP as an alternative medicine for the treatment of AD. However, more studies especially on the detailed pharmacy of its elements are still needed to explore its mechanism further.

Conflict of Interests

The authors declare no conflict of interests.

Acknowledgments

The authors would like to thank their colleagues in Central Laboratory of Peking University Third Hospital and Laboratory Animal Unit of Peking University Health Science Center for technology support. The study was supported by a fund provided by Chinese Association of the Integration of Traditional and Western Medicine.

References

[1] S. Bonness and T. Bieber, "Molecular basis of atopic dermatitis," *Current Opinion in Allergy and Clinical Immunology*, vol. 7, no. 5, pp. 382–386, 2007.

[2] N. Novak, "New insights into the mechanism and management of allergic diseases: atopic dermatitis," *Allergy*, vol. 64, no. 2, pp. 265–275, 2009.

[3] J. Verhagen, M. Akdis, C. Traidl-Hoffmann et al., "Absence of T-regulatory cell expression and function in atopic dermatitis skin," *Journal of Allergy and Clinical Immunology*, vol. 117, no. 1, pp. 176–183, 2006.

[4] T. Honda, G. Egawa, S. Grabbe, and K. Kabashima, "Update of immune events in the murine contact hypersensitivity model: toward the understanding of allergic contact dermatitis," *Journal of Investigative Dermatology*, vol. 133, no. 2, pp. 303–315, 2013.

[5] H. Matsuda, N. Watanabe, G. P. Geba et al., "Development of atopic dermatitis-like skin lesion with IgE hyperproduction in NC/Nga mice," *International Immunology*, vol. 9, no. 3, pp. 461–466, 1997.

[6] X. K. Gao, N. Nakamura, K. Fuseda, H. Tanaka, N. Inagaki, and H. Nagai, "Establishment of allergic dermatitis in NC/Nga mice as a model for severe atopic dermatitis," *Biological and Pharmaceutical Bulletin*, vol. 27, no. 9, pp. 1376–1381, 2004.

[7] Y. Tomimori, Y. Tanaka, M. Goto, and Y. Fukuda, "Repeated topical challenge with chemical antigen elicits sustained dermatitis in NC/Nga mice in specific-pathogen-free condition," *Journal of Investigative Dermatology*, vol. 124, no. 1, pp. 119–124, 2005.

[8] H. Jin, R. He, M. Oyoshi, and R. S. Geha, "Animal models of atopic dermatitis," *The Journal of Investigative Dermatology*, vol. 129, no. 1, pp. 31–40, 2009.

[9] N. Inagaki and H. Nagai, "Analysis of the mechanism for the development of allergic skin inflammation and the application for its treatment: mouse models for the development of remedies for human allergic dermatitis," *Journal of Pharmacological Sciences*, vol. 110, no. 3, pp. 251–259, 2009.

[10] B. G. Jung, S. J. Cho, H. B. Koh, D. U. Han, and B. J. Lee, "Fermented Maesil (*Prunus mume*) with probiotics inhibits development of atopic dermatitis-like skin lesions in NC/Nga mice," *Veterinary Dermatology*, vol. 21, no. 2, pp. 184–191, 2010.

[11] M. S. Choi, E. C. Kim, H. S. Lee et al., "Inhibitory effects of *Saururus chinensis* (Lour.) Baill on the development of atopic dermatitis-like skin lesions in NC/Nga mice," *Biological and Pharmaceutical Bulletin*, vol. 31, no. 1, pp. 51–56, 2008.

[12] K. Ogawa, M. Takeuchi, and N. Nakamura, "Immunological effects of partially hydrolyzed arabinoxylan from corn husk in mice," *Bioscience, Biotechnology and Biochemistry*, vol. 69, no. 1, pp. 19–25, 2005.

[13] K. Samukawa, Y. Izumi, M. Shiota et al., "Red ginseng inhibits scratching behavior associated with atopic dermatitis in experimental animal models," *Journal of Pharmacological Sciences*, vol. 118, no. 3, pp. 391–400, 2012.

[14] H. Tang, Q. P. Yang, D. Luo et al., "Qingpeng ointment in the treatment of eczema: a multi-center, randomized, double-blind, placebo-controlled study," *Chinese Journal of Dermatology*, vol. 44, no. 12, 4 pages, 2011.

[15] E. Proksch, J. M. Brandner, and J. Jensen, "The skin: an indispensable barrier," *Experimental Dermatology*, vol. 17, no. 12, pp. 1063–1072, 2008.

[16] S. Kezic, P. M. J. H. Kemperman, E. S. Koster et al., "Loss-of-function mutations in the filaggrin gene lead to reduced level of natural moisturizing factor in the stratum corneum," *Journal of Investigative Dermatology*, vol. 128, no. 8, pp. 2117–2119, 2008.

[17] M. J. Cork, S. G. Danby, Y. Vasilopoulos et al., "Epidermal barrier dysfunction in atopic dermatitis," *Journal of Investigative Dermatology*, vol. 129, no. 8, pp. 1892–1908, 2009.

[18] B. E. Kim, D. Y. M. Leung, M. Boguniewicz, and M. D. Howell, "Loricrin and involucrin expression is down-regulated by Th2

cytokines through STAT-6," *Clinical Immunology*, vol. 126, no. 3, pp. 332–337, 2008.

[19] N. Komatsu, K. Saijoh, C. Kuk et al., "Human tissue kallikrein expression in the stratum corneum and serum of atopic dermatitis patients," *Experimental Dermatology*, vol. 16, no. 6, pp. 513–519, 2007.

[20] N. Novak and D. Y. M. Leung, "Advances in atopic dermatitis," *Current Opinion in Immunology*, vol. 23, no. 6, pp. 778–783, 2011.

[21] H. Matsuoka, N. Maki, S. Yoshida et al., "A mouse model of the atopic eczema/dermatitis syndrome by repeated application of a crude extract of house-dust mite *Dermatophagoides farinae*," *Allergy*, vol. 58, no. 2, pp. 139–145, 2003.

[22] J. Li, C. Roubeix, Y. Wang et al., "Therapeutic efficacy of trehalose eye drops for treatment of murine dry eye induced by an intelligently controlled environmental system," *Molecular Vision*, vol. 18, pp. 317–329, 2012.

[23] K. J. Livak and T. D. Schmittgen, "Analysis of relative gene expression data using real-time quantitative PCR and the $2^{-\Delta\Delta CT}$ method," *Methods*, vol. 25, no. 4, pp. 402–408, 2001.

[24] M. Grewe, C. A. F. M. Bruijnzeel-Koomen, E. Schöpf et al., "A role for Th1 and Th2 cells in the immunopathogenesis of atopic dermatitis," *Immunology Today*, vol. 19, no. 8, pp. 359–361, 1998.

[25] D. Y. M. Leung, M. Boguniewicz, M. D. Howell, I. Nomura, and Q. A. Hamid, "New insights into atopic dermatitis," *Journal of Clinical Investigation*, vol. 113, no. 5, pp. 651–657, 2004.

[26] M. Boguniewicz and D. Y. M. Leung, "Atopic dermatitis: a disease of altered skin barrier and immune dysregulation," *Immunological Reviews*, vol. 242, no. 1, pp. 233–246, 2011.

[27] L. Yuan-Yuan and L. Lin-Feng, "Inhibitory effect of Qingpeng ointment on experimental atopic dermatitis in mice," *Chinese Journal of Dermatology*, vol. 46, no. 1, 5 pages, 2013.

[28] M. P. Laan, H. Koning, M. R. M. Baert et al., "Levels of soluble intercellular adhesion molecule-1, soluble E-selectin, tumor necrosis factor-α, and soluble tumor necrosis factor receptor p55 and p75 in atopic children," *Allergy*, vol. 53, no. 1, pp. 51–58, 1998.

[29] N. Behniafard, M. Gharagozlou, E. Farhadi et al., "TNF-α single nucleotide polymorphisms in atopic dermatitis," *European Cytokine Network*, vol. 23, no. 4, pp. 163–165, 2012.

[30] J. M. Reynolds, P. Angkasekwinai, and C. Dong, "IL-17 family member cytokines: regulation and function in innate immunity," *Cytokine and Growth Factor Reviews*, vol. 21, no. 6, pp. 413–423, 2010.

[31] H. Hamada, M. D. L. L. Garcia-Hernandez, J. B. Reome et al., "Tc17, a unique subset of CD8 T cells that can protect against lethal influenza challenge," *Journal of Immunology*, vol. 182, no. 6, pp. 3469–3481, 2009.

[32] N. Martin-Orozco, P. Muranski, Y. Chung et al., "T helper 17 cells promote cytotoxic T cell activation in tumor immunity," *Immunity*, vol. 31, no. 5, pp. 787–798, 2009.

[33] M. Huber, S. Heink, H. Grothe et al., "Th17-like developmental process leads to $CD8^+$ Tc17 cells with reduced cytotoxic activity," *European Journal of Immunology*, vol. 39, no. 7, pp. 1716–1725, 2009.

[34] J. D. Milner, "IL-17 producing cells in host defense and atopy," *Current Opinion in Immunology*, vol. 23, no. 6, pp. 784–788, 2011.

[35] D. Ma, X. Zhu, P. Zhao et al., "Profile of Th17 cytokines (IL-17, TGF-β, IL-6) and Th1 cytokine (IFN-γ) in patients with immune thrombocytopenic purpura," *Annals of Hematology*, vol. 87, no. 11, pp. 899–904, 2008.

[36] C. K. Wong, L. C. W. Lit, L. S. Tam, E. K. M. Li, P. T. Y. Wong, and C. W. K. Lam, "Hyperproduction of IL-23 and IL-17 in patients with systemic lupus erythematosus: implications for Th17-mediated inflammation in auto-immunity," *Clinical Immunology*, vol. 127, no. 3, pp. 385–393, 2008.

[37] T. Kawakami, T. Ando, M. Kimura, B. S. Wilson, and Y. Kawakami, "Mast cells in atopic dermatitis," *Current Opinion in Immunology*, vol. 21, no. 6, pp. 666–678, 2009.

[38] F. T. Liu, H. Goodarzi, and H. Y. Chen, "IgE, mast cells, and eosinophils in atopic dermatitis," *Clinical Reviews in Allergy and Immunology*, vol. 41, no. 3, pp. 298–310, 2011.

[39] D. A. Groneberg, C. Bester, A. Grützkau et al., "Mast cells and vasculature in atopic dermatitis—potential stimulus of neoangiogenesis," *Allergy*, vol. 60, no. 1, pp. 90–97, 2005.

[40] L. Zhao, H. Jin, R. She et al., "A rodent model for allergic dermatitis induced by flea antigens," *Veterinary Immunology and Immunopathology*, vol. 114, no. 3-4, pp. 285–296, 2006.

[41] T. Kanbe, Y. Soma, Y. Kawa, M. Kashima, and M. Mizoguchi, "Serum levels of soluble stem cell factor and soluble KIT are elevated in patients with atopic dermatitis and correlate with the disease severity," *The British Journal of Dermatology*, vol. 144, no. 6, pp. 1148–1153, 2001.

[42] P. M. Elias, Y. Hatano, and M. L. Williams, "Basis for the barrier abnormality in atopic dermatitis: outside-inside-outside pathogenic mechanisms," *Journal of Allergy and Clinical Immunology*, vol. 121, no. 6, pp. 1337–1343, 2008.